Experimental study of segregation mechanisms in bedload sediment transport

Ashley Dudill

Communauté
UNIVERSITÉ Grenoble Alpes

a place of mind
THE UNIVERSITY OF BRITISH COLUMBIA

THÈSE

Pour obtenir le grade de

DOCTEUR DE LA COMMUNAUTÉ UNIVERSITÉ GRENOBLE ALPES

préparée dans le cadre d'une cotutelle entre la *Communauté Université Grenoble Alpes* et The *University of British Columbia*

Spécialité : **Sciences de la terre et univers, environnement**

Arrêté ministériel : 25 mai 2016

Présentée par

Ashley DUDILL

Thèse dirigée par **Philippe FREY** et **Michael CHURCH**
codirigée par **Marwan HASSAN** et **Jeremy VENDITTI**

préparée au sein des **Laboratoires IRSTEA / Etna** et **UBC Geography**

dans **les Écoles Doctorales TUE (Terre, univers, environnement)** et **UBC Faculty of Graduate and Postdoctoral Studies**

Étude expérimentale de la ségrégation en transport solide par charriage

Thèse soutenue publiquement le **28 Septembre 2016**, devant le jury composé de :

M. Eric BARTHÉLÉMY Professeur, Université Grenoble Alpes	Président
Mlle. Lynne FROSTICK Professor, University of Hull	Rapporteur
M. Hervé PIÉGAY Directeur de recherche, CNRS, Université de Lyon	Rapporteur
M. Roger BECKIE Professor, University of British Columbia	
M. Michael CHURCH Professor Emeritus, University of British Columbia	
M. Philippe FREY Scientifique (HdR), IRSTEA, Université Grenoble Alpes	
M. Marwan HASSAN Professor, University of British Columbia	
M. Jeremy VENDITTI Professor, Simon Fraser University	

Abstract

This research focuses upon size segregation mechanisms in bedload sediment transport. Simplified experiments with fine grain inputs to a mobile coarse bed in equilibrium were undertaken in a small, narrow flume using spherical glass beads. The experiments demonstrate the influence of the size ratio between the bed (D_c) and the input (D_f) upon the channel response. Size ratios (D_c/D_f) between 7.14 and 1.25 were tested, with a constant coarse feed rate, and a variety of fine feed rates. Previous work has documented an increase in sediment transport rates as a result of a fine grain input; the experiments presented herein identify boundaries within this behaviour.

Kinetic sieving takes place in the mobile bed surface, with the finer sediment moving to the bottom of the bedload transport layer at the interface to the underlying quasi-static coarse bed. The behavior at this interface dictates how a channel responds to a fine sediment input. If, by spontaneous percolation, the fine sediment is able to infiltrate into the underlying quasi-static bed, the total transport increases and the bed degrades causing a reduction in the slope. However, if the fine sediment input rate exceeds the transport capacity or is geometrically unable to infiltrate into the underlying bed, it forms a quasi-static layer underneath the transport layer that inhibits entrainment from the underlying bed, resulting in aggradation and an increase in bed slope.

A formal test of the reproducibility of the aforementioned results was undertaken in a different laboratory, with the same experimental procedure. Comparison of the qualitative results reveals that the same dominant processes occur. Consistent differences, however, were present between the quantitative results; likely a result of differences in the experimental arrangement.

A final set of experiments assesses the differences and similarities between experiments undertaken with spherical glass beads and natural materials to examine the complexities introduced due to particle shape. While the experiments with ideal materials reveal fundamental mechanisms associated with granular transport of mixed sizes, several key new phenomena are apparent in the experiments with natural materials, including changes in the infiltration potential and the emergence of bed structures.

Résumé

Cette recherche porte sur les mécanismes de ségrégation dans le transport de sédiments par charriage. Des expériences simplifiées consistant à introduire un débit de particules fines sur un lit plus grossier, mobile, en équilibre, ont été entreprises dans un canal particulaire étroit en utilisant des billes de verre sphériques. Les expériences montrent des réponses différenciées en fonction du rapport de taille entre les particules grossières du lit (D_c) et les fines (D_f). Des rapports de taille (D_c/D_f) entre 7,14 et 1,25 ont été testés, pour différents débits solides de particules fines, tout en maintenant le débit solide des particules grossières constant. Des travaux antérieurs ont mis en évidence une augmentation des débits solides suite à l'introduction de grains fins. Les expériences présentées ici identifient les frontières au sein de ce comportement.

Le tamisage cinétique a lieu à la surface du lit mobile, avec des sédiments plus fins se déplaçant vers le bas de la couche de charriage à l'interface du lit grossier quasi-statique. Le comportement à cette interface dicte comment le système répond à l'introduction de sédiments fins. Si, par percolation spontanée, le sédiment fin est capable de s'infiltrer dans le lit quasi-statique sous-jacent, le débit solide total augmente et le lit s'incise (diminution de pente). Toutefois, si les fines ne peuvent géométriquement s'infiltrer ou dépassent la capacité de transport, elles forment une couche quasi-statique sous la couche de charriage, qui empêche l'entraînement du lit sous-jacent, résultant en un exhaussement (augmentation de pente).

Un essai formel de la reproductibilité des résultats ci-dessus a été effectué dans un autre laboratoire avec le même mode opératoire expérimental. La comparaison des résultats qualitatifs révèle les mêmes processus dominants. Cependant, des différences sont notées dans les résultats quantitatifs, du fait de la quasi-impossibilité de reproduire exactement la même expérience.

Une dernière série d'expériences évalue les différences et les similitudes entre les expériences menées avec des billes de verre sphériques et des matériaux naturels ce qui permet d'étudier l'influence de la forme. Alors que les expériences avec des matériaux idéaux révèlent des mécanismes fondamentaux associés au transport granulaire et à la ségrégation, plusieurs nouveaux phénomènes sont observés avec des matériaux naturels, notamment une modification du potentiel d'infiltration et l'émergence de formes du lit.

Preface

This dissertation is formatted in accordance with the regulations of the University of British Columbia and submitted in partial fulfillment of the requirements for a PhD degree awarded jointly by the University of British Columbia and the Université de Grenoble. Versions of this dissertation will exist in the institutional repositories of both institutions.

Chapter 1. Portions of the introductory text are taken from the papers under review in Chapters 2 and 3. I drafted the text, and M.Church and P.Frey provided advice and editing.

Chapter 2. A version of this chapter is under review at a journal as Dudill A., Frey P., and Church M. (2016) Infiltration of fine sediment into a coarse mobile bed: a phenomenological study. I designed, conducted and analysed the experiments, with the support of P.Frey. I was responsible for drafting the text. P.Frey and M.Church provided advice and edited the text.

Chapter 3. A version of this chapter has been prepared for submission at a journal as Dudill A., Lafaye de Micheaux H., Frey P., and Church M. (2016) Introducing finer grains into bedload: the transition to a new equilibrium. I designed, conducted and analysed the experiments, with the support of P.Frey. The image analysis techniques were developed by H.Lafaye de Micheaux. I was responsible for drafting the text. P.Frey and M.Church provided advice and edited the text.

Chapters 4 and 5. These chapters are original, unpublished work, which will later be submitted to a peer-reviewed journal. The experimental design was undertaken by myself, along with the support and guidance of J. Venditti, M.Church and P. Frey. I was responsible for conducting and analysing the experiments, and drafting the text. The image analysis techniques were developed by H. Lafaye de Micheaux.

Chapter 6. Portions of the discussion text are taken from the papers under review in Chapters 2 and 3. I drafted the text, and M.Church and P.Frey provided advice and editing.

Appendix A. The experiments detailed in Appendix A and presented in Figure A.1 were undertaken and analysed by P.Frey.

Table of Contents

List of Tables

List of Figures

List of Symbols

b	Decay timescale
D	Diameter
D_c	Diameter of the coarse sediment forming the bed
D_f	Diameter of the fine sediment
$D_{f,max}$	Size of the largest sphere which can fit into the largest void space
D_i	Intermediate diameter
D_x	Diameter at which X % of particles are below this size
g	Gravitational constant
h	Mean flow depth
k	Von Karman constant (0.4)
Q	Flow rate
q_s	Bedload transport rate per unit width
R	Submerged specific gravity
R_h	Hydraulic radius
R_{hb}	Bottom hydraulic radius
S	Bed slope
S_{eq}	Two-size equilibrium bed slope
S_o	Initial one-size equilibrium bed slope
t	Time
t_o	Start time: when the bed response commences
U	Mean velocity

u_*	Shear velocity
W	Channel width
w_s	Fall velocity
α	Channel angle
θ	Shields Number
μ	Dynamic viscosity
v	Kinematic viscosity
ρ	Water density
ρ_s	Sediment density
τ_o	Shear stress
Φ	Dimensionless solid discharge

Acknowledgements

Firstly, I would like to thank my two research supervisors, Mike Church and Philippe Frey, for their continued support throughout the past four years. This research would not have been possible, or as enjoyable, without their advice and enthusiasm. Professor Church asked the questions which pushed me to think harder, and took the time to help me become a better writer, for which I am sincerely grateful. Dr Frey taught me how to undertake experimental work, provided me with direction and inspiration, and introduced me to French coffee! Further, I am very grateful to both of them for providing me with so many opportunities, especially to attend conferences which allowed me to converse with researchers from all over the world. Marwan Hassan provided constant support and encouragement throughout. Jeremy Venditti allowed me to use his laboratory at SFU, and shared his expertise.

Veronica Leon Marin (at Irstea) and Indra Orgil (at SFU) were brilliant lab assistants. I am very grateful for their hard work, enthusiasm and companionship during the many, many months spent in the lab; they both made the experience much more enjoyable. I was also very fortunate to work with several great lab technicians. Á Irstea, je remercie Frédéric Ousset et Christian Eymond-Gris pour leur aide et leur patience. At SFU, I would like to thank Matt Akenhead who meticulously constructed the flume for the experiments. At UBC, I would like to thank Rick Kelter for always making time to give me advice.

Hugo Lafaye de Micheaux developed the image analysis tools for the experiments, which greatly enriched the analysis. Merci Hugo, for all of your patience and help with Matlab; it has been a pleasure to collaborate with you.

During my PhD, I've had the privilege of being part of several research groups. I am very grateful to the PhD students at Irstea for their warm welcome when I arrived in Grenoble, and for the wonderful coffee breaks! Marwan Hassan's research group at UBC has provided me with feedback, helpful advice and many lunch breaks. Jeremy Venditti's students in the SFU flume lab welcomed me and were great companions.

Finally, I am so thankful to my friends and family. Friends, near and far, old and new, have helped me to keep perspective and enjoy the opportunities of living in Vancouver and Grenoble. My Auntie Melinda and Uncle Hugh have been a constant source of advice and encouragement. And most importantly, my Mum, Dad and Jack. Without them, none this would have been possible. Parts of the past four years have been challenging, but I have always felt completely loved and supported. I cannot express how lucky I feel to have you all as my family.

Chapter 1: Introduction

1.1 Introduction

An alluvial river is one in which the channel is formed in sediments that the river has entrained, transported and deposited itself. Therefore, the type of sediment and process by which it is transported have a substantial influence upon the channel morphology. Bed material, which composes the bed and lower banks of the river, exerts the primary influence upon channel morphology (Church, 2006). Bed material is transported either as bedload or suspended load. Bedload is the sediment load that is transported in contact with the bed of a river, usually by rolling, traction (sliding) or saltation (hops). This research will focus upon gravel beds, wherein the coarse nature of the sediment means that the bed material is predominantly transported as bedload.

The bed material in a fluvial gravel system is formed of a wide range of grain sizes. When grains of different sizes are subjected to a shear flow, such as in a gravel-bed channel, they will segregate (Duran, 1999). There are two main types of vertical segregation, with the occurrence of each depending upon the mobility of the bed material (Frey and Church, 2011). The infiltration of fine sediment into an immobile gravel or boulder bed, a process termed 'spontaneous percolation' (Bridgwater et al., 1969) or 'static sorting' (Bacchi et al., 2014), has been extensively studied in fluvial geomorphology (see references below). However, the infiltration of fine sediment into a gravel bed in motion, a process termed 'kinetic sieving' (Middleton, 1970) or 'kinetic sorting' (Bacchi et al., 2014) has received far less attention. Due to the wide range of grain sizes present in a river, and the changing phases of sediment motion as a result of varying discharge, both of these segregation processes are likely to occur during

bedload sediment transport. The interaction of these differently sized grains within the channel bed has important implications for sediment transport rates (e.g. Curran and Wilcock, 2005b), channel morphology (e.g. Jackson and Beschta, 1984), stratigraphy (e.g. Frostick et al., 1984; Carling and Breakspear, 2006; Carling et al., 2006) and fluvial ecology (e.g. Lisle, 1989; Kemp et al., 2011).

The aim of this research is to employ flume experiments to further our understanding of the processes of spontaneous percolation and kinetic sieving. Specific attention will be given to understanding these processes in the context of a channel responding to a finer grain input. These experiments will be undertaken using a simplified, reductionist approach, which enables us to isolate the sediment infiltration behaviour for attention. The intention for these experiments is to elucidate the fundamental processes occurring in grain mixtures, not to simulate a river channel.

1.2 Background and Theory

1.2.1 Spontaneous Percolation

Spontaneous percolation is the process of fine particles infiltrating into an immobile coarse bed through the void spaces. Research on spontaneous percolation has been undertaken experimentally (e.g. Einstein, 1968; Sakthivadivel and Einstein, 1970; Beschta and Jackson, 1979; Carling, 1984; Diplas and Parker, 1992; Gibson et al., 2009; 2010; Dermisis and Papanicolaou, 2014), in the field (e.g. Frostick et al., 1984; Carling and McCahon, 1987; Lisle, 1989), and using models (Cui et al., 2008; Wooster at al., 2008).

Einstein (1968) explored the infiltration of suspended silica flour into an initially clean, static, gravel bed. He showed that the fine sediment infiltrated the gravel framework to the base of the deposit without clogging, and proceeded to fill the voids from the base upwards. Since that

work, the process of spontaneous percolation has been examined numerous times in a fluvial context. A particular focus of interest has been investigation of the influence of grain size ratio (the ratio between the diameter of the coarse sediment forming the bed framework, D_c, and the fine infiltrating sediment, D_f) on this process (e.g. Beschta and Jackson, 1979; Frostick et al., 1984; Diplas and Parker, 1992; Gibson et al., 2009). In these works it has been demonstrated that the larger the grain size ratio (D_c/D_f), the greater the amount of fine sediment infiltration. The control of grain size ratio over the amount of fine sediment infiltration is understandable as it dictates how much finer sediment can fit in the voids of a gravel deposit.

The influence of the grain size ratio on the vertical gradational profile formed due to spontaneous percolation has also been investigated. Depending upon the ratio, finer sediment has been shown to undergo 'unimpeded static percolation', form a 'bridge' layer, or not infiltrate into the bed. Table 1.1 summarizes experiments that have assigned boundaries to the formation of these different types of profile.

The term 'unimpeded static percolation' describes fine sediment infiltration to the base of a deposit so that the voids in the matrix fill from the base upward. Gibson et al. (2010) showed that, following unimpeded static percolation, the sand content is relatively constant over the depth and fills nearly all the void space. Einstein (1968), Gibson et al. (2009) and Gibson et al. (2010) observed unimpeded static percolation.

A 'bridge' layer is formed when the void geometry causes the fines to become blocked, or lodged, in void throats so that fine sediment can infiltrate only to a limited depth. Bridging has been observed both in the field (Frostick et al., 1984; Lisle, 1989) and in the flume (Beschta and Jackson, 1979; Diplas and Parker, 1992; Allan and Frostick, 1999; Gibson et al., 2009; Gibson et al., 2010; Dermisis and Papanicolaou, 2014). The depth of a bridge layer into the gravel deposit

is commonly reported to be between 2.5 and 5 D_{90} of the gravel (Beschta and Jackson, 1979; Lisle, 1989; Diplas and Parker, 1992). The bridge, or seal, layer prevents infiltration farther into the bed, with additional fine sediment entering the bed being stored above the bridges. Once the bed has become saturated with fine sediment above the bridge layer, if more fines are introduced, then they have been observed to appear on the bed surface (Diplas and Parker, 1992).

Table 1.1 Experiments demonstrating the formation of different vertical gradational profiles*

Author	**Material**	**Criterion**	**Profile**
Gibson et al. (2009)	Natural materials	$D_{15,gravel}/D_{85,sand} \geq 15.4$	Unimpeded static percolation
Gibson et al. (2010)	Natural materials	$12 < D_{15,gravel}/D_{85,sand} < 14$	Transitional (profile between bridging and unimpeded static percolation)
Gibson et al. (2009)	Natural materials	$D_{15,gravel}/D_{85,sand} \leq 10.6$	Bridging
Sakthivadivel and Einstein (1970)	Unisize spheres packed regularly and crushed styron particles	$7 < D_c/D_f \leq 14$	Bridging
Sakthivadivel and Einstein (1970)	Unisize spheres packed regularly and crushed styron particles	$D_c/D_f < 6.35$	No infiltration

***D_x: Diameter at which X % of particles are below this size.**

Sakthivadivel and Einstein (1970) put forward different theories to explain the formation of these bridges, including two fine particles arriving simultaneously and forming a bridge (their experiments did not support this theory) or, alternatively, one fine particle either moving slowly, or being retained in ‘dead space’, being joined by another particle and forming a bridge. The

formation of bridges or ‘arches’ by spherical material is well known in granular mechanics (e.g. To et al., 2002; Pugaloni and Barker, 2004).

To understand spontaneous percolation behavior as a function of grain size ratio, the geometry of the grain arrangements and void spaces must be known. As an ideal case, the packing of uniform spheres has been studied for a long period of time. In 1611, Johannes Kepler hypothesized that the densest packing arrangement for cannonballs yields a void fraction of approximately 0.26 (Andreotti et al., 2013), yet this was not proven until recently by Hales (2005). This packing arrangement is the theoretically densest possible packing, and would be difficult to achieve in a real system. In contrast, the loosest possible packing arrangement in which the system is stable was shown by Onoda and Liniger (1990) to have a void fraction of approximately 0.45 (but see next paragraph regarding cubic packing); this state is termed ‘random loose packing’. Between these two extremes, Scott and Kilgour (1969) defined ‘random close packing’, which is formed by spheres randomly arranged in a rigid container and vibrated to ensure close packing; this has a void fraction of approximately 0.36. Between the limit states, there exists a wide range of stable packing arrangements (see Allen, 1982).

Allen (1982) summarized work undertaken by Manegold et al. (1931), Horsfield (1934) and White and Walton (1937) on the size of the largest sphere which could fit into the largest void space for various packing arrangements. For cubic, orthorhombic and rhombohedral packing arrangements, the void fractions are 0.4764, 0.3954 and 0.2595, respectively. If D_c is the diameter of the spheres forming the packing arrangement, and $D_{f,max}$ is the size of the largest sphere which can fit into the largest void space, values of $D_c/D_{f,max}$ for the different packing arrangements are 1.366, 1.895 and 2.414, respectively. These values are much smaller than those

reported from fluvial experiments in Table 1.1, demonstrating that factors other than grain size ratio play a role in the infiltration behaviour.

Other factors which have been shown to modify the amount of fine sediment infiltration into a static coarse bed include:

(1) Flow conditions: Huston and Fox (2015) undertook a macroanalysis and statistical analysis of multiple previously published studies on fine grain infiltration into gravel beds in hydraulically rough turbulent open flows. They discovered that, whilst the grain size ratio was a good predictor for whether a bridge layer would form, it was not a good predictor of the maximum depth of bridging. Instead, they found that a combination of the bed porosity and the roughness Reynolds number, which indicates a control of the pore water velocity distribution, was a better predictor of maximum bridging depth.

(2) Fine feed rate: Wooster et al. (2008) undertook experiments wherein sand at varying feed rates was input to a clean gravel bed. Higher sand feed rates resulted in less infiltration into the bed.

(3) Other sediment properties: It has been noted that the framework packing arrangement is influenced by sediment shape (Frostick et al., 1984) and the grain size distribution (Lisle, 1989). These, in turn, influence the void sizes and consequently the infiltration behavior.

A great deal is known about spontaneous percolation, however the question arises, how would this grain sorting process change if the surface of the gravel bed were in motion, as is often the case in nature? Would the moving surface layer cause changes to the spontaneous percolation process in the underlying static bed?

1.2.2 Kinetic Sieving

Kinetic sieving occurs when granular materials containing particles of different sizes are in motion. The process of kinetic sieving has been extensively addressed in granular physics literature to gain insight for industrial purposes. For example, research has been undertaken to improve understanding on the segregation of granular materials in hoppers and of medical ingredients for the pharmaceutical industry.

Savage and Lun (1988) used different sizes of dry granular material to experimentally and theoretically study the process of kinetic sieving in an inclined free surface flow. They assumed that flow within a granular medium takes place in layers which move relative to each other. For relatively slow flows, where collisions are not too vigorous, they proposed two mechanisms to explain the transfer of particles between the layers:

(1) The particles are continually rearranging as the layers are moving relative to one another. If a void space opens up into which a particle from the layer above is able to fall, the particle will change layers. There is a higher probability of finding a void space for a small particle to fall into than a larger one. Therefore fines move towards the base of the deposit.

(2) As the fine sediment is moving towards the channel base in (1), there must be some mechanism that moves particles upward to preserve mass conservation. They attributed this to an imbalance of instantaneous forces acting on a particle, which causes it to be squeezed into a different layer. This process has no preference for direction of movement, or size of grain involved.

Although the majority of research on kinetic sieving has been focused in industrial contexts, there is an increasing body of literature documenting the process in a fluvial context. The process of ‘kinetic sieving’ was introduced into fluvial sedimentology as an explanation for

inverse sorting observed in sediment deposits (Middleton, 1970). Since then the process has been invoked to partly explain the formation of bed pavements (Parker and Klingeman, 1982) and 'mobile armour layers' (Mao et al., 2011). Additionally, kinetic sieving in coastal environments, due to waves, is becoming an increasingly explored topic (e.g. Calantoni and Thaxton, 2008).

Allan and Frostick (1999) investigated how the formation of a fine sediment matrix is influenced by flows that are capable of entraining the gravel bed compared to flows which cannot. They observed that, when the coarse particles 'jostle' and 'shake', the fine sediment is able to fall past the surface layer into the subsurface. Then, just before the coarse particle is entrained, the framework[1] lifts and dilates, and fluid is drawn into the space created, along with fine sediment.

Bacchi et al. (2014) undertook experiments comparing the size sorting behavior between a run with mobile coarse material and a run with static coarse material. The two runs led to different bed behaviours and morphologies, and in the run in which kinetic sieving was possible, it was noted that highly efficient vertical sorting occurred.

Whilst awareness of kinetic sieving is increasing, we do not have a complete description of this process in a fluvial context. This research will contribute to an improved understanding by examining how the grain size ratio between the segregating grains impacts upon the behaviour.

[1] Coarse grains forming the structure of the bed.

1.2.3 Sediment Mobility

In addition to examination of the size sorting processes, investigation of the consequences of a fine grain input to a channel has been undertaken due to observed impacts upon sediment mobility.

Imagine a channel with a mobile uniform bed (constant grain diameter) in equilibrium, whereby the sediment input rate is equal to the sediment output rate. An increase in sediment supply to the channel, with the additional material being finer than that forming the bed, has been shown to cause an increase in the coarse sediment transport rate in comparison to the preceding uniform conditions. The superior mobility of grain size mixtures was first demonstrated by Gilbert (1914), and has since been explored experimentally (Jackson and Beschta, 1984; Iseya and Ikeda, 1987; Ikeda and Iseya, 1988; Wilcock et al., 2001; Cui et al., 2003; Curran and Wilcock, 2005b; Venditti et al., 2010a, 2010b), and also observed in the field (e.g., Ferguson et al., 1989; Montgomery et al., 1999; Major et al., 2000).

The increase in transport rates resulting from a fine sediment addition may even be so large as to increase the sediment output rate above the sediment input rate, despite the increased supply to the system, which leads to channel degradation and a reduced equilibrium bed slope (Iseya and Ikeda, 1987; Ikeda and Iseya, 1988; Curran and Wilcock, 2005b). In contrast, an increase in sediment supply to the channel with the additional material being the same size as that forming the bed, would result in a steeper channel slope (Lane, 1955), as more energy would be required to transport the larger load.

The superior mobility of mixtures has been attributed to several causes. (1) Enhanced entrainment potential: Houssais and Lajeunesse (2012) demonstrated that, in a bimodal bed, an increasing fraction of fine sediment on the bed surface leads to a reduction in the critical Shields

number for the coarse component. (2) Elimination of 'deposition' locations: infilling of the bed surface with fines will remove potential 'deposition' locations (Venditti et al., 2010b), consequently once a particle is entrained, it is less likely to stop again. (3) Changes in the flow structure: infilling of fines on the bed surface will result in a smoother top layer, which has been observed to cause flow acceleration close to the bed, resulting in an increased drag force on the coarse particles (Venditti et al., 2010b). (4) Pivoting angle: Komar and Li (1986) examined the pivoting angle required for the threshold of motion. For a grain to be entrained, it must pivot about a contact point with an underlying grain; the angle through which it must rotate is the 'pivoting angle'. The pivoting angle of a grain is, amongst other things, a function of the ratio of the diameter of the grain to the diameter of the underlying grain, with a greater difference in diameter leading to a smaller pivoting angle (Komar and Li, 1986). (5) Exposure: the projection of a larger grain above a bed formed of finer material increases the exposure of the grain to the flow (Fenton and Abbott, 1977), therefore resulting in a lower critical Shields number for the larger grain when compared to uniform conditions (Parker and Klingeman, 1982). However, the finer grains have a higher critical Shields number as they are 'hidden' from the flow.

The extent of the increase in sediment transport rates following the introduction of fines to a channel has been shown to depend upon the proportion of fines in the total feed (Jackson and Beschta, 1984; Iseya and Ikeda, 1987; Ikeda and Iseya, 1988; Wilcock et al., 2001, Curran and Wilcock, 2005b). However, the relation between the proportion of fines and the equilibrium slope of the bed varies:

(1) Iseya and Ikeda (1987) held the gravel feed rate constant, and varied the sand feed rate between 0 and 58 % of the total feed rate. They observed a reduction in the equilibrium slope between 0 and 48 % sand content, and then a slope at 58 % no different than that at

48 %. During this experiment, the D_{50} of the gravel was 2.6 mm, and the D_{50} of the sand was 0.37 mm; therefore a grain size ratio of 7.03.

(2) Curran and Wilcock (2005b), using the same method, saw a reduction in the equilibrium bed slope between 33 and 72 % sand feed content, and then a more gradual decrease between 72 and 86 %. In this experiment the grain size ratio indexed by D_{50} was approximately 25.

(3) Ikeda and Iseya (1988) held the total feed rate constant, and varied the feed rates of the fine (D=0.2 mm) and coarse (D=1 mm) components (grain size ratio of 5). Between 0 and 43 % fine content, they observed a reduction in the equilibrium bed slope, but above a 43 % content, there was a slight increase in slope.

(4) Ikeda and Iseya (1988) undertook experiments with sand (D_{50}=0.37mm) and gravel (D_{50}=2.6mm) (grain size ratio of 7.03). In this experiment the total feed rate was kept constant. A reduction in the equilibrium bed slope was observed until the sand content reached 54%. As the sand content increased beyond this point, the slope increased slightly.

In the previous sections, it was made clear that the grain size ratio influences the amount of fine infiltration into a sediment bed. Additionally, the grain size ratio has been shown to influence pivoting angle (Komar and Li, 1986) and will influence the smoothness of the bed surface. Therefore it can be hypothesised that the enhancement of mobility due to a mixture will depend upon the grain size ratio. Yet, only a small amount of work has focused on the influence of grain size ratio upon levels of mobility within a bimodal mixture. Gilbert (1914) measured the mass transported for bimodal mixtures with five different grain size ratios (16.2, 9.7, 8.5, 3.4 and 2.9), with each grain size ratio exhibiting different behaviour. Additionally, Venditti et al. (2010a)

used two different infiltrating sizes of fine sediment and found that bed mobility was higher when coarse gravels were infiltrated by finer pulses as opposed to by coarser pulses.

Understanding how grain size ratio influences sediment mobility is an important research gap, and its investigation will test the applicability of previous results demonstrating an enhancement of mobility due to a finer grain input. Additionally, examination of the link between infiltration processes and changes in mobility may enhance our overall understanding of channel responses to fine grain inputs.

1.2.4 Research Gaps

The infiltration of fine sediment into a static coarse bed, spontaneous percolation, has been studied extensively. However, less is known in a fluvial context about the process of kinetic sieving, when the bed surface is in motion. Additionally, despite the possibility of spontaneous percolation and kinetic sieving occurring simultaneously, there has been no examination of how the sorting processes interact.

The introduction of fines has been documented to enhance the mobility of the coarse sediment. Reasons for this enhancement of mobility have been attributed to interactions between the differently sized grains and to changes in the flow properties. However, whether the infiltration behaviour plays a role in this enhancement has not been explored. Given that grain size ratio (D_c/D_f) is known to heavily influence spontaneous percolation, and therefore the bed structure, it is hypothesised that the enhancement of mobility following a fine grain input will also be a function of D_c/D_f, and this behaviour will be controlled by the infiltration processes.

Contribution to this field of research should ideally stem from an improved understanding of the sorting processes and how they influence the overall channel response in the context of

transport of mixed grain sizes. To achieve this goal, decomposition of the problem, which will enable examination at a simplified scale, should be undertaken. It is common, in the field of granular physics, to use simplified models to gain understanding of complex systems (e.g. Hill et al., 2003; Hill and Zhang, 2008). Further, the use of idealized materials in specially adapted flumes to study the fundamental mechanisms of sediment transport has been shown to reveal the most essential aspects of the physical processes that underlie complex field situations (e.g. Hergault et al., 2010; Dermisis and Papanicolaou, 2014; Frey, 2014; Martin et al., 2014; Houssais et al., 2015). Here, we will undertake simplified experiments utilizing two-size mixtures of idealized materials and a specialized flume to facilitate detailed observations of grain interactions.

1.3 Wider Considerations

In addition to improving understanding of sorting processes, and their influence upon channel response, this research will have two other research goals.

(1) As the current scientific climate places a great deal of emphasis on publishing new findings, the failure or success in reproducing[1] the results of others often goes underreported. However, recent assessment of the reproducibility of scientific results has revealed worrying conclusions in the fields of biomedicine (e.g. Begley and Ellis, 2012), psychology (e.g. Open Science Collaboration, 2015) and economics (e.g. Camerer et al., 2016). Further, a recent survey of *Nature* readers across a wide range of disciplines,

[1] Repeatability is defined as, how closely the results of independent tests agree when undertaken using the same material and the same conditions of measurement (including the same operator, equipment, laboratory, and the repeat takes place after a short period of time) (IUPAC, 1997). Whereas, reproducibility is defined as, how closely the results of independent tests agree when undertaken using the same material but different conditions of measurement (examples of changed conditions include: operator, equipment, laboratory) (IUPAC, 1997).

revealed that over 70 % of researchers have been unable to reproduce another scientist's experiment, and over 50 % have been unable to reproduce their own experiments (Baker, 2016).

The *Nature* survey also revealed that researchers thought selective reporting was the largest factor contributing to irreproducible research (Baker, 2016). The inability to reproduce the results of others also suggests flawed findings, or inadequately described methods. The need to encourage reporting of, and discussion around, reproducibility has led to the creation of a new open-access journal in the field of biomedicine (Kaiser, 2016).

Despite growing awareness in other fields, formal testing of the reproducibility of results in fluvial geomorphology is rare. Although there is implicit evidence within geomorphological classifications of reproducibility, e.g. sand wave classifications (Allen, 1982). This research will therefore take the opportunity to undertake a formal test of reproducibility within the domain of fluvial geomorphology.

(2) Natural fluvial sediments vary in shape depending upon the material properties, degree of wear and the conditions surrounding its transport and deposition (Fraser, 1935). Yet simplified experiments to reduce complex situations often involve the use of idealised materials, whereby the shape of the grains is different than that of natural sediment. This is particularly apparent in experiments undertaken with spherical beads (e.g. Hergault et al., 2010). However, the difference in sediment behaviour depending upon whether the grains are natural or spherical beads has received little attention in the context of sediment mixtures (but see, Miller and Byrne, 1966; Li and Komar, 1986). In this research, a preliminary examination of this issue is undertaken.

1.4 Research Questions

The following questions, which will be tackled during this research:

Question 1: The main body of research on kinetic sieving has been undertaken in an industrial context. What are the defining characteristics of this sorting process in a fluvial context?

Question 2: A bed with a mobile surface will be subject to both spontaneous percolation and kinetic sieving. How do the two sorting processes interact and influence each other? Is the previously observed spontaneous percolation behaviour modified by the presence of a mobile bed surface?

Question 3: How does grain size ratio (D_c/D_f) impact upon spontaneous percolation and kinetic sieving processes in a bed with a mobile surface?

Question 4: How does grain size ratio influence sediment mobility within the bed?

Question 5: Can changes in mobility at different grain size ratios be explained by the sorting processes? (The purpose of the research is not to simply observe the effect of changing the grain size ratio upon the mobility, but to understand the cause).

Question 6: Are the results of an experiment in the domain of fluvial geomorphology reproducible?

Question 7: What is the impact of using spherical beads instead of natural materials?

The experiments will be ‘exploratory’ in that they will serve to develop initial phenomenological descriptions of the behaviour. The concept of ‘exploratory’ experiments was suggested by Flueck (1978); ‘an attempt at “staking a claim” on a planned or unplanned relation(s) among events based on a plausible (though often crude) conceptual model and appropriate scientific evidence’ (Flueck, 1978; pg 386).

Through the use of simplified, artificial experiments, we are able to focus upon one aspect; these experiments will isolate the grain-grain interactions, with only estimates of certain summary values being calculated for the hydraulics and sediment transport parameters. Primary observations, such as these, are essential to understanding larger, complex, problems.

The reductionist view involved in these experiments, whilst being advantageous in its ability to reveal the fundamental processes, also has limitations. It is acknowledged that the results of these experiments will not be directly applicable to the field, but rather constitute an initial step towards building understanding.

Chapter 2 will present results from experiments undertaken at the National Research Institute of Science and Technology for Environment and Agriculture (Irstea), Grenoble, France using a short, narrow flume with two-size mixtures of narrowly graded spherical glass beads. It will address research questions 1 to 5, in a qualitative manner. Chapter 3 will present the quantitative results from the Irstea experiments, specifically addressing research questions 3 and 4. References to the experiments undertaken at Irstea will be identified by ‘I’. Chapter 4 will present results from experiments undertaken using two-size mixtures of narrowly graded spherical glass beads at Simon Fraser University (SFU), Vancouver, Canada. These experiments address research question 6 by testing the reproducibility of the Irstea results. Chapter 5 will

present the results of experiments undertaken at SFU with natural materials, therefore addressing research question 7. References to the experiments undertaken at SFU will be identified by ‘S’.

Chapter 2: Infiltration of fines into a coarse mobile bed: a phenomenological study

The purpose of this chapter is to provide phenomenological descriptions of how fine sediment inputs to a coarse bed in motion behave with regards to spontaneous percolation and kinetic sieving. The chapter examines both of these sorting processes, considering how and when they occur, the infiltration profiles formed, and identifies limits to the behavior for spherical grains with given grain size ratios. This is achieved through the presentation of experimental results that elucidate the influence of both the grain size ratio and the quantity of the fine sediment input. Additionally, by observing the bed slope response following the fine sediment input, it is possible to determine whether or not a given fine sediment input leads to an enhancement in the sediment transport capacity.

2.1 Experimental Arrangements

Experiments were undertaken using artificial media (spherical glass beads) in a glass-sided, steel-framed sediment-feed flume (Figure 2.1), located at Irstea, Grenoble, France. The channel width was 10.3 mm, which permitted clear observation over the entire width of the bed. The slope was 10.1±0.01 %; the relatively high gradient facilitated mobility of the coarse grains and the accompanying processes of infiltration of the finer sizes. In order to prevent regular arrangements of grains developing within the sediment bed, the flume has an irregularly corrugated bottom. An obstacle of 64 mm height, in lieu of a tailgate, was inserted into the end of the flume to cause bed formation.

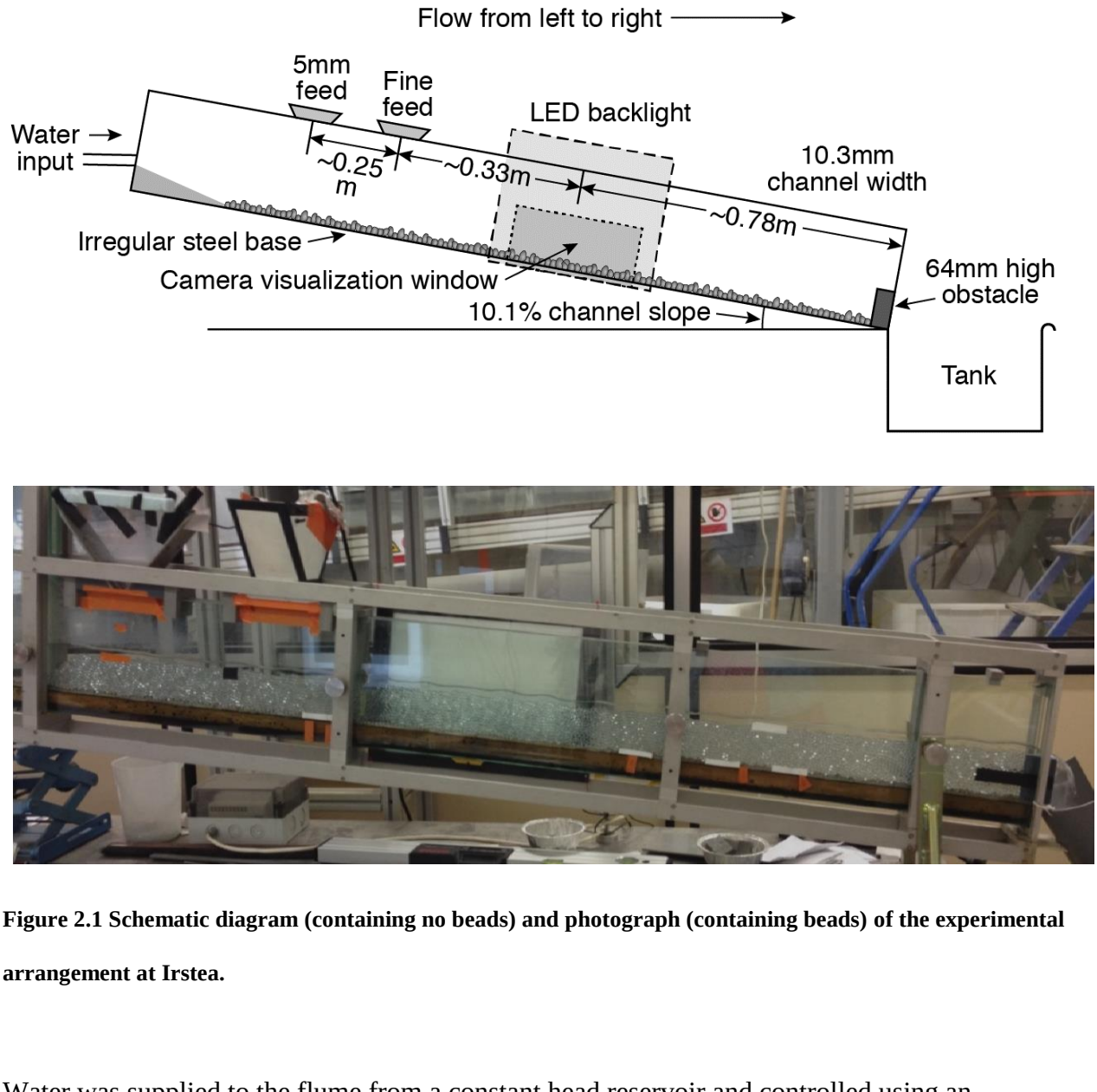

Figure 2.1 Schematic diagram (containing no beads) and photograph (containing beads) of the experimental arrangement at Irstea.

Water was supplied to the flume from a constant head reservoir and controlled using an electromagnetic flow meter. Flow rate was held constant in all experiments at 0.0495 L/s; this was essential as the influence of flow structure upon fine sediment infiltration has been prominently noted in literature (e.g. Sakthivadivel and Einstein, 1970; Beschta and Jackson, 1979; Cui et al., 2008; Huston and Fox, 2015). This flume, during supercritical flows, has been

shown to produce sediment transport parameters in good agreement with classic semi-empirical bedload formulae (Frey et al., 2006; Böhm et al., 2006; and see Appendix A).

Experiments were undertaken using two-size mixtures of spherical glass beads. The diameter of the coarse component remained fixed at 5.0±0.3 mm. This ensured that the pore space within the bed was consistent between experiments. The diameter of the fine component varied; diameters of 1.5±0.2 mm, 2.0±0.2 mm, 3.0±0.3 mm and 4.0±0.3 mm were used. Additionally, two sets of material below 1mm in diameter were used: one with D_{50} of 0.7 mm (D_{75}/D_{25}=1.15) and another with D_{50} of 0.9 mm (D_{75}/D_{25}=1.12). All of the beads used in the experiments have a density of 2500 kg/m^3, and all were transparent except for the 3 mm beads, which were translucent blue. In all of the experiments, the fine sediment moved as bedload, the weight of the sediment being supported by the bed of the channel, but including short saltation hops. This is consistent with the field observation of Lisle (1989) that most of the infiltrated sediment came from the finest bedload as opposed to the suspended load.

Two sediment-feeders were utilized during the experiments. The 5 mm bead feeder, a K-Tron© Bulk Solids Pump^{TM} Loss-in-Weight feeder, was located 1.36 m upstream of the flume outlet. The fine bead feeder, a 'Tinker' distributor , was located 1.11 m upstream of the flume outlet. This distributor consists of a rotating pipe within a reservoir filled with beads and is shown in Figure 2.2.

The experiments were recorded using a Photon Focus© camera, provided by Alliance Vision©. The camera was inclined to the same angle as the flume, and run at 130 frames per second. A LED backlight panel was placed behind the flume, approximately 0.78 m upstream from the flume outlet, which provided stable and uniform lighting for the camera. The images from the camera visualization window are 1024 by 500 pixels.

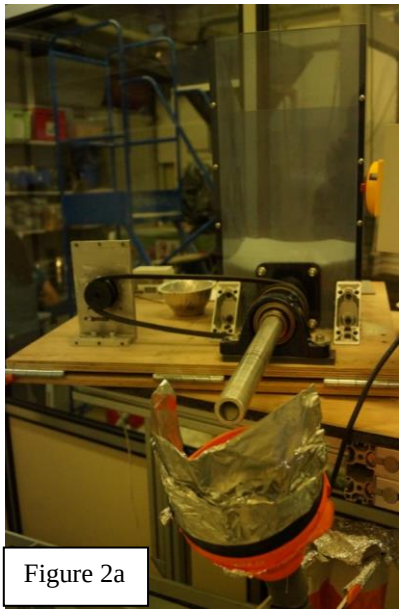
Figure 2a

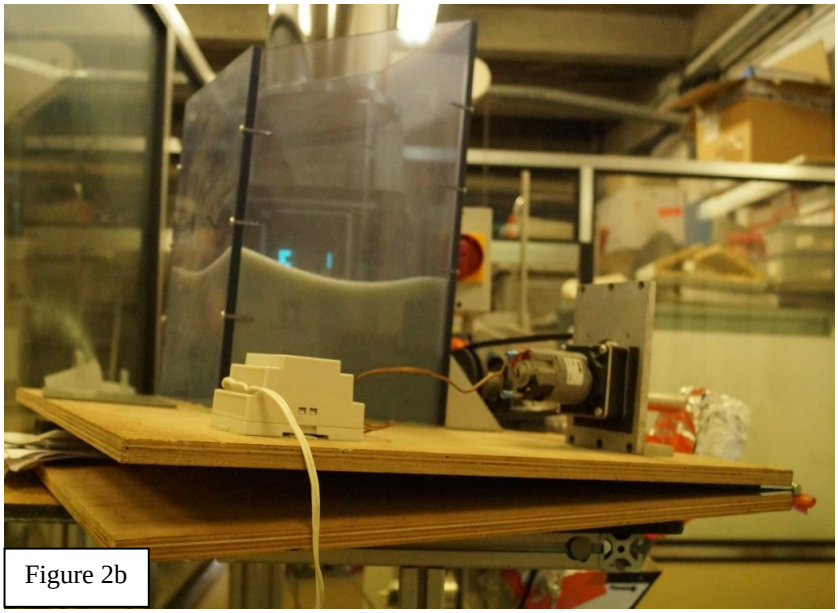
Figure 2b

Figure 2.2 Photograph of the 'Tinker' distributor. (a) Front view. (b) Side view.

2.2 Experimental Procedure

Each experiment was undertaken in two stages:

- Stage 1: The sediment bed was formed of 5 mm beads alone, and then maintained in equilibrium such that the sediment input rate was equal to the sediment output rate, and the bed slope and water slope were parallel to the flume slope. The conditions necessary to maintain one-size equilibrium of the 5 mm beads were predetermined: a convenient sediment feed rate of 2.22 g/s required the flow rate of 0.0495 L/s. The packing of the 5 mm beads was 'haphazard' (Gray, 1968) as the beads were predominantly disordered, but with small locally ordered structures (Allen, 1982) occurring (see Figure 2.3). Consequently, the void spaces between the particles were of a variety of sizes and shapes (Allen, 1985). Due to the high slope of the flume, the submergence (flow depth: grain diameter) was relatively low, and the flow was supercritical and turbulent (see Table 2.1).

• Stage 2: The fine bead supply was introduced to the flume (either 0.7, 0.9, 1.5, 2, 3 or 4 mm in diameter) and the response of the channel was recorded using the camera.

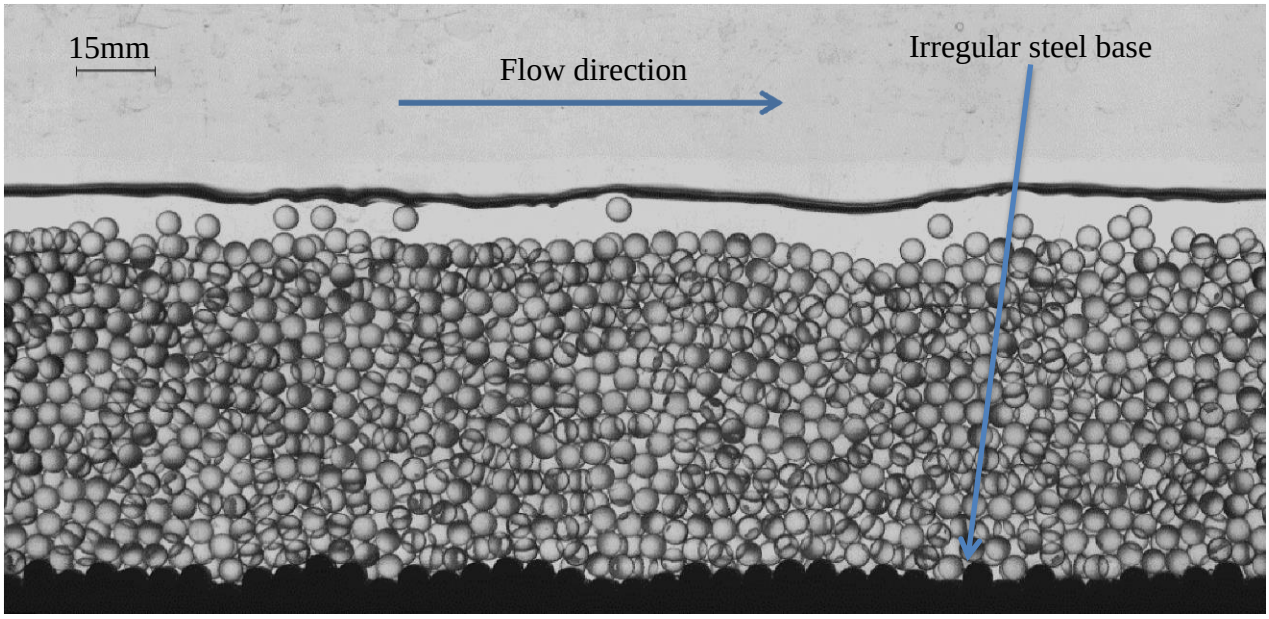

Figure 2.3 5 mm bed in one-size equilibrium.

Two sets of experiments were undertaken:

• Set 1 explored the influence of grain size ratio. During these experiments the fine sediment feed rate remained constant (at approximately 1.57 g/s), but the diameter of the fine sediment varied. The proportion (by feed rate) of fine sediment in the total feed was approximately 41%. A summary of these experiments is given in Table 2.2.

• Set 2 explores the influence of fine sediment feed rate using selected grain size ratios. The coarse feed rate and flow rate remaining the same as in Set 1. A summary of these experiments is given in Table 2.3.

Table 2.1 Experimental conditions for 5 mm one-size equilibrium*.

Flow rate (mL/s)	**5 mm feed rate (g/s)**	**Mean flow depth, *h* (mm)**	**Submergence ratio (h/D_c)**	**Side-wall corrected dimensionless shear stress**	**Mean velocity, *U* (m/s)**	**Froude number ($\frac{U}{\sqrt{gh}}$)**	**Reynolds Number ($\frac{4UR_h}{\nu}$)**	**Roughness Reynolds Number $\left(\frac{u_* D_c}{\nu}\right)$**	**Rouse Number $\left(\frac{w_s}{ku_*}\right)$**
49.5	2.22	8.02 ± 0.38	1.6 ± 0.18	0.076 ± 0.011	0.60 ± 0.03	2.14 ± 0.15	8420 ± 237	417 ± 25	16.3 ± 0.5

***Details of how the hydraulic parameters were calculated are given in Appendix B.**

Table 2.2 Summary of the experimental results: Set 1*.

Experimental Conditions				**Experimental Results**			
Experiment number	**Fine bead diameter D_f (mm)**	**Grain size ratio (D_c/D_f)**	**Fine bead feed rate (g/s)**	**Spontaneous Percolation**		**Kinetic Sieving**	**Bed slope response to fine input**
				Partially impeded static percolation	**Bridging**		
I.1	0.7	7.14	1.54	Yes	No	Yes	Degrade
I.2	0.9	5.56	1.54	Yes	No	Yes	Degrade
I.3	1.5	3.33	1.60	No	Yes	Yes	Degrade
I.4	2	2.5	1.57	No	Yes	Yes	Degrade
I.5	3	1.67	1.59	No	No	Yes	Aggrade
I.6	4	1.25	1.55	No	No	Yes	Aggrade

***Coarse bead diameter (*D*c): 5 mm; coarse bead feed rate: 2.22 g/s; flow rate: 0.0495 L/s; fine bead feed rate/total feed rate: ~41%**

Table 2.3 Summary of the experimental results: Set 2*.

Experimental Conditions					**Experimental Results**			
Experiment number	**Fine bead diameter D_f (mm)**	**Grain size ratio (D_c/D_f)**	**Fine bead feed rate (g/s)**	**Fine feed rate / Total feed rate (%)**	**Spontaneous Percolation**		**Kinetic Sieving**	**Bed slope response to fine input**
					Partially Impeded Static Percolation	**Bridging**		
I.7	0.7	7.14	0.64	22	Yes	No	Yes	Degrade
I.1	0.7	7.14	1.54	41	Yes	No	Yes	Degrade
I.8	0.7	7.14	4.82	68	Yes	No	Yes	Degrade
I.9	2	2.5	0.62	22	No	Yes	Yes	Degrade
I.4	2	2.5	1.57	41	No	Yes	Yes	Degrade
I.10	2	2.5	4.72	68	No	Yes	Yes	Aggrade

***Coarse bead diameter (D_c) 5 mm; coarse bead feed rate: 2.22 g/s; flow rate: 0.0495 L/s.**

The experiments were continued until, over five minutes, the sediment output rate for each size component was generally equal to the sediment input rate for that component: within ± 4 %, except for Experiment I.9 (5.5% difference for the coarse component and 6.5 % difference for the fine component) and Experiments I.1 and I.4 (5.8 % and 8.3 % differences for the fine components respectively). This was defined as the new equilibrium. Under two-size equilibrium conditions, the bed and water slopes were equal, but no longer parallel to the flume slope.

2.2.1 Supporting Information

The phenomena described in this chapter were identified from the experimental videos. Clips taken from these video recordings can be accessed at: http://hdl.handle.net/2429/54751

The details of these clips are reported in Appendix C.

2.3 Observations

2.3.1 Coarse Sediment Alone

In each experiment, before the fine sediment feed was introduced, a two-minute recording of the 5 mm beads in one-size equilibrium was taken. Figure 2.3 illustrates the characteristic bed structure (supporting video: Video_S1); the average local intergrain roughness is approximately $D_c/4$, and the longer wavelength bed undulations are on average approximately $0.8D_c$ in amplitude, and reach a maximum of approximately $1.3D_c$.

During 5 mm equilibrium, the bedload was formed predominantly of a single layer of beads saltating, but with occasional rolling beads (see Video_S1). The rolling beads remained in contact with the bed surface whilst moving downstream, whereas the saltating beads bounced consecutively over the bed surface, sometimes touching the water surface.

2.3.2 Experiments: Set 1

A summary of the experimental results is given in Table 2.2. Pairs of fines that displayed similar behavior are discussed together.

2.3.2.1 0.7 mm and 0.9 mm Fine Input: Partially Impeded Static Percolation

Infiltration Characteristics

Once the 0.7 mm feed was introduced, kinetic sieving took place in the bedload transport layer; consequently the layer was formed of mobile fine sediment at the bottom, upon which the 5 mm grains moved. Once at the base of the bedload layer, the 0.7 mm sediment then spontaneously percolated into the underlying quasi-static 5 mm bed, falling through the coarse framework to the base, filling the bed from the bottom upward (supporting video: Video_S2).

Figure 2.4a shows the bed after the 0.7 mm infiltration wave had passed through the camera visualization window. Whilst there are substantial areas of the bed that the fine sediment had infiltrated, there are also areas where there was no infiltration. The projected area of the bed within the camera visualization window that had been infiltrated purely due to spontaneous percolation was 77 % (see Table 2.4). According to Gibson et al. (2010), under 'unimpeded static percolation' the fine content over the depth should be relatively uniform. In this case, the fine content over the depth was not uniform, and therefore the infiltration profile cannot be classified as 'unimpeded static percolation'. In some locations, the infiltration profile contains the features of a 'bridging' profile, however, the infiltration into the bed is much deeper than that observed for typical 'bridging' (usually reported as 2.5 to 5 D_{90} in depth). Consequently, the infiltration profile formed under these circumstances is akin to the transitional profile observed

by Gibson et al. (2010); a profile that falls between the conditions for unimpeded static percolation and bridging. This profile will be termed ‘partially impeded static percolation’.

The 0.9 mm experiment exhibited behavior similar to the 0.7 mm case, but less infiltration into the bed occurred. Figure 2.4b (supporting video: Video_S3) shows the bed state after the 0.9 mm infiltration wave had passed through the camera visualization window. Due to spontaneous percolation alone, the projected area of infiltration within the camera visualization window was 27 % (see Table 2.4). The fine sediment penetrated to the base of the deposit in some locations, but a bridging profile occurred in others. The infiltration profile in this case will also be termed ‘partially impeded static percolation’.

Bed Response

Once the fine beads formed part of the bedload layer, the motion of the 5 mm beads changed. Under one-size conditions, the 5 mm beads mainly saltated along the bed surface. However, under two-size conditions, they mainly rolled over the bed surface, which was now covered in fine grains; saltation became far less frequent.

Almost immediately after the fine sediment became present on the bed surface, the bed began to degrade, indicating an increase in coarse sediment transport over the input rate, despite the addition of the fine sediment to the formerly equilibrium flow. During the degradation, the 5 mm beads on the surface of the underlying quasi-static coarse bed became mobilized and joined the bedload layer. Through examination of the experimental videos (supporting Video_S4 for the 0.7 mm experiment), it was observed that the mobilisation of a grain forming the quasi-static 5 mm bed was predominantly caused by collisions with another 5 mm grain rolling along the bed surface.

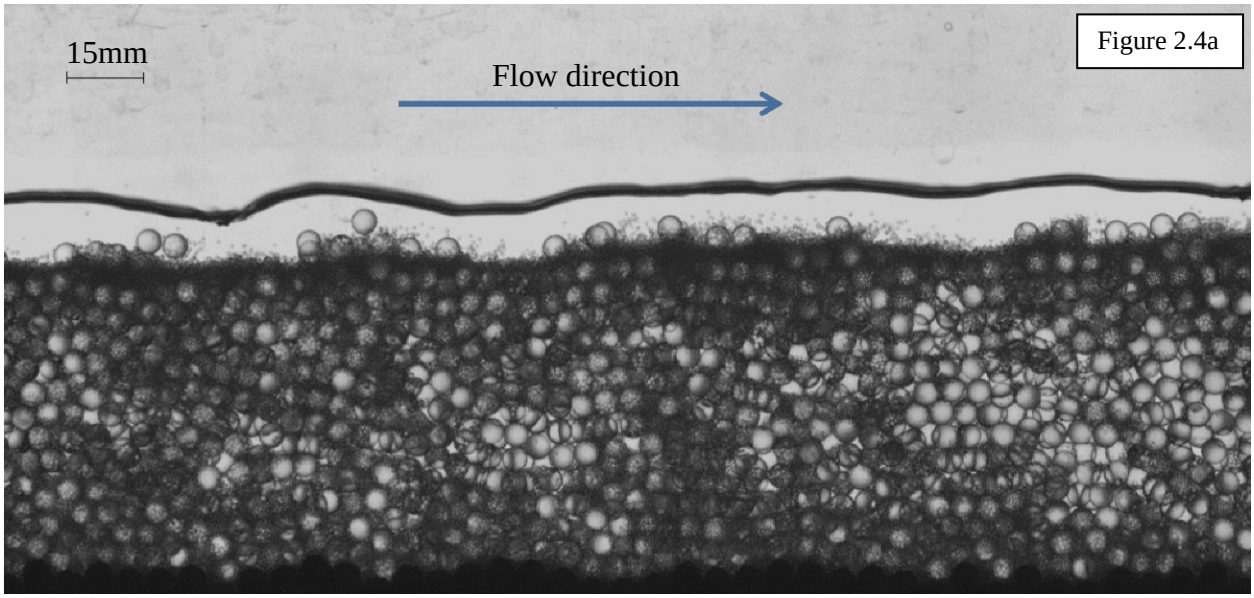

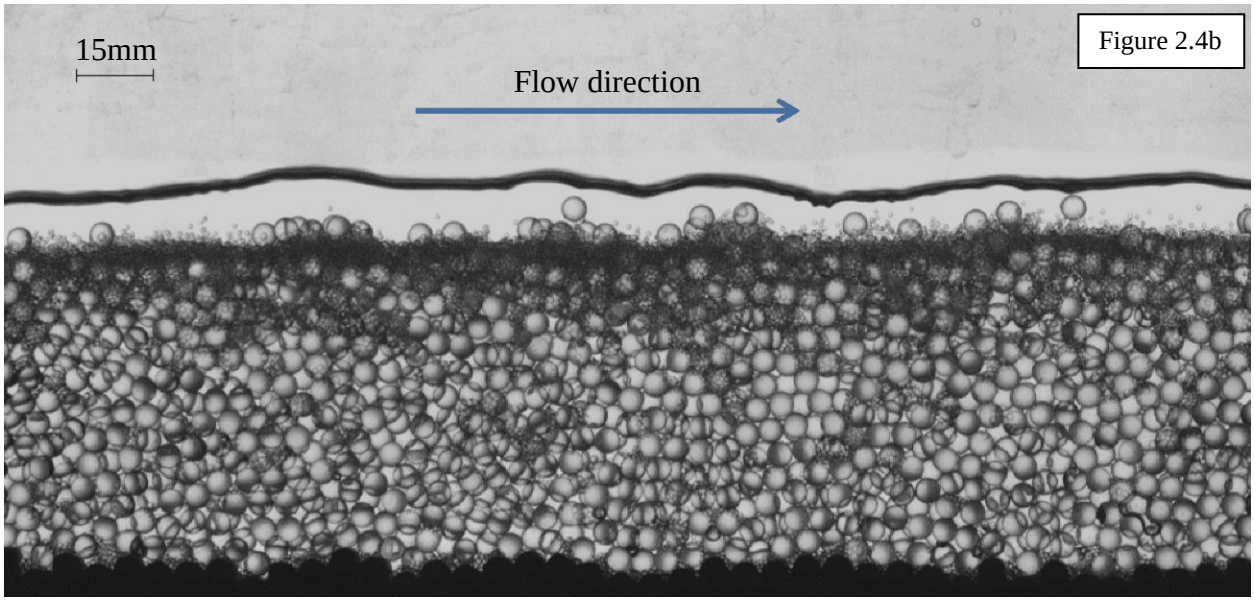

Figure 2.4 (a) Experiment I.1: 0.7 mm fines. Snapshot of the bed approximately 99 seconds after the fine sediment has been introduced, showing partially impeded static percolation. (b) Experiment I.2: 0.9 mm fines. Snapshot of the bed approximately 47 seconds after the fine sediment has been introduced, showing partially impeded static percolation.

Table 2.4 Percentage of the projected area within the camera visualization window of the 5 mm bed infiltrated by the fines due to spontaneous percolation*.

Experiment number	Fine bead size	Percentage of the bed infiltrated due to spontaneous percolation
I.1	0.7mm	77
I.2	0.9mm	27
I.3	1.5mm	6
I.4	2mm	4
I.5	3mm	0
I.6	4mm	0

*** The measurements were taken immediately after the initial wave of fine sediment had passed through the entire length of the visualization window.**

When a framework grain on the bed surface was nudged (pushed slightly) by a rolling 5 mm grain, fine beads moved into the space created, as also observed by Allan and Frostick (1999). If the coarse grain became entrained, the fine sediment filled the gap left behind. If this coarse grain movement revealed previously blocked void spaces, further spontaneous percolation into the quasi-static bed occurred.

Once a 5 mm grain was mobilized, it moved into the bedload layer, rising to the surface due to kinetic sieving. Once the 5 mm bead was entrained, it continued to move, leaving the camera visualization window (a process known as 'overpassing' (Allen, 1983)). This was due to the fine sediment filling the interstices (dips) in the bed surface, resulting in a smoother profile, and the removal of deposition opportunities. The entrainment of the pre-existing 5 mm bed

which, once in motion left the channel due to a lack of deposition locations, caused the bed degradation.

Eventually the bed reached a new equilibrium state, with a reduced slope, whereby the input rate was equal to the output rate for each size component. When the bed reached two-size equilibrium, the fine sediment layer on the bed surface was thicker than during the slope evolution (supporting video: Video_S5). This thicker fine sediment layer was formed of both a moving bedload section on top and a quasi-static section underneath, isolating the coarse bed beneath.

2.3.2.2 1.5 mm and 2 mm Fine Infiltration: Bridging

Infiltration Characteristics

Both 1.5 mm and 2 mm beads spontaneously percolated into the quasi-static bed below the moving bedload layer (see supporting videos: Video_S6 and Video_S7 respectively). In these experiments, the infiltration occurred only to a depth of several grain diameters within the quasi-static deposit; 'bridging' occurred. Figure 2.5a shows the depth of infiltration into the bed, at 2.3 mm intervals along the x-axis of the camera visualization window, in the 2 mm experiment.

Figure 2.5b shows a cumulative distribution of the depth of infiltration in the 2 mm case from Figure 2.5a; in some locations the depth of infiltration was very low (to $1D_c$); sometimes it was around $2 – 3D_c$ and, very occasionally, as deep as $3.75D_c$. In the 2 mm experiment, the projected area of infiltration due to spontaneous percolation alone was 4 % (see Table 2.4). In the 1.5 mm case more infiltration occurred, and to a greater depth, but still a bridging profile was formed. In this case, the projected area within the camera visualization window infiltrated purely due to spontaneous percolation was 6 %.

Bed Response

Following 1.5 mm and 2 mm inputs, the bed degraded in a manner similar to the experiments with the 0.7 mm and 0.9 mm fines. As the 5 mm grains were mobilized from the bed surface, kinetic sieving took place and additional fine sediment infiltrated into the underlying quasi-static bed due to spontaneous percolation. Consequently, during bed degradation there was always a fine sediment bridge layer present in the quasi-static deposit (supporting video: Video_S8 of the 2 mm experiment).

From close observation of the videos, one can observe that the additional spontaneous percolation did not always take place at the moment when the 5 mm grain became entrained, but rather just beforehand due to the 5 mm grain first being nudged by a grain in motion. Consequently, when the 5 mm framework grain came to move, it was already 'cushioned on' fine sediment. The movement of the fines into this space meant that the coarse grain was unable to return to its original location; instead it rested on the newly located fines, at a higher elevation. This action increased the projection of the coarse grain into the flow, reduced the pivoting angle and therefore enhanced the probability of entrainment.

It was noted in the 0.7 and 0.9 mm experiments that the fine sediment surface caused the 5 mm bedload grains to roll, as opposed to mainly saltate as in the 5 mm one-size case. In the 1.5 and 2 mm cases also, rolling was observed. However, in these cases the rolling was less smooth than in the 0.7 and 0.9 mm cases, and included hops of low amplitude.

In a manner similar to the 0.7 and 0.9 mm cases, the fine sediment layer thickness at the bed surface increased when the bed reached two-size equilibrium, comprising both a section in motion and an underlying quasi-static section.

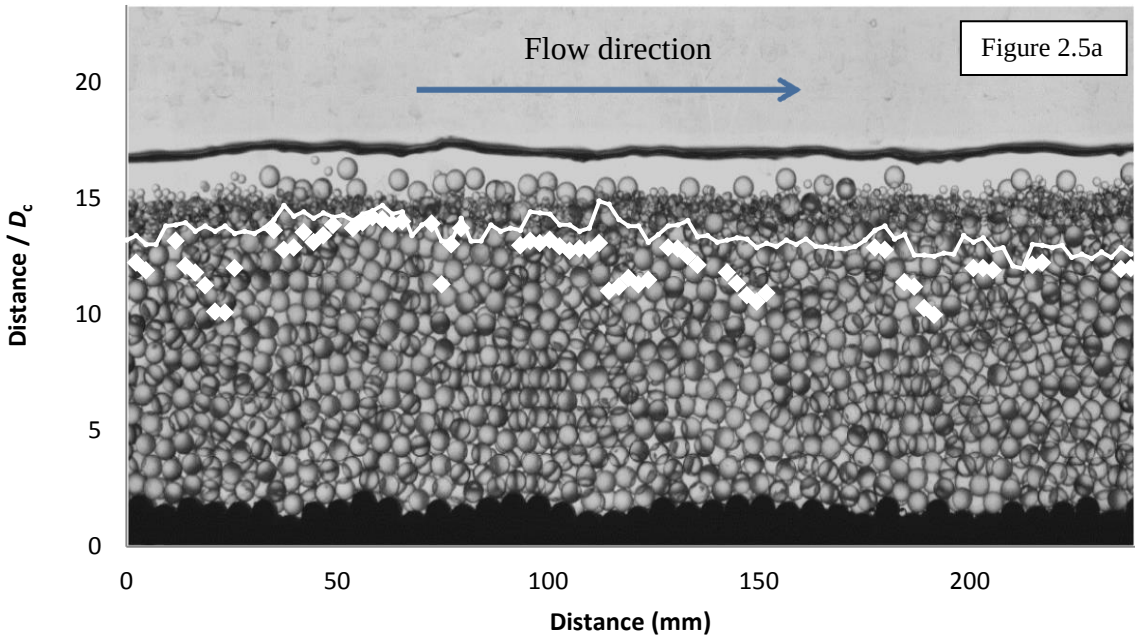

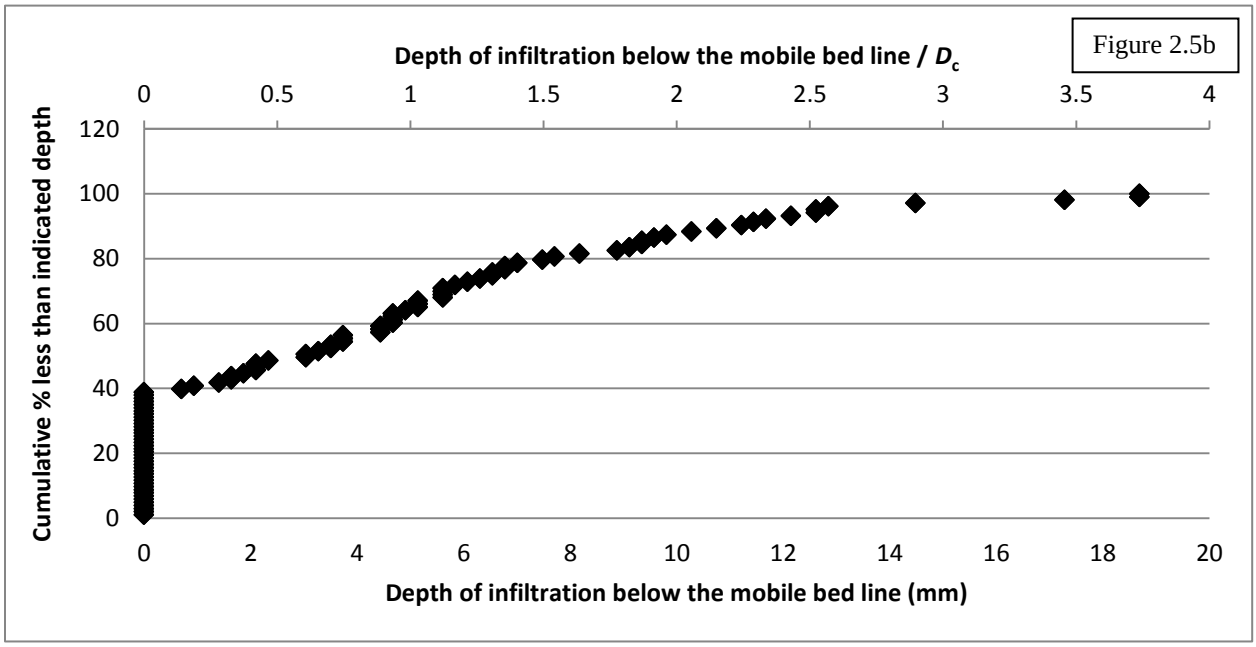

Figure 2.5 (a) Experiment I.4: 2mm fines. Snapshot of the bed approximately 27 seconds after the fine feed has been introduced. The solid white line shows the boundary between the bedload layer and the quasi-static bed. The white diamonds show the maximum depth of 2mm infiltration into the bed due to spontaneous percolation at 2.3 mm intervals across the horizontal axis. (b) Cumulative distribution of the infiltration depths due to spontaneous percolation presented in Figure 2.5a.

2.3.2.3 3 mm and 4 mm Fine Infiltration: No Spontaneous Percolation

Infiltration Characteristics

When the fine sediment feed was turned on, the first grains to enter the visualization window generally fell into gaps in the bed surface, where they became sheltered from the flow, and remained; they were not re-entrained. There was no fine sediment infiltration below the bed surface into the quasi-static deposit; spontaneous percolation did not occur (supporting video: Video_S9). As the dips in the bed surface were filled, a fine sediment quasi-static layer on the bed surface began to form and then thicken. The bedload layer, above, was composed of both 5 mm and fine beads, with the finer grains falling to the base of the bedload layer due to kinetic sieving.

Bed Response

To enable the transport of the larger supply, the bed aggraded to increase the slope through the formation of a quasi-static 3 mm layer upon the bed surface. Once the quasi-static fine sediment layer had been created, the pre-existing 5 mm framework below became isolated from the transport process and did not move again. Consequently, the bed structure became very distinct; the bottom layer was the pre-existing 5 mm bed, overtop was the deposited, quasi-static 3 mm grains, then on the surface was the moving bedload layer with the 3 mm grains on the bottom and the 5 mm grains on the surface. The structure of the sediment bed, once the channel had reached two-size equilibrium, is shown in Figure 2.6 (supporting video: Video_S10). The resulting bed structure in the 4 mm fine case was the same except that the deposited 4 mm layer was thicker than that in the 3 mm case.

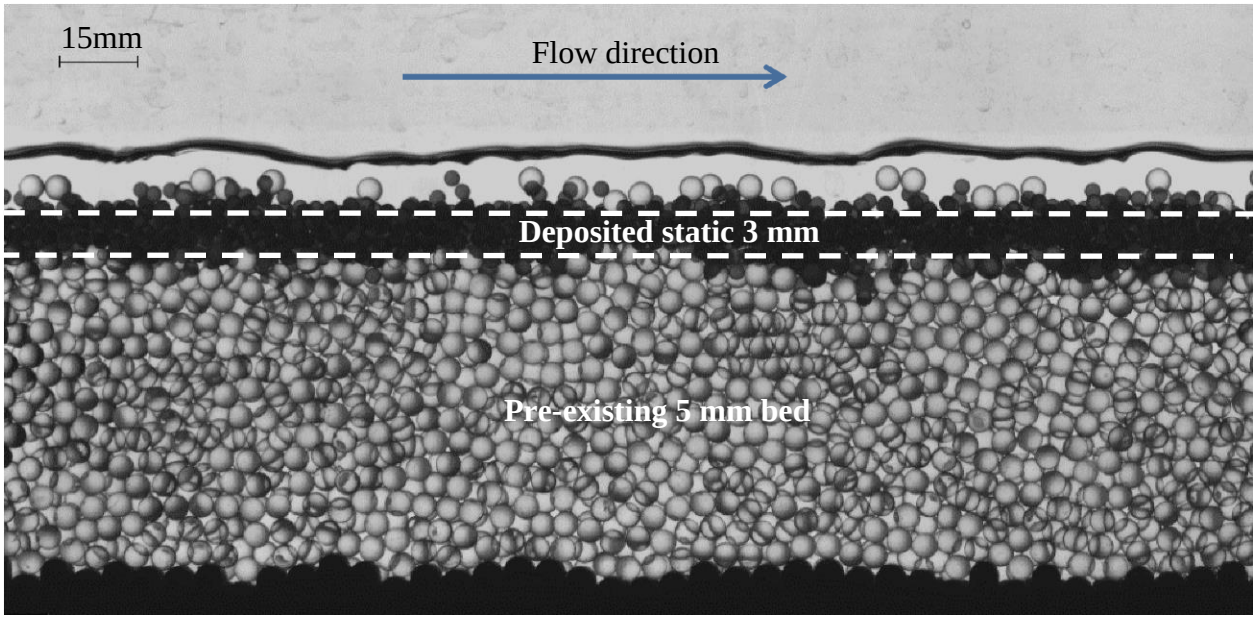

Figure 2.6 Experiment I.5: 3 mm fines. Snapshot of the bed approximately 18.5 minutes after the fine sediment has been introduced. Bed is in two-size equilibrium.

2.3.3 Experiments: Set 2

The aim for the second set of experiments was to explore the influence of the fine sediment feed rate upon the infiltration behaviour and channel response. Experiments were undertaken using the 0.7 mm and 2 mm diameter beads as this permitted further examination of both the partially impeded static percolation and the bridging behaviour. The fine sediment feed rates tested were both lower and higher than the rate used in Set 1, whilst the coarse sediment feed rate remained the same. A summary of the experimental results is given in Table 2.3.

2.3.3.1 0.7 mm Fine Input

In the 0.7 mm experiments, the same infiltration characteristics were observed as in the first set of experiments, as was the channel response. However, differences in the grain behavior were apparent.

A striking characteristic that differentiated the experiments with varying fine sediment feed rates was the number density of 5 mm particles moving over the bed surface. Figures 2.7a and 2.7b show the camera visualization window when the initial fine sediment wave had just passed through, with fine sediment feed rates of 0.64 g/s (Experiment I.7) and 4.82 g/s (Experiment I.8) respectively. The number density of moving coarse grains on the bed surface was much greater when the fine sediment feed rate was lower, and decreased at higher fine sediment feed rates; compare Figure 2.7a with Figure 2.7b. This characteristic persisted, even when the bed reached two-size equilibrium; Figure 2.7c shows the number of 5 mm bedload grains on the bed surface within the camera visualization window at 5 second intervals, over 300 seconds when the channel was in two-size equilibrium for Experiments I.7 and I.8. As the coarse sediment transport rate was the same in all of the experiments, this indicates that the velocity of coarse grains is related to the fine sediment feed rate. In Experiment I.7, when the fine sediment feed rate was relatively low, the coarse bedload was formed of long, slow-moving trains of grains rolling along the surface, or as saltating grains (supporting video: Video_S11 of the bed in two-size equilibrium). However, in Experiment I.8 (high fine sediment feed rate), the coarse sediment bedload was formed of individual grains quickly moving along the bed surface (supporting video: Video_S12 of the bed in two-size equilibrium). A difference in the vertical profile was also noted between Experiments I.7 and I.8. In Experiment I.8 there was a 4.7 ± 1.8 mm thick fine layer (including both the moving and the quasi-static fine sections) above the

quasi-static 5 mm framework bed when the bed was in two-size equilibrium whereas, in Experiment I.7, the layer was 1.4 ± 0.9 mm thick.

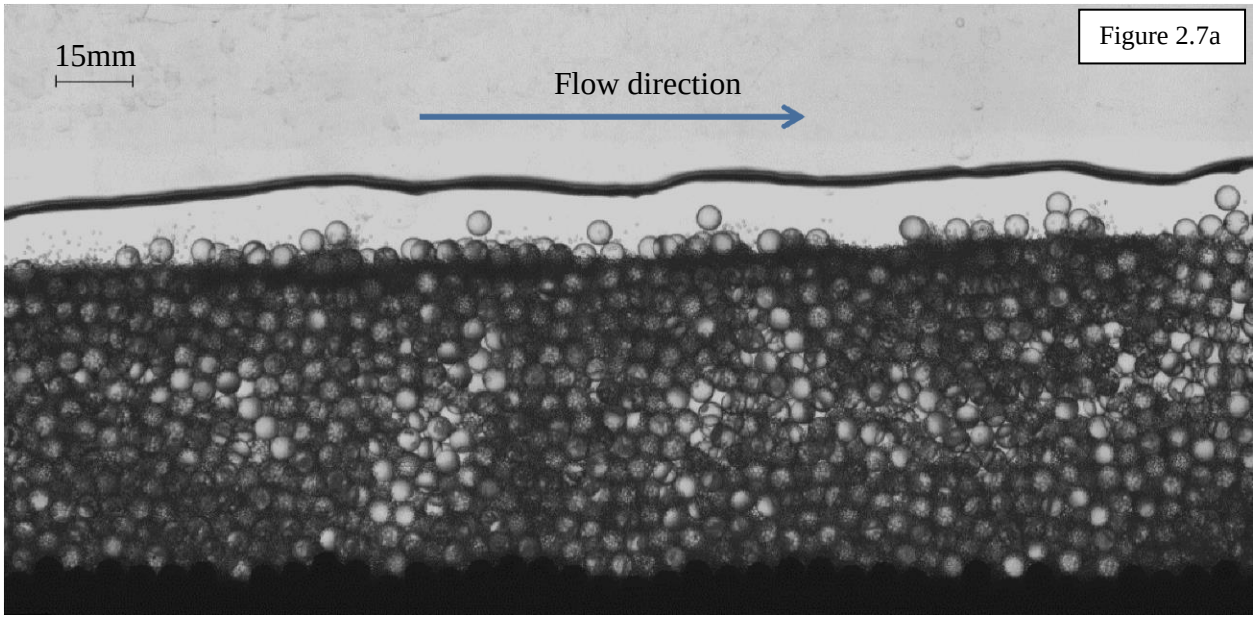

Figure 2.7a

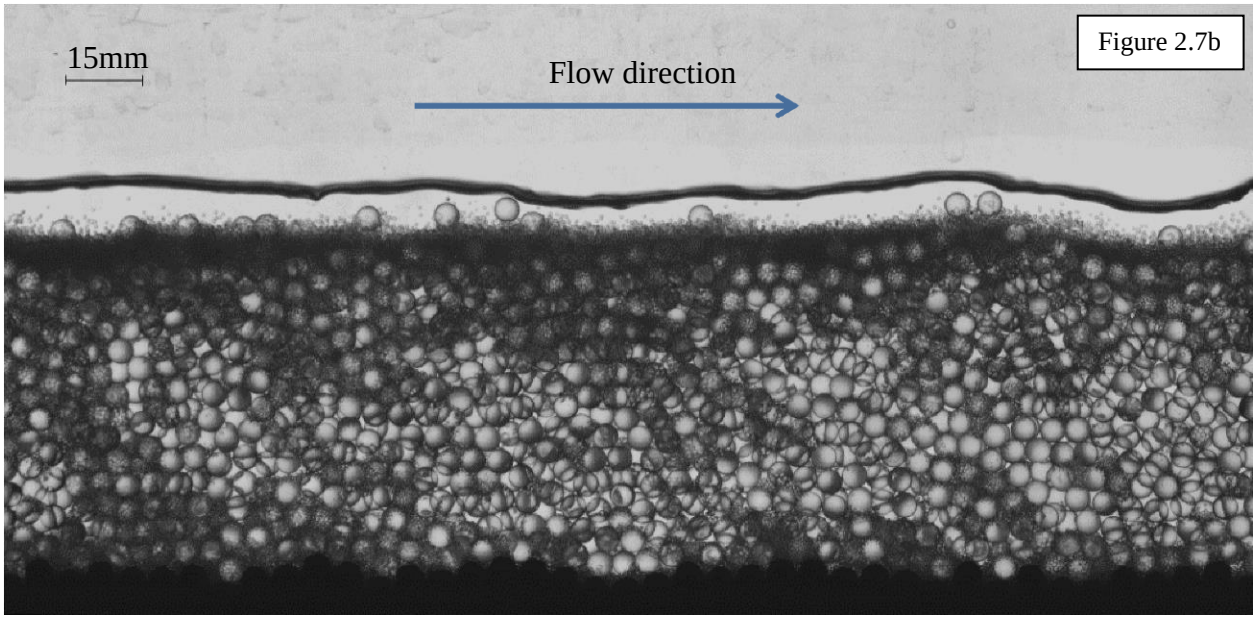

Figure 2.7b

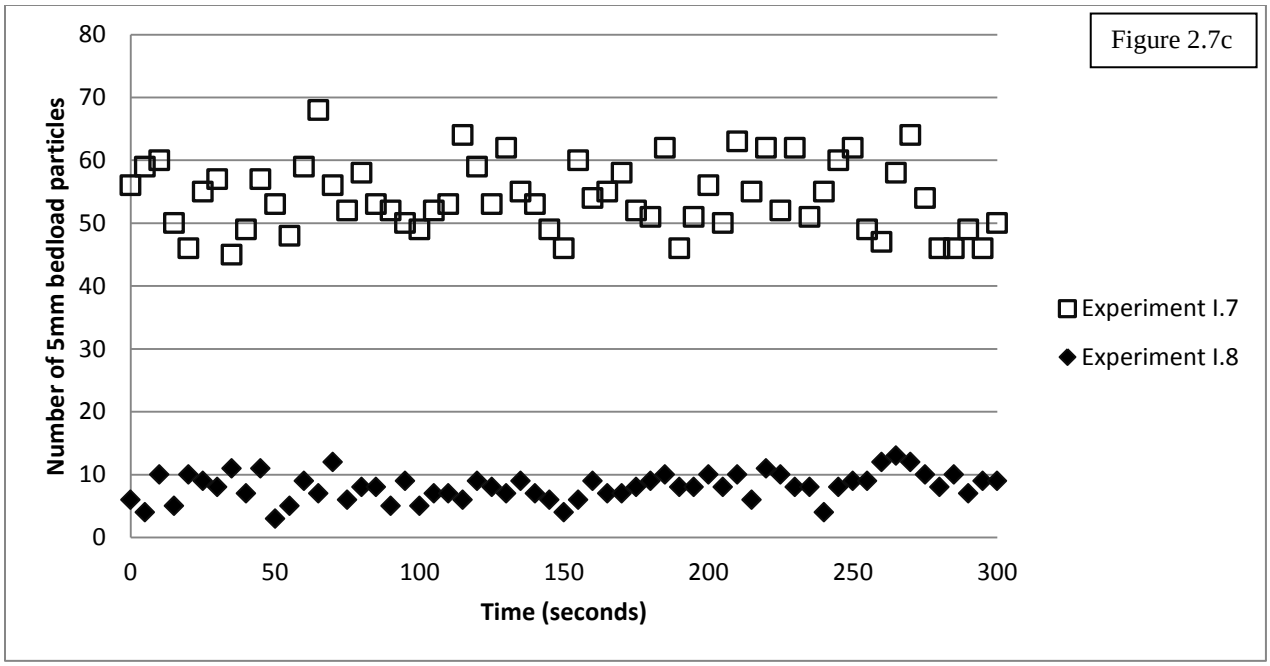

Figure 2.7 (a) Experiment I.7: 0.7 mm fines at 0.64 g/s. Snapshot of the bed approximately 227 seconds after the fine sediment has been introduced. (b) Experiment I.8: 0.7 mm fines at 4.82 g/s. Snapshot of the bed approximately 26 seconds after the fine sediment has been introduced. (c) Number of 5 mm bedload particles within the camera visualization window for Experiment I.7 and Experiment I.8 whilst the bed was in two-size equilibrium.

In all of the experiments with the 0.7 mm fine sediment, the channel degraded in response to the fine sediment input. For Experiment I.7 (0.64 g/s) and Experiment I.1 (1.54 g/s), the slope of the bed in two-size equilibrium was very similar (7.0±0.24 % and 7.4±0.41 %, respectively). However, in Experiment I.8 (4.82 g/s), the slope of the bed in two-size equilibrium was higher (9.2±0.11 %). Shortly after the bed started to degrade in Experiment I.8, the fine sediment layer on the bed surface was observed to thicken, inhibiting interaction between the bedload layer and underlying bed. Beyond this point the coarse sediment transported through the flume was equal to the coarse sediment supplied and no further degradation took place.

2.3.3.2 2 mm Fine Input

In the 2 mm experiments, the same infiltration profiles were formed as in the 2 mm experiment in 'Set 1', but in Experiment I.10 the bed response was different. In all of the experiments with the exception of Experiment I.10, when spontaneous percolation occurred, the channel response was degradation. In Experiment I.10 the channel aggraded (see Figure 2.8). The 2 mm sediment 'flooded' the bed surface very quickly (supporting video: Video_S13), covering the pre-existing 5 mm bed, isolating it from the bedload layer, consequently inhibiting any degradation. This layer then thickened, causing aggradation, until the channel reached two-size equilibrium.

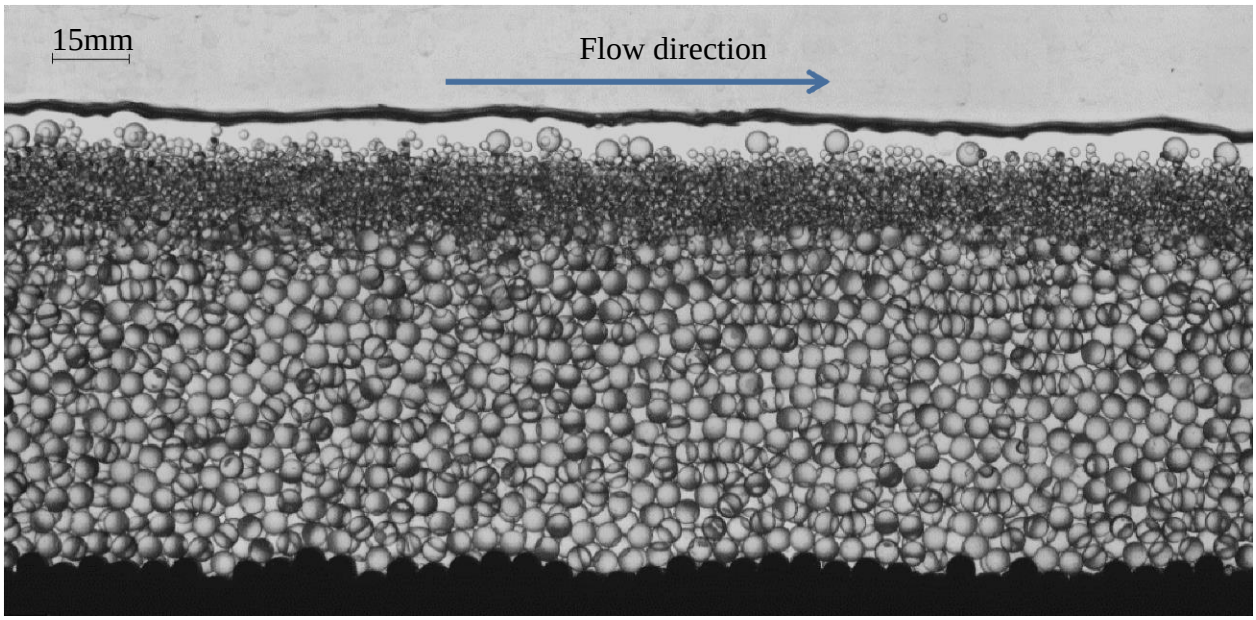

Figure 2.8 Experiment I.10: 2 mm fines at 4.72 g/s. Snapshot of the bed approximately 15 minutes after the fine sediment has been introduced.

The same inverse relation between mobile coarse sediment number density on the bed surface and fine sediment feed rate was observed with the 2 mm fine experiments as in the 0.7 mm fine experiments.

2.4 Discussion

A summary of the grain sorting behavior exhibited in the experiments is given in Figure 2.9.

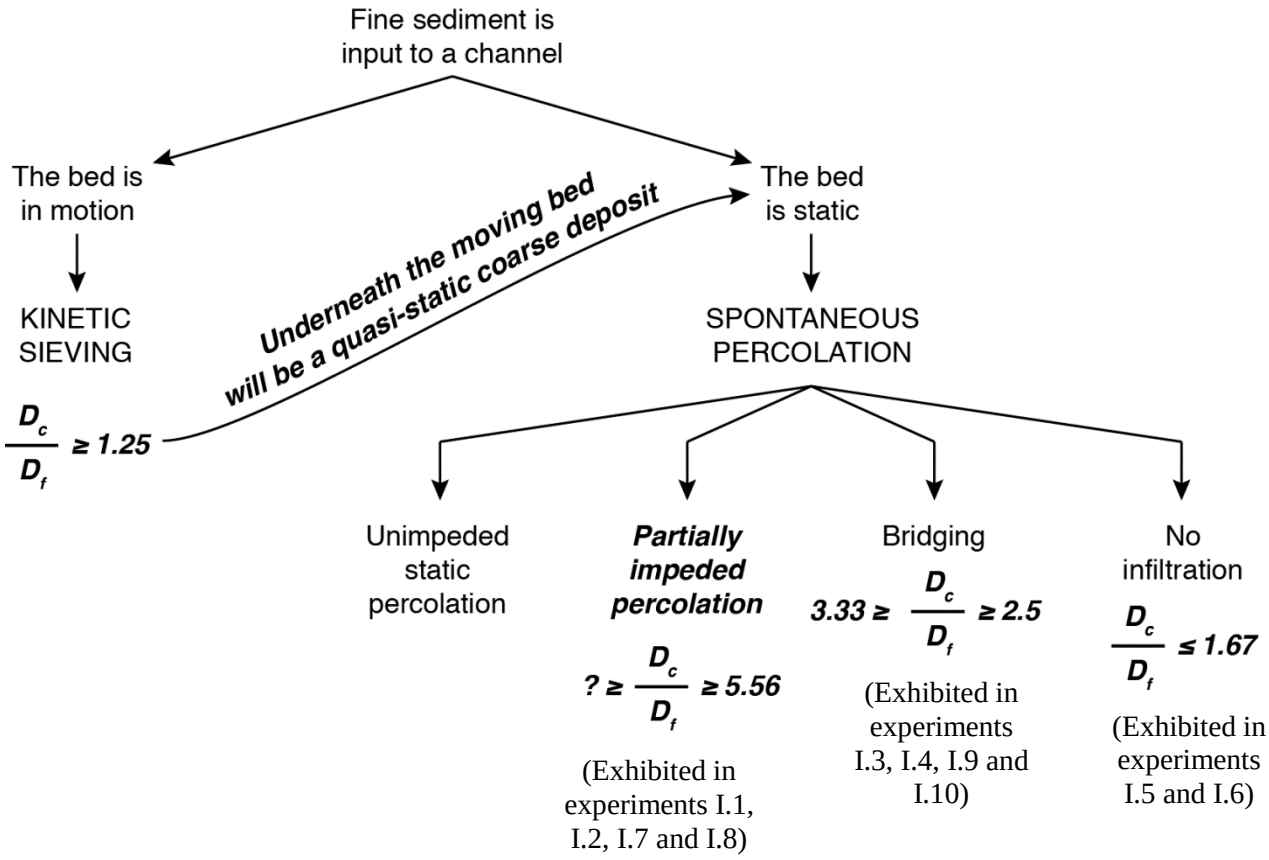

Figure 2.9 Flow chart for the grain sorting processes exhibited during the experiments*.

***Limits shown are specific to these experiments. The non-bold text indicates the state of knowledge before this research. The bold text shows the knowledge gained from this research. When the bed surface is in motion, kinetic sieving will occur within the mobile layer. Underneath this moving layer will be a quasi-static coarse deposit, into which the fines may infiltrate by spontaneous percolation if the geometry permits. The upper limit for partially impeded percolation is unknown, and shown with a question mark.**

Consistent with previous work (Beschta and Jackson, 1979; Frostick et al., 1984; Diplas and Parker, 1992; Gibson et al., 2009), increasing amounts of spontaneous percolation occurred at increasing grain size ratios. Additionally, the control of grain size ratio upon the vertical infiltration profile formed was exhibited (as documented in Sakthivadivel and Einstein, 1970; Gibson et al., 2009; Gibson et al., 2010). However, the limits on the spontaneous percolation behavior presented in Figure 2.9 differ from those documented in previous literature, presented in Table 1.1.

This difference is likely due to differences in material properties and experimental conditions. The Gibson et al. (2009; 2010) experiments used natural materials with wider grain size distributions. When fines are infiltrating into a coarse deposit, the amount of infiltration depends upon the void spaces available and the ability of the fines to fit into these void spaces. In comparison with our experiments, using spherical glass beads with narrow size distributions and haphazard (Gray, 1968) packing of the framework grains, experiments using natural materials, which have a variety of shapes, and also wider grain size distributions, will vary the size of the voids available and will also change how the fines fit into these spaces, causing different behaviors to emerge at given grain size ratios. Sakthivadivel and Einstein (1970) used spheres for the coarse component in their experiments, but used irregularly shaped crushed ‘styron’ for the fine component. Additionally, the coarse particles were regularly arranged in a vertical column with the minimum possible void spacing. Consequently, the amount of void space will have been smaller than in our experiments, leading to the larger size ratios than we observed for bridging behavior and non-infiltration. The quantitative ratios expressing the limits in behaviour for all of the experiments depend on the particular grain sizes used and the coarse fraction packing achieved: they are by no means universal numbers.

Set 1:

The purpose of 'Set 1' was to explore the role of grain size ratio at a fixed sediment feed rate. The diameter of the coarse grains was consistently 5 mm, and the diameter of the fine grains varied between 0.7 and 4 mm. The varying diameter of the fine grains means that each grain size ratio will result in a different bed roughness, and this will have an influence upon the channel response to the fine grain input. However, during these experiments, a link was also observed between the infiltration behavior and the channel response. In the experiments when spontaneous percolation was geometrically feasible ($D_c/D_f \geq 2.5$), degradation occurred in response to the fine grain input. Our step-by-step understanding of the process under these circumstances is as follows:

- The fine beads are introduced to the channel and move to the bottom of the bedload transport layer due to kinetic sieving.
- Once at the base of the bedload transport layer, the fines reach the interface with the underlying quasi-static coarse bed.
- Spontaneous percolation of the fines into the quasi-static coarse bed occurs to the extent permitted by the geometry and the amount of remaining void space. The depth of spontaneous percolation for a given grain size ratio varies due to the haphazard packing arrangement of the 5 mm beads forming the bed, creating variable void spacing.
- Once the infiltration capacity of the bed has been reached, the fines begin to appear in the bed surface layer. This behavior was also observed by Diplas and Parker (1992).
- The fine sediment begins to surround the coarse grains forming the bed surface.
- The fines fill the dips and gaps in the bed surface, removing potential deposition locations. Consequently, once a grain is entrained it does not come to rest again.

- A 5 mm framework grain is nudged by a 5 mm grain in motion, and fines fall into the space which was previously occupied. The movement of fines into this space means that the 5 mm grain will now rest at a higher elevation on the fines, consequently enhancing its projection above the bed and exposure to the flow, therefore increasing the probability of entrainment. The requirement of projection and exposure of a grain for entrainment has been previously documented (Fenton and Abbott, 1977; Kirchner et al., 1990). Additionally, when the movement of the coarse framework grain results in the opening of a previously blocked, uninfiltrated void space, additional fine sediment will infiltrate into the quasi-static bed. It was observed that the additional spontaneous percolation did not always take place at the moment when the 5 mm grain became entrained, but rather just beforehand. Our observations lead us to believe that rocking (or vibration) of the coarse grain before it was entrained (a phenomenon observed by Schumm and Stevens (1973) and Carling et al. (1992)), mainly due to impacts from coarse grains in motion, allowed the fine sediment to move into the space created and infiltrate into the quasi-static bed.
- When a 5 mm grain is entrained, the fines will ultimately fill the space left behind on the bed surface.
- This process continues until the channel reaches two-size equilibrium. The slope of the bed at two-size equilibrium is that which is sufficient to transport the coarse and fine components of the supply. It was observed that, when the bed reaches two-size equilibrium, the bedload transport layer is no longer in contact with the quasi-static coarse sediment bed; a layer of quasi-static fine sediment exists between the two. Hence, the lowermost bed formed of quasi-static 5 mm grains is isolated from the transport process as there is no longer any interaction between these grains and the bedload. From this point onwards, the 5 mm transport is equal to the supply.

In the experiments when $D_c/D_f \leq 1.67$ the fine sediment is geometrically unable to infiltrate into the underlying quasi-static coarse bed. The fine sediment creates a quasi-static layer above the coarse bed, immediately isolating the underlying bed from the transport process and preventing degradation from occurring. This quasi-static fine layer thickens, and the channel aggrades, increasing its slope, until the flow is sufficient to transport the added finer load.

In all of the experiments, the fine grain feed rate was consistent, hence the total supply was consistent. Yet, the infiltration of the fine grains into the quasi-static coarse bed through spontaneous percolation when the $D_c/D_f \geq 2.5$ will also result in a smaller increase in load for the flow to transport compared to when the fines are geometrically unable to spontaneously percolate. As the flow will have a given transport capacity, this difference in sediment load due to the varying infiltration characteristics will play a role in the bed response.

Set 2:

A link is observed between the fine sediment feed rate and the motion of the 5 mm grains on the bed surface. At a higher fine sediment feed rate, the number density of the moving coarse grains on the bed surface is lower, and the velocity higher (Figure 2.7c). At the higher fine sediment feed rates, a thick fine sediment layer exists between the bedload layer and the quasi-static 5 mm bed, whereas for the lower fine sediment feed rates, this layer is much thinner. At the higher fine sediment feed rates, the bedload moves upon this thicker fine sediment layer which reduces the surface roughness and enhances the projection of the coarse grains into the flow, enabling the higher bedload velocity and lower number density. At the lower fine sediment feed rates, the bed surface is much rougher, which may cause the grains to stall, resulting in the slow movement and clustering of the bedload particles. This relation between fine feed rate and bedload density was

also observed experimentally by Iseya and Ikeda (1987); when there was an abundance of fines on the bed surface, the coarse particles were transported rapidly, which they termed a 'smooth' bed state. In contrast, in conditions of low fine sediment content, there was a high number density of coarse particles, moving slowly, which they termed a 'congested' bed state.

As with the first set of experiments, a control of the channel response to a fine sediment input was observed to be the behavior at the interface between the bedload transport layer and the quasi-static coarse bed. In the 2 mm experiments, when the fine sediment feed rate is 0.62 and 1.57 g/s the channel responds by degrading, yet when the fine sediment feed rate is increased to 4.72 g/s, the channel aggrades. In the latter case the total supply is much higher, and a fine sediment layer on the bed surface is created and thickens almost immediately after the input, creating a quasi-static layer of fines between the bedload transport layer and the 5 mm bed, therefore isolating the 5 mm bed and preventing the channel from degrading. During the 0.7 mm experiments with the highest fine sediment feed rate (4.82 g/s), the channel was observed to degrade by a smaller amount than in 0.7 mm experiments with lower fine sediment feed rates. The reduced degradation in the 4.82 g/s experiment is also attributed to the creation of a thick, fine, quasi-static surface layer. At the highest fine sediment feed rate, our observations lead us to believe that the channel degrades in the 0.7 mm case, but not in the 2 mm case because the 0.7 mm sediment infiltrates deeper into the 5 mm bed, 'consuming' the initial influx of fine sediment, consequently, the channel is able to degrade before the fine sediment layer builds. The limited infiltration of the 2 mm fines means that this does not occur with the larger fine fraction. Consequently, the grain size ratio is observed to have an important control over the channel response to a fine grain input.

2.5 Conclusion

This chapter has employed phenomenological descriptions to diagnose the critical processes exhibited during vertical sediment sorting due to both kinetic sieving and spontaneous percolation following a fine grain input to a coarser mobile bed, and has described the corresponding channel response. Specific attention has been given to how these processes are modified as the grain size ratio between the sediment forming the bed and the fine sediment input changes.

It is known that varying the grain size ratio and the feed rate of the fines will result in varying bed roughness and transport rates, influencing the channel response. However, during these experiments, a physical control of the channel response to a fine grain input was observed at the boundary between the bedload transport layer and the quasi-static coarse bed. The first set of experiments varied the grain size ratio between the fine sediment input and the coarse sediment bed. Once the fine sediment has moved to the base of the bedload transport layer, through kinetic sieving, it is capable of infiltrating into the quasi-static coarse deposit when $D_c/D_f \geq 2.5$. Under these conditions, the channel responds to the fine sediment input by degrading, despite the addition of fine sediment contributing an increase in the total sediment supply. If $D_c/D_f \leq 1.67$, then the fine sediment is unable to infiltrate into the quasi-static coarse bed beneath the bedload transport layer. The fine sediment then forms a quasi-static layer underneath the bedload transport layer, which thickens, leading to channel aggradation.

An additional set of experiments was performed to elucidate the influence of the fine sediment feed rate upon the results. These experiments reveal that the channel does not always degrade following a fine sediment input capable of infiltrating into the bed through spontaneous percolation but rather, the bed response is controlled by the vertical profile at the interface

between the bedload and the quasi-static bed. At high fine sediment feed rates, the surface of the bed is very quickly overwhelmed by the fine sediment input. The maximum amount of fine sediment capable of infiltrating is soon reached, and additional fine sediment arriving causes the formation of a quasi-static fine sediment layer underneath the bedload transport layer, isolating the underlying bed from the transport process. The rate at which this occurs depends upon the grain size ratio.

Chapter 3: Introducing finer grains into bedload: the transition to a new equilibrium

The purpose of this chapter is to quantitatively analyse the channel response of the experiments presented in Chapter 2, along with additional experiments, which were also undertaken with two-size mixtures of spherical glass beads. This chapter investigates the transition from initial to final transport equilibrium with a variety of fine feed proportions (fine feed / total feed) and over a range of grain size ratios (D_c/D_f). This is achieved through examination of the adjustment in bed slope following a fine grain input. Further analysis will be presented in the form of the rate of sediment output from the channel, the characteristics of the bedload movement and the vertical bed composition.

3.1 Experimental Arrangement

The experimental arrangement was the same as in Chapter 2.

3.2 Experimental Procedure

In order to explore the question of how the proportion of fines within a sediment feed influences grain mobility, two types of sediment-feed experiments have previously been undertaken. The first type, utilised by Ikeda and Iseya (1988; chapters 3 and 6), involves fixing the total feed rate, and varying both the fine and coarse feed rates. The second type involves fixing the coarse feed rate, and varying both the fine and total feed rate (e.g. Jackson and Beschta, 1984; Iseya and Ikeda, 1987; Ikeda and Iseya, 1988 (chapter 4); Curran and Wilcock, 2005b). The experiments

presented in this chapter were undertaken using the second approach for two reasons. First, from a scientific perspective, by fixing the coarse feed rate, the flow rate required for one-size equilibrium of the coarse-grain bed, which is the initial condition in these experiments, is constant. Second, from an applied perspective, this approach allows us to explore how the response of a channel varies if a source of fine sediment is introduced, depending upon the rate and grain size of the input.

As with the experiments in Chapter 2, a consistent procedure, with two stages, was followed for each experiment. (1) One-size equilibrium was achieved with the 5 mm grains only. An example frame from the camera visualisation window of the bed in one-size equilibrium is shown in Figure 3.1a. One-size equilibrium was achieved when the sediment input rate equaled the sediment output rate and the bed and water slope matched the flume slope. The 5 mm feed rate and the flow rate remained constant throughout the experiment (details are given in Table 2.1). (2) Fines of a fixed diameter and a fixed feed rate were introduced into the channel (see Table 3.1 for details). The bed response to the fine grain input was filmed using the high-speed camera.

Nineteen experiments were undertaken in two sets:

- Set 1: A variety of grain size ratios were tested (D_c/D_f from 7.14 to 1.25), the bed response was examined at three different fine feed proportions (fine feed/total feed): approximately 22, 41 and 68 %. A summary of these experiments is given in Table 3.1: Set 1. Experiments with 3 mm and 4 mm fine components at approximately 68 % were not feasible as the flow rate was not sufficient to transport the load.

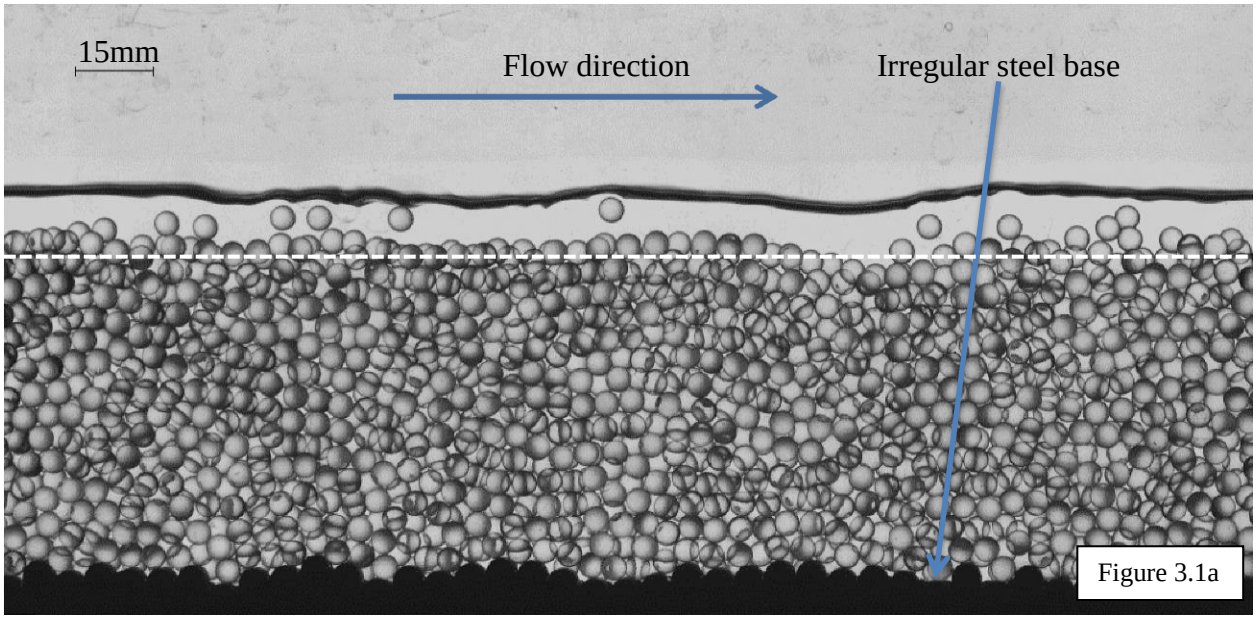

Figure 3.1a

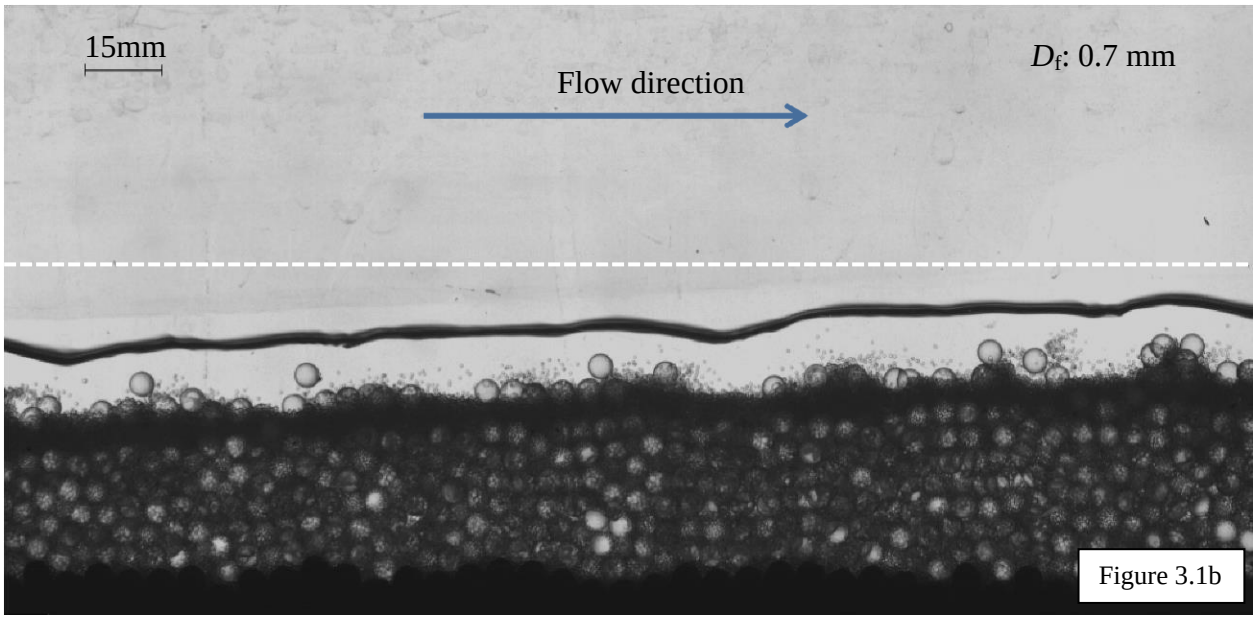

Figure 3.1b

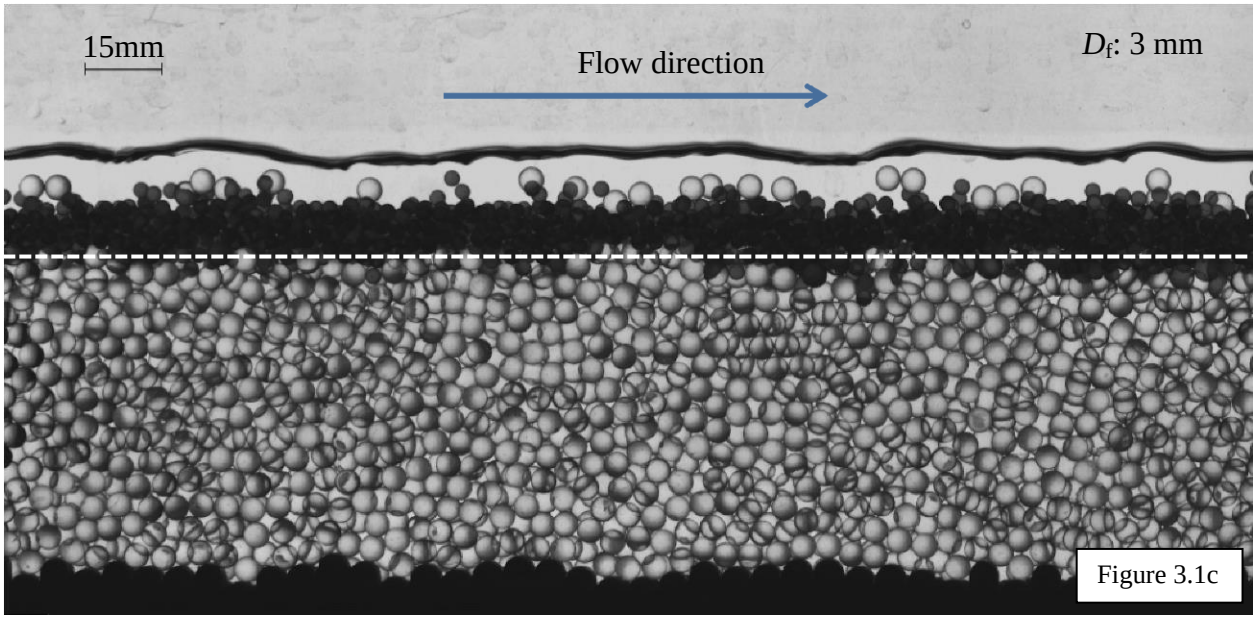

Figure 3.1 (a) Example frame from the camera visualisation window of the bed: in one-size equilibrium (b) Experiment I.1: The bed in two-size equilibrium. (c) Experiment I.5: The bed in two-size equilibrium. The white dashed line consistently shows the height of the bed in one-size equilibrium from Figure 3.1a.

- Set 2: The fine grain size was fixed at 1.5 mm (therefore $D_c/D_f = 3.33$), and three additional fine feed proportions were investigated. A summary of these experiments is given in Table 3.1: Set 2.

Following the fine sediment input, the channel passed through a transient phase to ultimately reach a new, two-size equilibrium bed slope, whereby the sediment output rate was again approximately equal to the sediment input rate for each size component. In many cases the channel had aggraded or degraded to reach this new equilibrium slope, consequently the bed and water slopes were no longer parallel to flume slope. Figures 3.1b and 3.1c show the bed in two-size equilibrium in Experiment I.1 ($D_f = 0.7$ mm) and Experiment I.5 ($D_f = 3$ mm) respectively.

Table 3.1 Experimental conditions for the fine grain inputs.

Experiment Set	Experiment number	Fine grain diameter (D_f) (mm)	Grain size ratio (D_c/D_f)	Fine grain feed rate (g/s)	Total feed rate (g/s)	Fine feed rate/ Total feed rate (%)
1	I.7	0.7	7.14	0.63	2.85	22
	I.1			1.54	3.76	41
	I.8			4.82	7.04	68
	I.11	0.9	5.56	0.62	2.84	22
	I.2			1.54	3.76	41
	I.12			4.92	7.14	69
	I.13	1.5	3.33	0.65	2.87	23
	I.3			1.60	3.82	42
	I.14			4.74	6.96	68
	I.9	2	2.5	0.62	2.84	22
	I.4			1.57	3.79	41
	I.10			4.72	6.94	68
	I.15	3	1.67	0.62	2.84	22
	I.5			1.59	3.81	42

Experiment Set	**Experiment number**	**Fine grain diameter (D_f) (mm)**	**Grain size ratio (D_c/D_f)**	**Fine grain feed rate (g/s)**	**Total feed rate (g/s)**	**Fine feed rate/ Total feed rate (%)**
1	I.16	4	1.25	0.65	2.87	23
	I.6			1.55	3.77	41
2	I.17	1.5	3.33	1.01	3.23	31
	I.18			2.70	4.92	55
	I.19			3.74	5.96	63

During the Set 1 experiments, samples of the sediment output were taken for the entire duration of the experiment. The first sample of the 5 mm bed in one-size equilibrium was taken for two minutes. Then, once the fine sediment had been introduced to the channel, the samples were initially taken for 30 seconds, however, as the experiment progressed, the samples were taken for longer periods of time. The final sample, of the bed in two-size equilibrium was taken for five minutes. The samples were oven dried and then sieved to separate the fine and coarse components to enable comparison between the input and output rates. The results from the five minute samples are presented in Table 3.2: Set 1. For the Set 2 experiments, two two-minute samples of the sediment output from the channel were taken at the end of each experiment to ensure that the bed had reached two-size equilibrium. The results of these samples are also presented in Table 3.2: Set 2.

Once in two-size equilibrium, the distance from the base of the bed to the bed surface was measured manually in five locations along the length of the channel, allowing computation of the bed slope. These measurements were repeated five times for each experiment.

Using a combination of image analysis techniques, detailed in Lafaye de Micheaux et al. (2015), on the images taken by the high-speed camera, the bed elevation could be detected, permitting computation of the bed slope. Consequently, it is possible to document the evolution of the slope over time, from the start of the fine grain input until the bed reached a stable two-size equilibrium state. For the slope evolution graphs presented within this chapter, the analysis was undertaken on one frame per second. Figure 3.2 presents the two-size equilibrium bed slopes measured manually, and also those determined from image analysis for the experiments with an approximately 41 % fine feed content; good agreement between the two techniques is observed.

Table 3.2 Results of the samples taken to confirm that the channel had reached two-size equilibrium[1].

Experiment Set	Experiment Number	Fine grain diameter (D_f) (mm)	Coarse output rate (g/s)	Percentage difference between input and output	Fine input rate (g/s)	Fine output rate (g/s)	Percentage difference between input and output
1	I.7	0.7	2.28	2.7	0.63	0.63	0.0
	I.1		2.29	3.2	1.54	1.45	-5.8
	I.8		2.24	0.9	4.82	4.94	2.5
	I.11	0.9	2.25	1.4	0.62	0.58	-6.5
	I.2		2.25	1.4	1.54	1.48	-3.9
	I.12		2.21	-0.5	4.92	5.04	2.4
	I.13	1.5	2.30	3.6	0.65	0.66	1.5
	I.3		2.23	0.5	1.60	1.54	-3.8
	I.14		2.28	2.7	4.74	4.81	1.5
	I.9	2	2.32	4.5	0.62	0.66	6.5
	I.4		2.27	2.3	1.57	1.44	-8.3

[1] In all experiments, the coarse input rate was 2.22 g/s.

Experiment Set	Experiment Number	Fine grain diameter (D_f) (mm)	Coarse output rate (g/s)	Percentage difference between input and output	Fine input rate (g/s)	Fine output rate (g/s)	Percentage difference between input and output
1	I.10		2.17	-2.3	4.72	4.85	2.8
	I.15	3	2.33	5.0	0.62	0.63	1.6
	I.5		2.21	-0.5	1.59	1.65	3.8
	I.16	4	2.25	1.4	0.65	0.60	-7.7
	I.6		2.23	0.5	1.55	1.53	-1.3
2	I.17-1	1.5	2.27	2.3	1.01	1.02	1.0
	I.17-2		2.35	5.9	1.01	0.90	-10.9*
	I.18-1		2.27	2.3	2.70	2.78	3.0
	I.18-2		2.22	0.0	2.70	2.84	5.2
	I.19-1		2.19	-1.4	3.74	3.87	3.5
	1.I9-2		2.15	-3.2	3.74	3.96	5.9

***The percentage difference between the input and output rate during this sample is higher than average. However, over the two minute sample, this is a difference of just 13.2 g, which is not substantial.**

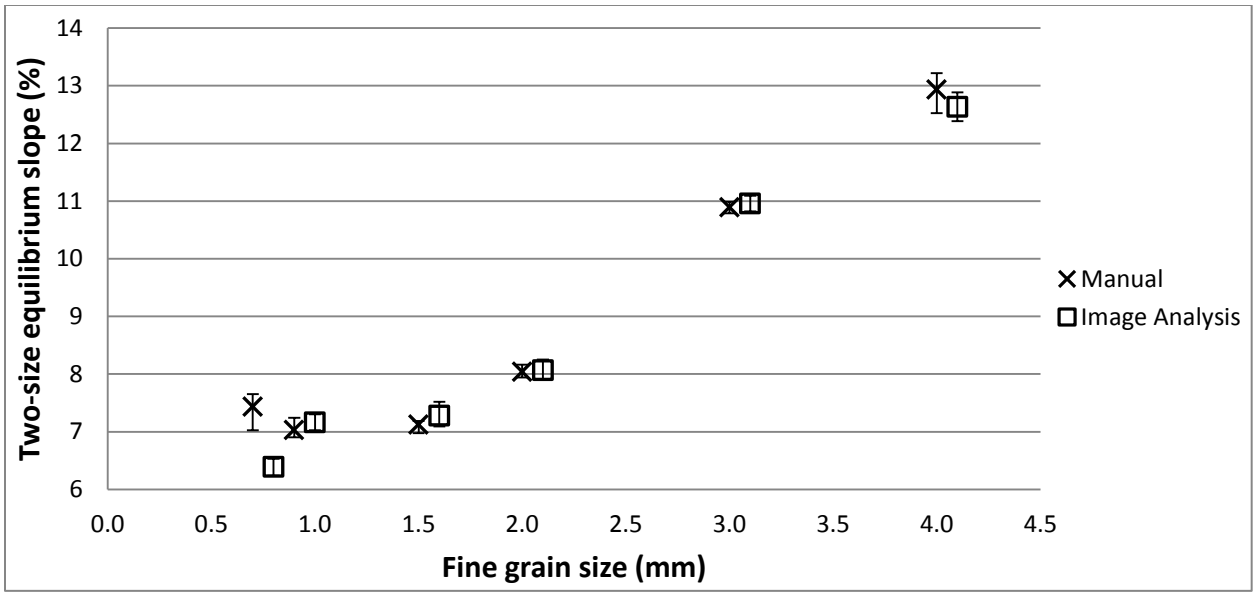

Figure 3.2 Comparison of the two-size equilibrium bed slope values measured manually and determined from image analysis for the experiments with an approximately 41 % fine feed proportion*.

***The image analysis data have been offset by 0.1 mm on the x-axis to permit comparison of the data. Error bars show absolute range of measurements.**

3.3 Results

3.3.1 Experiments: Set 1

Figure 3.3 presents the two-size equilibrium bed slope measured manually for each of the experiments in Set 1, permitting comparison under various conditions. Experiments with final two-size equilibrium slopes less than 10.1 % underwent degradation, while those with slopes greater than 10.1 % aggraded. Figure 3.3 shows influences of both the grain size ratio and the proportion of fines within the feed upon the two-size equilibrium bed slope. Particular note should be made of the transition in behaviour between fine diameter ≤2 mm and ≥3 mm. For comparison, degradation of the bed is shown in Figure 3.1b (D_f = 0.7 mm), and aggradation in Figure 3.1c (D_f = 3 mm).

Near agreement is shown, in Figure 3.3, between the two-size equilibrium bed slopes when the fine size composes 22 % and 41% of the total feed for all of the grain size ratios tested. However, when the fine size composes 68 % of the total feed, the two-size equilibrium slope is consistently substantially higher.

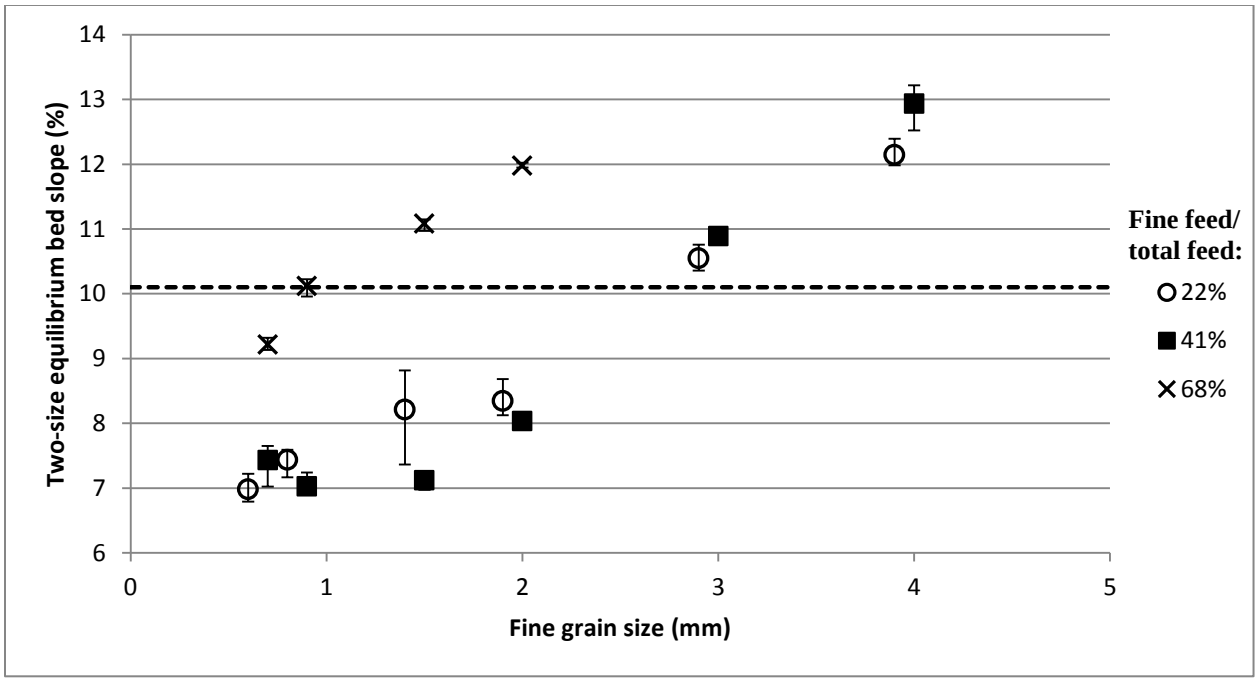

Figure 3.3 Manual measurements of the two-size equilibrium bed slope for the experiments in Set 1*. *For each experiment the slope was measured five times. Error bars show absolute range of measurements. The initial bed slope (10.1 %) before the fine sediment introduction is shown using a dashed black line. The 22 % data have been offset by 0.1 mm (decreased) on the x-axis to permit comparison of the data.

Figure 3.4 presents the evolution of the bed slope over the duration of each experiment, illustrating how the bed slope transitions from one-size equilibrium to two-size equilibrium due to the addition of fines to the bed. To ensure that the full bed slope evolution was captured, the fine sediment was introduced two minutes into the recording. Consequently, the first two

minutes of the slope evolution curves in Figure 3.4 are of the bed in one-size equilibrium. Following the fine sediment introduction, an initial small increase in the bed slope before an eventual fall can be seen in several experiments. Viewing of the experimental videos revealed that this initial upwards peak in the bed slope is due to the wave of fine sediment which moves downstream on the bed surface following the fine sediment introduction, causing the bed to temporarily thicken before it starts to degrade.

Fluctuations in the bed slope can be observed in some of the experiments presented in Figure 3.4. These fluctuations are particularly prominent and regular in the experiments utilising 1.5 mm fines with a content of 22 % and 41 %. Possible causes of these fluctuations are addressed in the discussion.

For each of the experiments presented in Figure 3.4, an exponential decay curve was fitted to the data:

$$S(t) = S_{eq}+(S_o-S_{eq}).\exp(-t/b)$$

wherein S is the bed slope, S_{eq} is the two-size equilibrium bed slope, S_o is the initial slope (10.1%), b is the decay timescale, and t is time from the commencement of the adjustment (t_o, defined below). The values of (S_o-S_{eq}), b and S_{eq} are presented in Table 3.3. The exponential decay curve was fitted between the final data point for the experiment (when the bed is in two-size equilibrium) and a pre-determined start time, t_o (presented in Table 3.3). The start time, t_o, for the aggradation cases is the time when the fine sediment is introduced. Due to the initial upward peak in the bed slope following the fine grain input for the degradation cases, the start time, t_o, is when the bed slope passes through 10.1 % again after this initial upward peak.

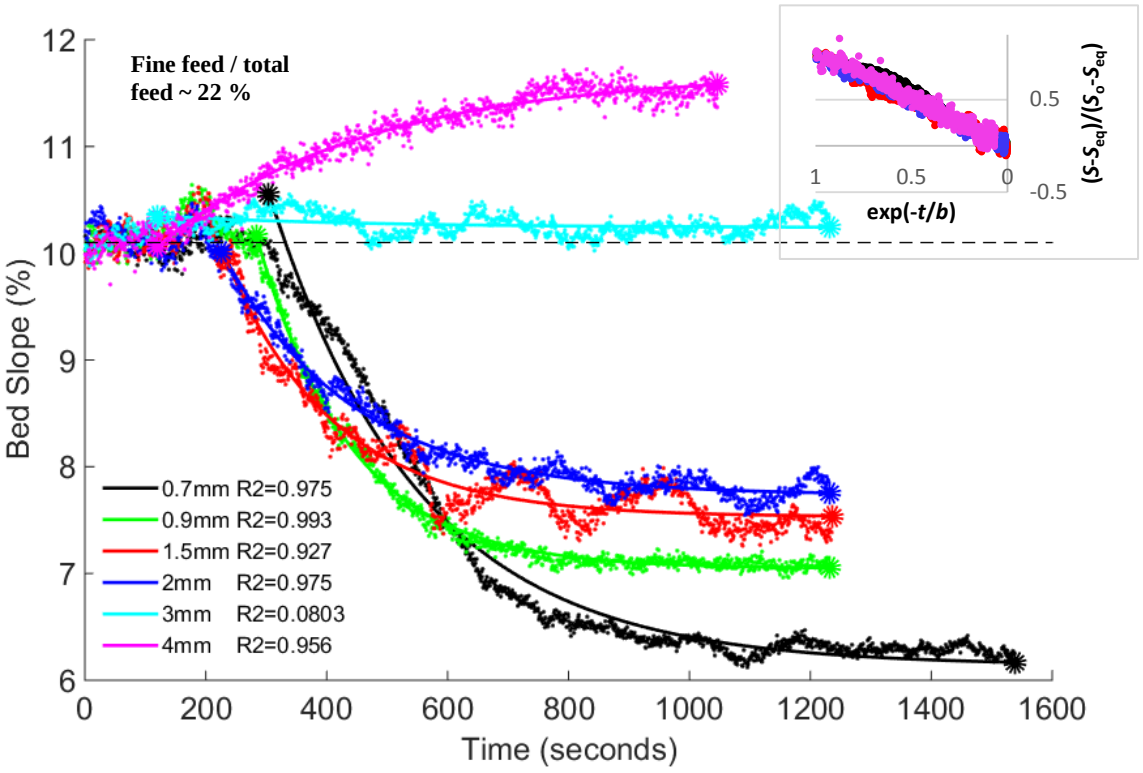
Fine feed / total feed ~ 22 %
Bed Slope (%)
Time (seconds)
0.7mm R2=0.975
0.9mm R2=0.993
1.5mm R2=0.927
2mm R2=0.975
3mm R2=0.0803
4mm R2=0.956
exp(-t/b)
(S-Seq)/(So-Seq)

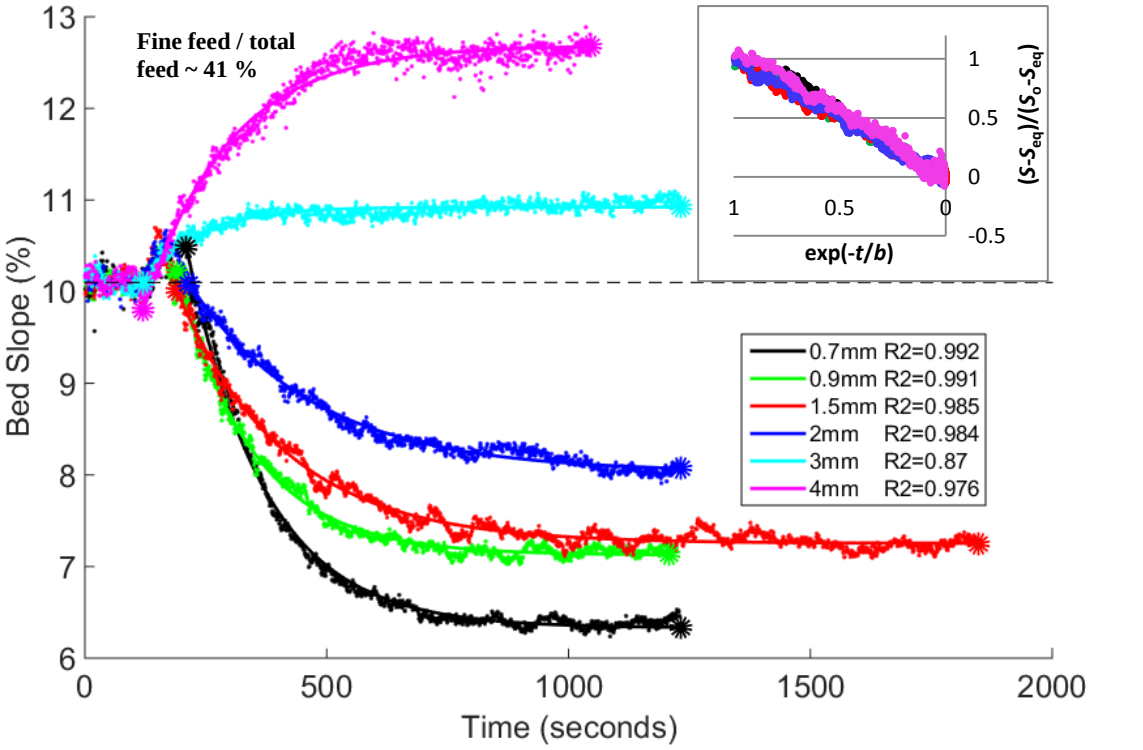
Fine feed / total feed ~ 41 %
Bed Slope (%)
Time (seconds)
0.7mm R2=0.992
0.9mm R2=0.991
1.5mm R2=0.985
2mm R2=0.984
3mm R2=0.87
4mm R2=0.976
exp(-t/b)
(S-Seq)/(So-Seq)

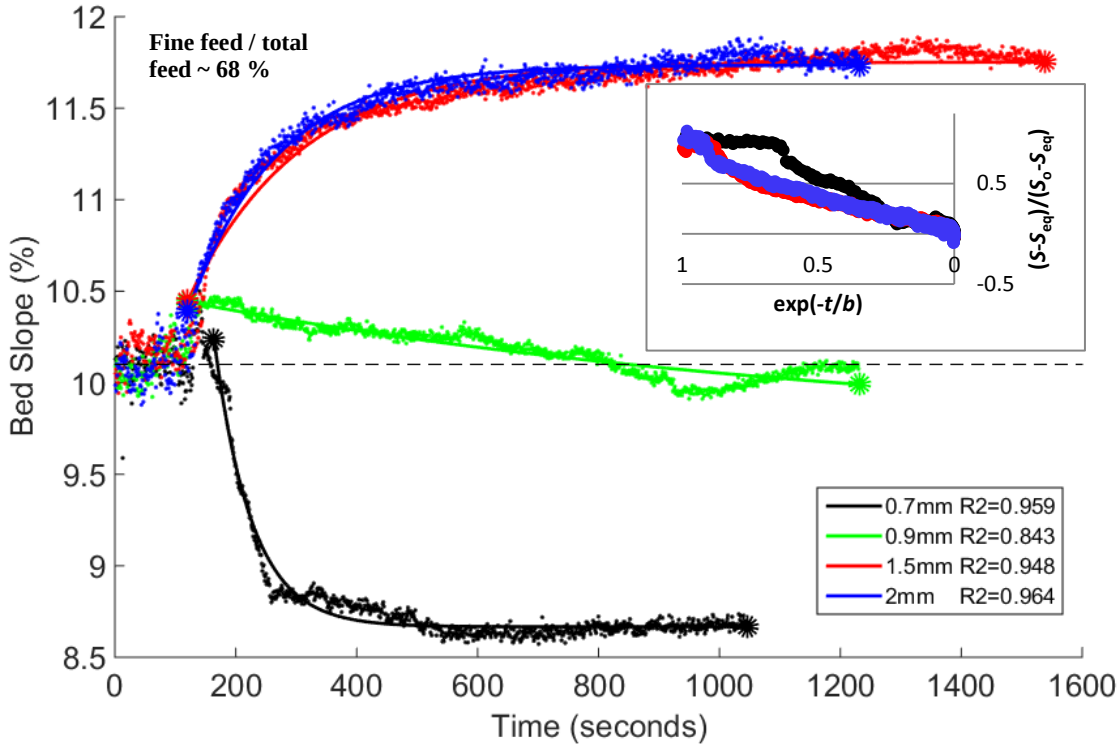

Figure 3.4 Main figures: Bed slope evolution over time*. Insets: Collapse of the bed slope evolution profiles. * The initial bed slope (10.1 %) before the fine sediment was introduced is shown using a dashed black line. The fine sediment was introduced to the channel after 120 seconds. An exponential decay curve (start and end points indicated with spots) has been fitted to each of the bed slope evolution curves, with the R^2 value included in the legend, and the parameter values shown in Table 3.3.

The start time for the degradation cases consequently varied as, depending upon the fine grain size and the fine feed proportion, it required different lengths of time for the fine sediment to reach the camera visualisation window from the feeder. The R^2 value for each of the curves is presented in the legend of the figure. With the exception of three experiments, for which there is little difference between S_o and S_{eq}, the R^2 values are greater than 0.9.

Insets in Figure 3.4 show the collapse of the slope evolution curves. The data used for the collapse in each case lie between the initial and final data points used for the exponential fitting.

Cases for which little slope adjustment occurred (the R^2 values are less than 0.9), have been discounted from the collapse plots.

Table 3.3 The data for the exponential decay curves shown in Figure 3.4.

Approximate fine feed/total feed	**Start time for curve fitting, t_o (s)**	**Fine sediment size (mm)**	**R^2 value**	**S_o-S_{eq}**	***b***	**S_{eq}**
22 %	300	0.7	0.98	4.4	250	6.1
	280	0.9	0.99	3.1	160	7.0
	230	1.5	0.93	2.4	180	7.5
	230	2	0.98	2.3	220	7.7
	120	3	0.080	0.11	360	10.2
	120	4	0.96	-1.6	340	11.7
41 %	210	0.7	0.99	4.2	160	6.3
	190	0.9	0.99	3.1	160	7.1
	180	1.5	0.99	2.8	220	7.3
	220	2	0.98	2.1	260	8.0
	120	3	0.87	-0.83	110	10.9
	120	4	0.98	-2.9	180	12.7
68 %	160	0.7	0.96	1.6	62	8.7
	120	0.9	0.84	0.73	1100	9.7
	120	1.5	0.95	-1.3	190	11.8
	120	2	0.96	-1.4	150	11.7

The sediment output was measured over the duration of the experiments. Figure 3.5 shows the difference between the cumulative input and the cumulative output for the 5 mm grains in each of the experiments, and Figure 3.6 does the same for the fine sediment. The difference between the cumulative sediment input to the channel and the cumulative sediment output over a period of time measures either how much additional sediment has been stored in the channel (if input > output), or how much has been extracted from the bed (if output > input). Figure 3.5, similar to Figure 3.3, shows an influence of both the grain size ratio and the proportion of fines within the feed upon the channel response to the fine grain input; under certain conditions, 5 mm beads are stored within the channel and under other conditions 5 mm beads are extracted from the bed. Figure 3.6 shows fines being retained in the channel in every experiment.

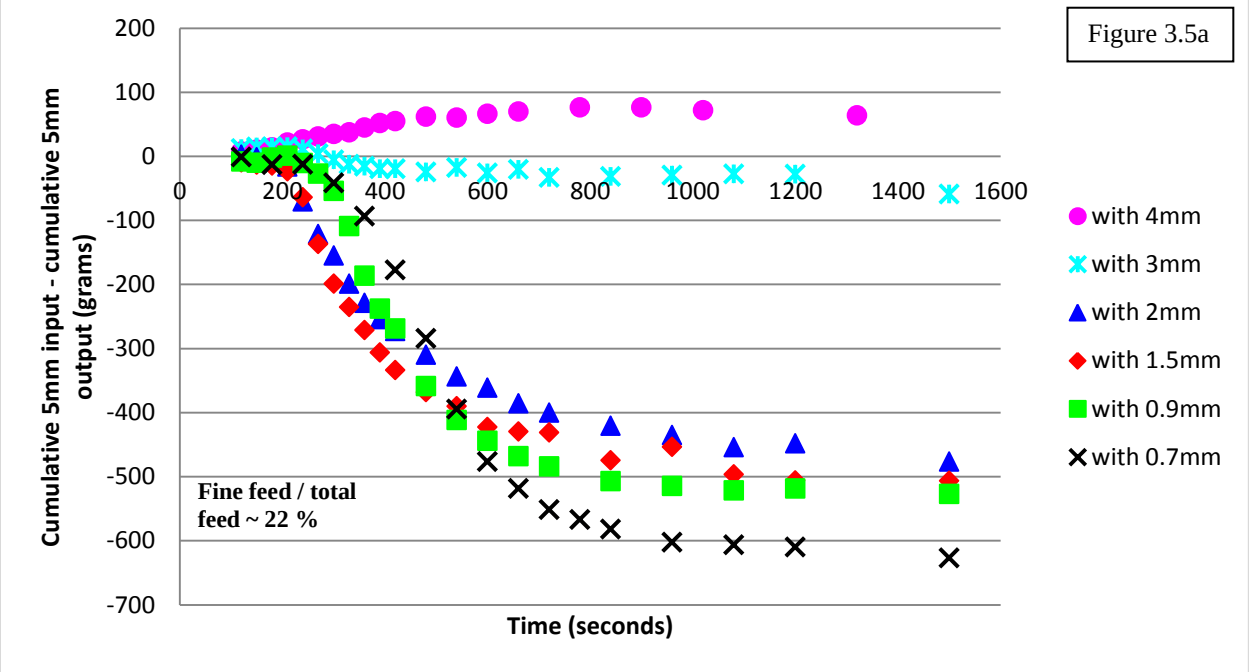

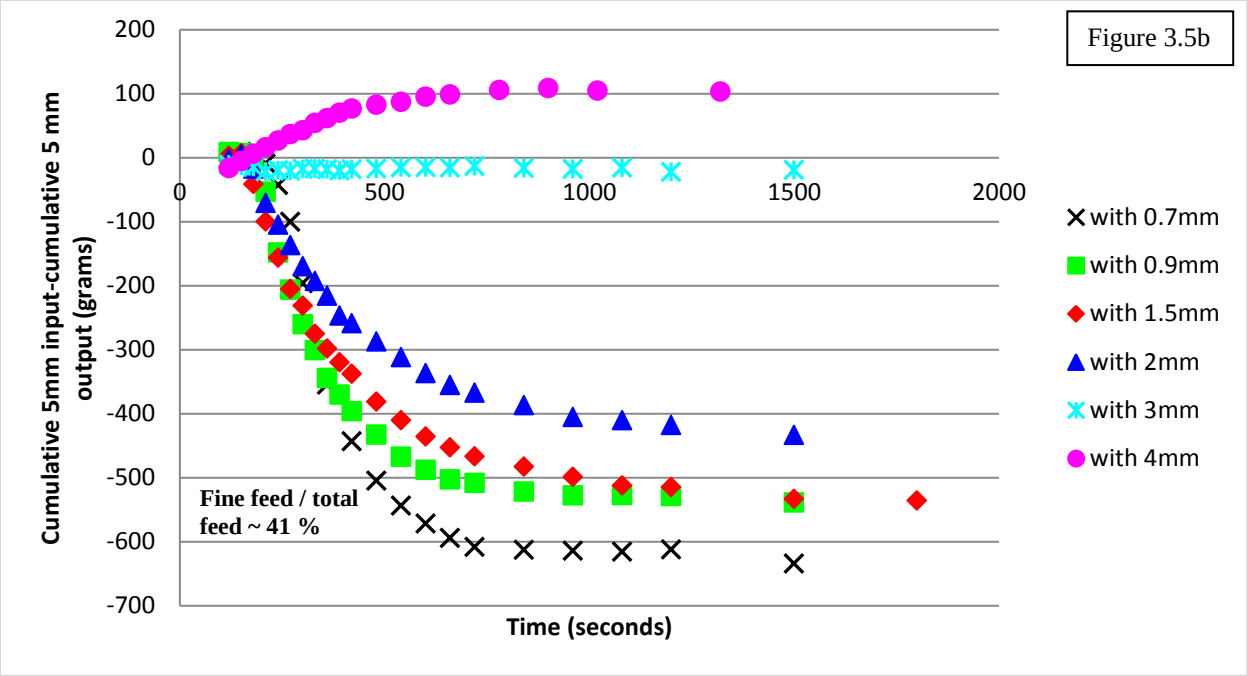

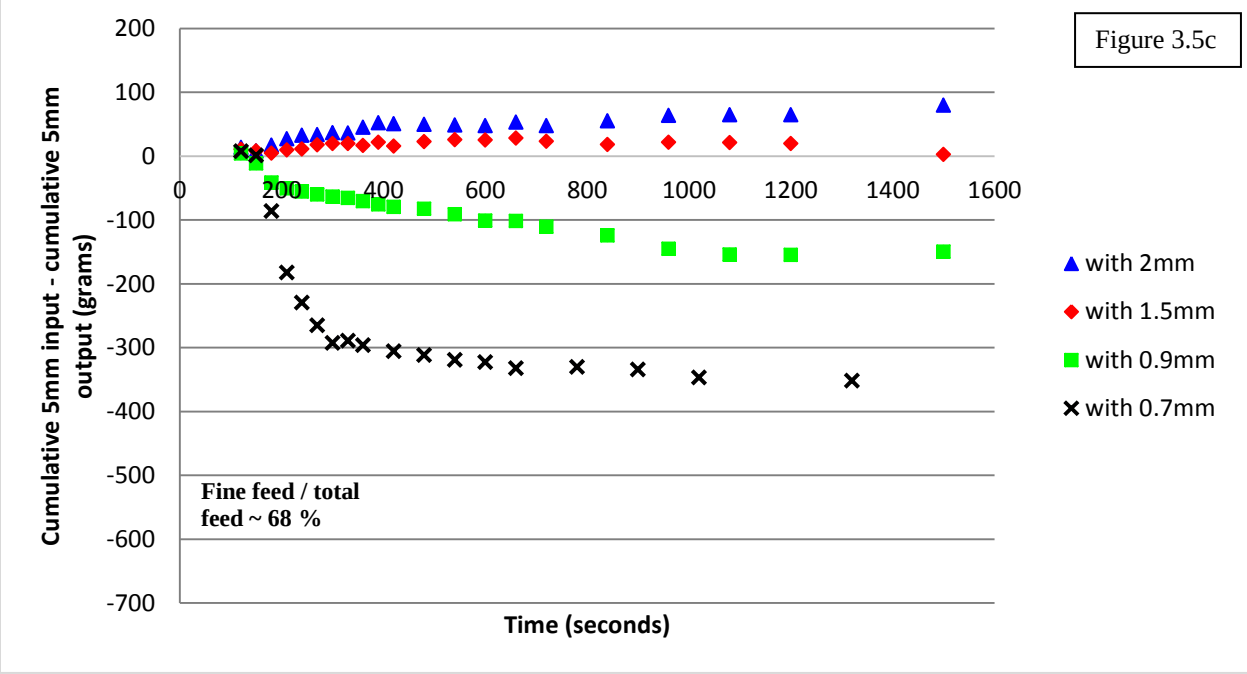

Figure 3.5 Cumulative 5 mm input minus cumulative 5 mm output over time*.

***The fine sediment was introduced after 2 minutes.**

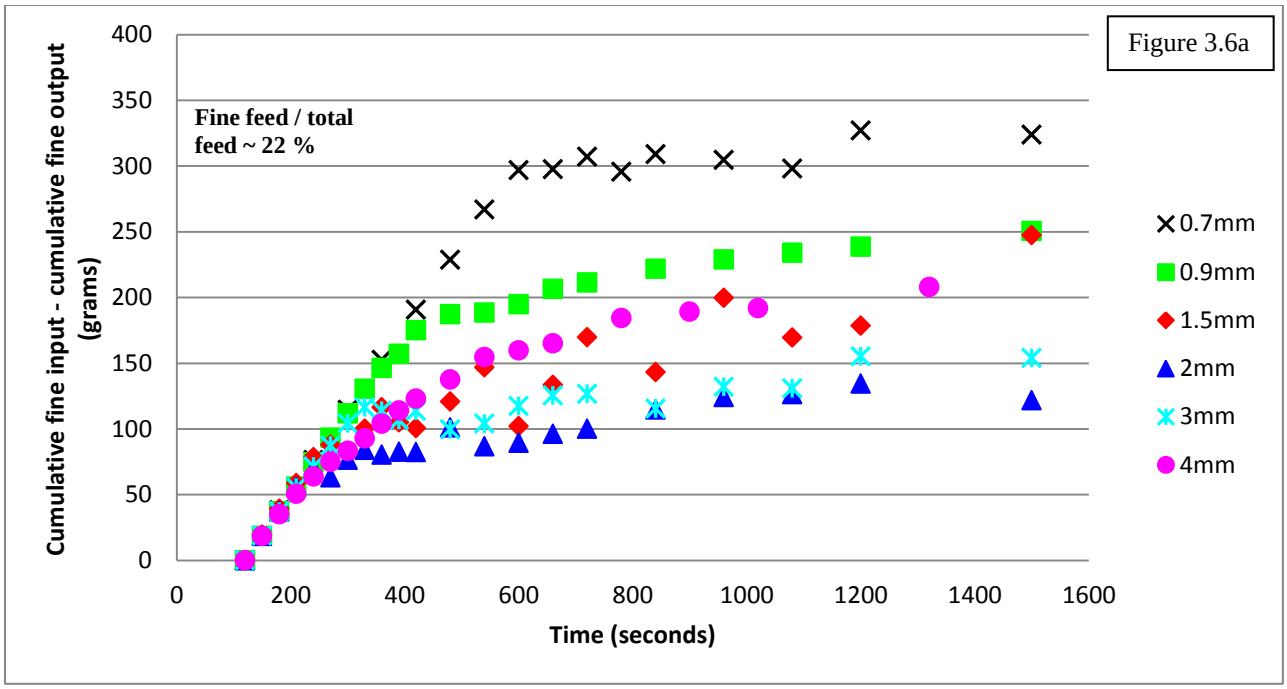
Figure 3.6a
Fine feed / total feed ~ 22 %
Cumulative fine input - cumulative fine output (grams)
Time (seconds)
0.7mm
0.9mm
1.5mm
2mm
3mm
4mm

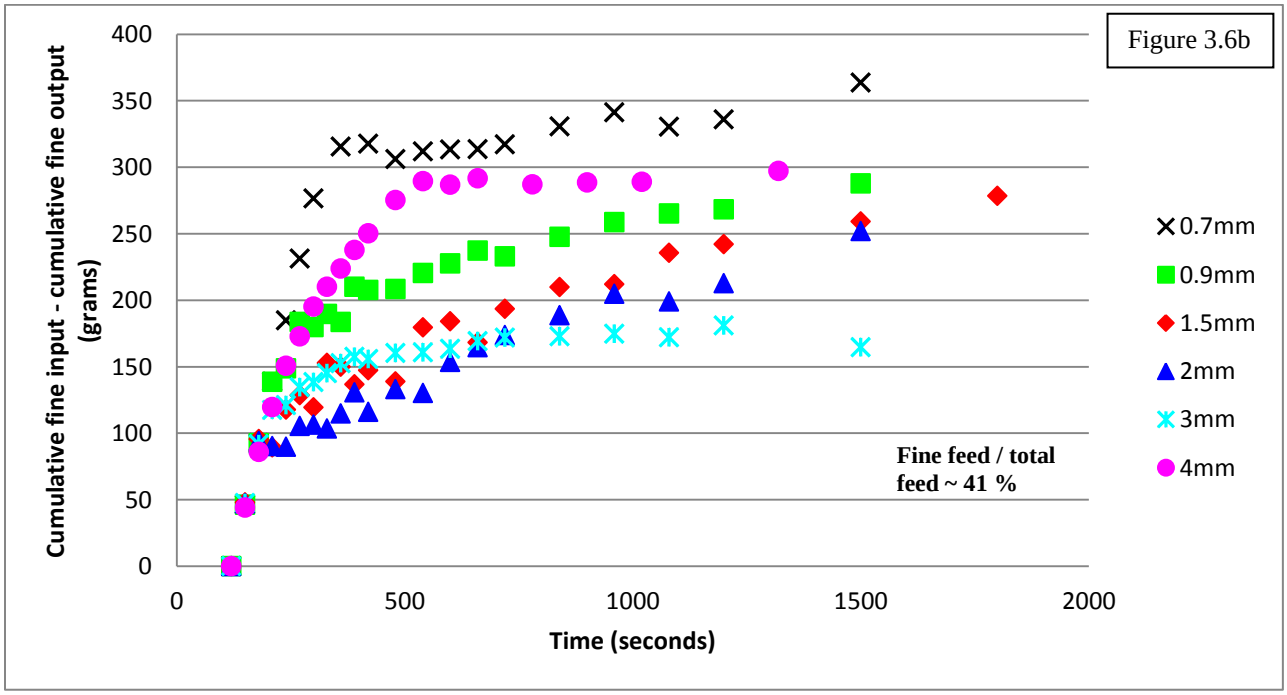
Figure 3.6b
Fine feed / total feed ~ 41 %
Cumulative fine input - cumulative fine output (grams)
Time (seconds)
0.7mm
0.9mm
1.5mm
2mm
3mm
4mm

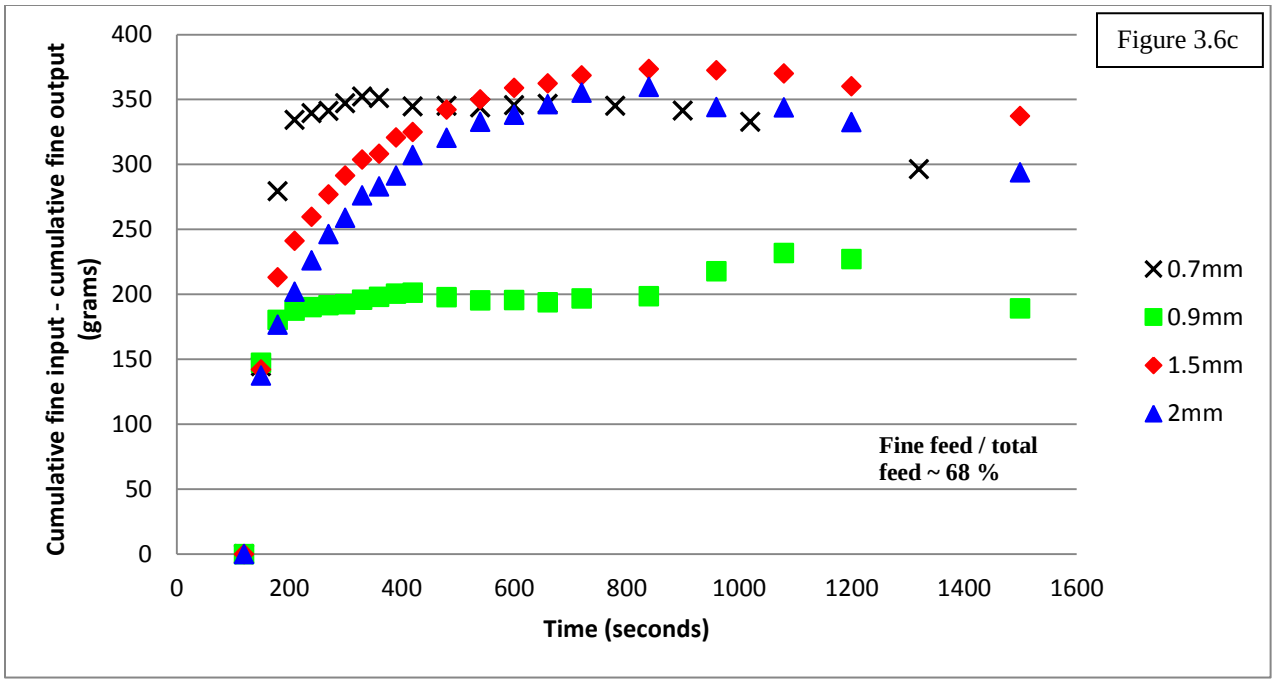

Figure 3.6 Cumulative fine input minus cumulative fine output over time*.

***The fine sediment was introduced after 2 minutes.**

3.3.2 Experiments: Set 2

During the Set 2 experiments, the fine sediment was introduced as soon as the camera recording started. Figure 3.7 shows the bed slope evolution for the 1.5 mm experiments. The experiments in which the fines composed approximately 63 and 68 % of the total feed aggraded following the fine grain input whereas, in the other experiments, the bed degraded in response to the input. In Figure 3.7, 'time 1' is when the bed slope is still responding to the fine grain input, and 'time 2' is when the bed appears to be in two-size equilibrium in all of the experiments. However, as is shown in Figure 3.7, in the 23 %, 31 % and 42 % experiments, the bed slope oscillated whilst in two-size equilibrium.

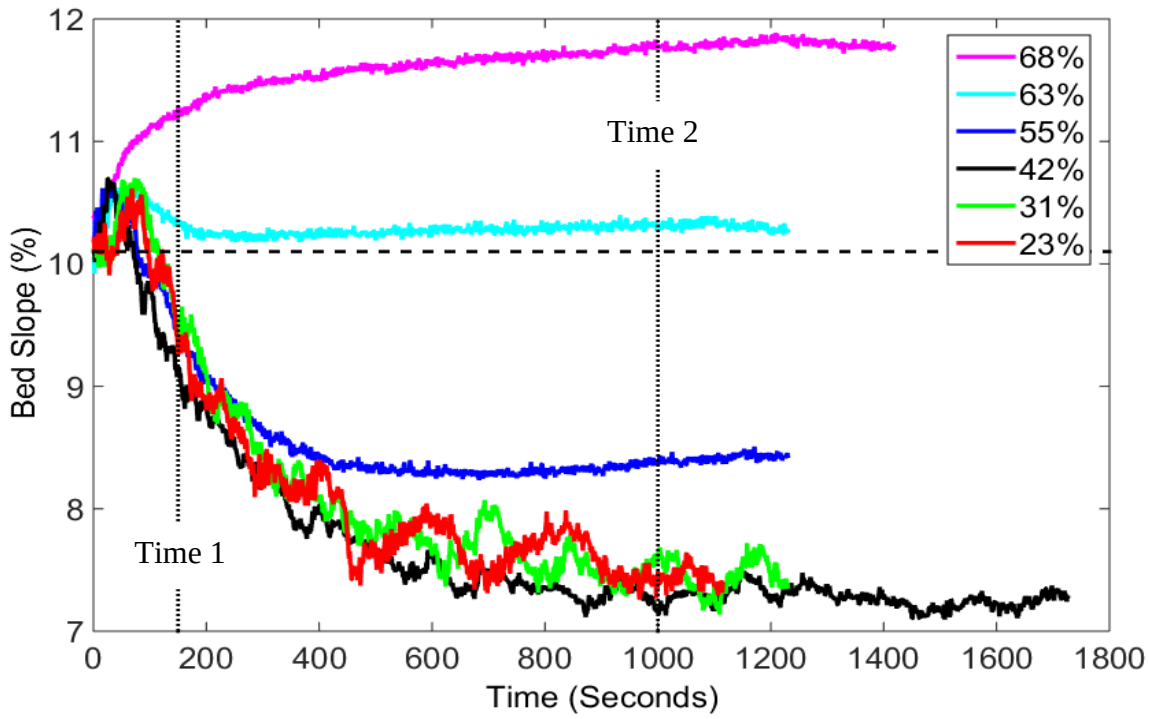

Figure 3.7 Bed slope evolution over time for the experiments with the 1.5 mm fines*.

*** The initial bed slope (10.1 %) before the fine sediment was introduced is shown using a dashed black line. The fine sediment was introduced to the channel at 0 seconds. 'Time 1' and 'time 2' are defined in the text.**

In Chapter 2, the importance of the vertical bed structure, and particularly the occurrence of a quasi-static fine layer, in determining a channel response to a fine sediment input was described. If the introduced fines are unable to infiltrate into the quasi-static coarse bed, they form a quasi-static fine layer upon the coarser bed; the isolation of the coarse bed from the bedload layer prevents degradation from occurring as grain-grain collisions and therefore entrainment are not feasible. Figure 3.8 shows the thickness of the quasi-static fine layer at 'time 1' and 'time 2' for the Set 2 experiments. In all of the experiments, the quasi-static fine layer was thicker at 'time 2' than at 'time 1'. At 'time 1' there is a positive relation between the quasi-static fine layer thickness and the proportion of fines in the total feed. For all of the experiments, excluding the

68 % fine content, the thickness of the quasi-static fine layer at ‘time 2’ is similar. The thickness of the quasi-static fine layer at ‘time 2’ in the experiment with a 68 % content is higher.

The number density of the 5 mm bedload grains present within the camera visualisation window at ‘time 1’ and ‘time 2’ is presented in Figure 3.9. For both ‘time 1’ and ‘time 2’, a decrease in the number density of the 5 mm bedload grains can be seen as the proportion of fines in the total feed increases. Additionally, it is shown that the number density of bedload grains is clearly lower at ‘time 2’ compared to ‘time’ 1 for the experiments with fine feed contents less than or equal to 42 %.

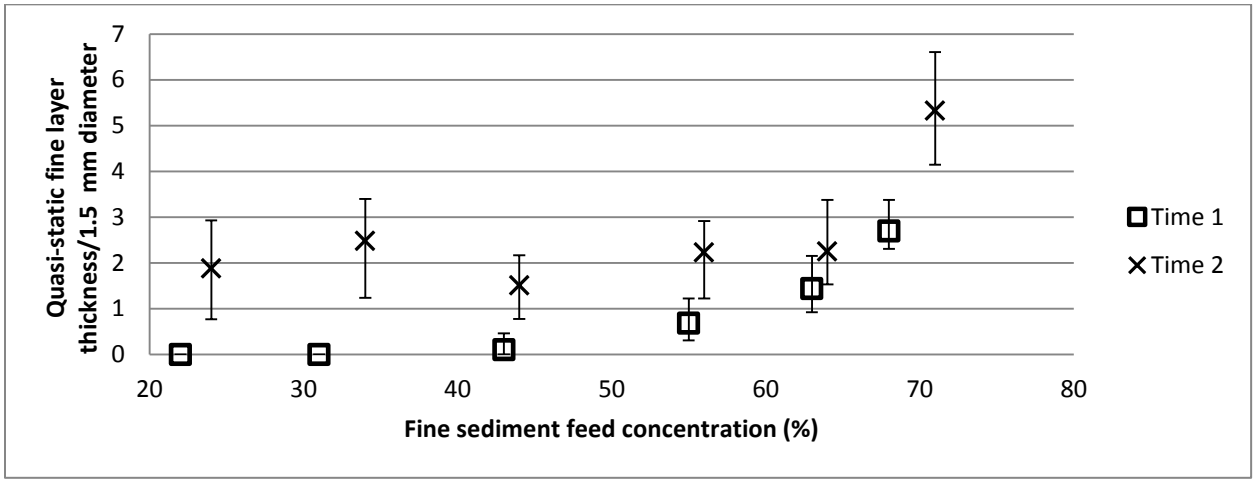

Figure 3.8 Quasi-static fine layer thickness for the 1.5 mm experiments at ‘time 1’ and ‘time 2’ divided by the fine grain diameter*.

***‘Time 1’ and ‘time 2’ are explained in the text. Measurements were taken over 10 seconds, every second starting at ‘time 1’ and ‘time 2’, the error bars show the range in quasi-static fine layer thickness over these ten measurements. The ‘time 2’ data have been offset by 1 % on the x-axis to permit comparison of the data.**

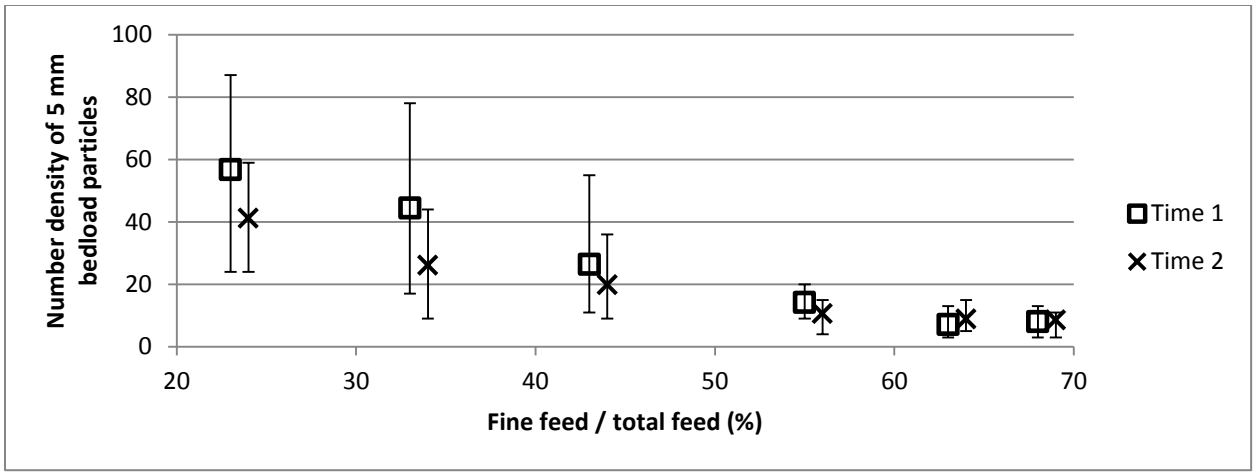

Figure 3.9 Number density of 5 mm bedload particles within the camera visualisation window for the 1.5 mm experiments at 'time 1' and 'time 2'*.

***'Time 1' and 'time 2' are explained in the text. Measurements were taken over two minutes, with the number density counted every 5 seconds starting at 'time 1' and 'time 2'. The error bars show the range in number density over the twenty four measurements. The 'time 2' data have been offset by 1 % on the x-axis to permit comparison of the data.**

3.4 Discussion

Grains which are finer than those forming the channel bed can be input to a river due to natural or anthropogenic occurrences, for example, landslides or land use changes including agriculture, forest management or mining. In 1914, Gilbert undertook experiments which explored the influence of the grain size ratio within a mixture upon the transport rate, and demonstrated that the capacity transported varied depending upon the size ratio. Since that work, over 100 years ago, no further work, involving a wide range of grain size ratios in this context, has been undertaken. The results of these experiments confirm Gilbert's (1914) observations of a relation between the grain size ratio and the capacity transported.

The experimental results confirm our hypothesis that the size ratio (D_c/D_f) between a fine grain input and a coarse bed influences the two-size equilibrium bed slope when the fine content is varied. This explains why Curran and Wilcock (2005b) observed a reduction in the equilibrium slope over a wider range of sand contents than Iseya and Ikeda (1987): the Curran and Wilcock (2005b) experiments used a larger grain size ratio.

The inverse relation between two-size equilibrium bed slope values and grain size ratios when the proportion of fines in the total feed is constant may be attributable to a number of factors. Firstly, to the negative relation between grain size ratio and pivoting angle; according to Komar and Li (1986), the pivoting angle required for entrainment, decreases as the difference between the diameter of a grain and the diameter of the underlying grain around which it needs to pivot increases, potentially explaining why experiments with larger grain size ratios degraded further. Additionally, the finer the grains introduced, the smoother the bed surface. A smoother bed surface was shown by Venditti et al. (2010b) to cause flow acceleration close to the bed and therefore increase drag upon the coarse particles.

The evolution of the bed to reach two-size equilibrium is particularly interesting in the 22 % case (Figure 3.4a). The 0.7 mm experiment reaches the lowest two-size equilibrium bed slope, but evolves the most slowly; similar behaviour is exhibited for the 0.9 mm experiment. The larger the size ratio (D_c/D_f), the more infiltration can take place into the bed, as demonstrated in Chapter 2. The more infiltration takes place, the more time it takes for the fine sediment to fill the void spaces and become present upon the bed surface. Therefore it takes longer for the deposition locations to be filled and for the bed surface to become smoother. Hence the channel takes longer to respond.

The coefficients of the exponential curves from Figure 3.4 are reported in Table 3.3. The parameter *b* is the decay timescale. Discounting the 0.7 mm results, a positive relation is present between the fine grain diameter and the decay timescale for the degradational cases. The results for the 0.7 mm experiments do not conform to this behaviour. It is possible that in the 0.7 mm experiments, the fines were sufficiently small that different controlling processes were emerging. Through examination of Figure 3.1b, a camera image from a 0.7 mm experiment, and videos from the experiments, it can be seen that the 0.7 mm material is present within the water column, occasionally as high as the free surface, indicating that part of the transported 0.7 mm load may have moved temporarily in suspension; yet the shear velocity: settling velocity $\left(\frac{u_*}{w_s}\right)$ is 0.57, which suggests that it is moving as bedload. The high trajectories of the material may be explained by the wave-like behaviour of the 0.7 mm beads within the bedload layer, which looks similar to a Kelvin-Helmholtz instability (Meiron et al., 1982). Despite this, excluding the 68 % fine content case, in Figure 3.4 (insets) the 0.7 mm data collapses in line with the other experiments, suggesting that the behaviour controlling the channel response is similar.

Examination of Figure 3.3 reveals closely matched two-size equilibrium bed slopes in the 22 % and 41 % cases over the full range of size ratios explored. The match between these equilibrium slopes is consistent with the similar behaviour in the sediment output results presented in Figure 3.5a (22 %) and 3.5b (41 %) for the 5 mm grains and Figure 3.6a (22 %) and 3.6b (41 %) for the fine grains. In the 3 and 4 mm experiments, the introduction of finer material to the channel did not result in an increase in the coarse sediment transport rate, and the channel aggraded in response to the input. The 0.7, 0.9, 1.5 and 2 mm experiments, however, did respond to the fine sediment introduction with an increased coarse sediment transport rate. In these cases,

Figures 3.5a and 3.5b show net loss of 5 mm material from the channel following the fine grain input, consequently leading to bed degradation. This therefore suggests a transition in the channel response from degradation to aggradation for fine grain inputs with D_c/D_f somewhere between 1.67 and 2.5. In Chapter 2, it was suggested that this difference in channel response is a result of the infiltration behaviour.

In contrast, Figure 3.3 shows that in the 68 % case the two-size equilibrium bed slope is consistently higher than in the 22 % and 41 % experiments. This is likely to be a result of the much higher total sediment supply in the 68 % case.

In Figures 3.5a, b and c, the data presenting the sediment output for the 5 mm beads are organized with respect to the fine grain input diameter. This pattern is a result of the bed slope response to the fine grain input. The larger the grain size ratio, the greater the amount of degradation (see Figures 3.3 and 3.4). The greater the amount of degradation, the larger the amount of 5 mm material evacuated from the flume. As the grain size ratio decreases, the bed response changed from degradation to aggradation. In the experiments with aggradation, additional 5 mm material was often retained in the flume.

Figure 3.6 presents the sediment output for the fine material. The fine material output is more complex than the 5 mm output behaviour, and the plots, when considering all of the data, are not organized according to the fine grain input diameter. This is due to competing factors. In the experiments with the 0.7 mm, 0.9 mm, 1.5 mm and 2 mm beads, the fine material infiltrated into the bed due to spontaneous percolation and was therefore retained in the channel. Additionally, the finer the input diameter, the more spontaneous percolation took place, and the greater the amount of fine material retained in the channel. In the 22 % (Figure 3.6a) and 41 % (Figure 3.6b) fine feed content experiments, the 0.7-2 mm fine inputs all resulted in degradation

of the bed. It can be seen in Figure 3.6a and 3.6b, when only the degradation experiments are considered, that these data are arranged according to the fine grain diameter; with the greatest amount of material retained for the smallest fine grain diameter. In the 3 mm and 4 mm experiments, spontaneous percolation was not possible, but the channel aggraded in response to the fine grain inputs due to a deposited layer of fines upon the bed surface (see Figure 2.6 for the 3 mm case), therefore fines were retained in the channel, causing the data to overlap with the 0.7-2 mm cases. Considering just the 3 mm and 4 mm cases, in Figure 3.6a and 3.6b, it can be seen that the greater the fine grain diameter, the larger the amount of fines retained in the channel, which is due to the bed aggrading more at lower grain size ratios.

In the 68 % fine feed content experiments, infiltration due to spontaneous percolation was feasible in all cases; again with more fine infiltration at smaller fine grain diameters. However, in the experiments with the 1.5 mm and 2 mm inputs, the bed responded by aggrading, with a layer of deposited fines upon the bed surface (see Figure 2.8 for a 2 mm example), therefore increasing the amount of fines retained. Consequently, the 1.5 mm and 2 mm data in Figure 3.6c plot higher than expected.

The second set of experiments was designed to gain further insight into the influence of fine feed content at a given grain size ratio. Following a fine grain input to a coarse bed in motion, the two-size equilibrium bed slope has previously been found to be dependent upon the proportion of fines in the total feed (Jackson and Beschta, 1984; Iseya and Ikeda, 1987; Ikeda and Iseya, 1988; Wilcock et al., 2001; Curran and Wilcock, 2005b), this was confirmed during these experiments. Figure 3.7 shows that there is a positive relation between the fine feed content and the two-size equilibrium bed slope, with a transition from degradation to aggradation occurring between 55 % and 63 % fine feed content. In order to understand why the 63 % and

68 % cases lead to aggradation, but the other cases lead to degradation, it is important to examine the quasi-static fine layer thickness at ‘time 1’, presented in Figure 3.8. For both the 63 % and the 68 % cases at ‘time 1’, there is a quasi-static fine layer at least one grain diameter thick covering the coarse bed surface, consequently isolating the underlying bed, preventing degradation. At ‘time 2’, when the bed has reached two-size equilibrium, it can be seen in Figure 3.8 that the quasi-static fine layer in all of the experiments is thicker than at ‘time 1’, and always greater than one fine grain diameter in thickness. Further degradation is not able to take place under these conditions as the thick quasi-static fine layer isolates the underlying bed.

This thickening of the layer at ‘time 2’ compared to ‘time 1’ has a substantial impact upon the number density of bedload grains only in the experiments with a quasi-static fine layer thickness of approximately zero at ‘time 1’ (see Figure 3.9). In these experiments, the number density is reduced at ‘time 2’, compared to ‘time 1’ as the thicker quasi-static fine layer results in a smoother bed. The thickening of the quasi-static fine layer from ‘time 1’ to ‘time 2’ did not substantially impact the number density of bedload grains in the experiments wherein the quasi-static fine layer thickness at ‘time 1’ was greater than zero.

In an experiment by Ikeda and Iseya (1988), the transition between the ‘congested’ and ‘smooth’ bed states occurred around a 50:50 fine to coarse ratio within the feed. A similar transition is shown in Figure 3.9 during the present experiments, with a much lower number density occurring when the fine content is greater than 50 %, and vice versa. Although the bedload number density appears not to reach a stable value until the fine content is greater than or equal to 63 %. The experiments undertaken during this research present a link between the quasi-static fine layer thickness and the bedload number density. The thickness of the quasi-static

layer will dictate how rough or smooth the bed surface is, and therefore influences the bedload number density.

In Figure 3.7, an oscillatory pattern can be seen in the bed slope for the cases when the fine feed composed 23 %, 31 % and 42 %. The amplitude of the oscillations appears to grow as the slope declines. During these experiments it could be seen that the thickness of the fine grain layer upon the bed surface oscillated in thickness, causing the bed slope oscillations. This behaviour explains the spread in manual slope measurements for the 1.5 mm experiments in Figure 3.3, and also the variations in quasi-static fine layer thickness between these cases in Figure 3.8.

3.5 Conclusions

Experiments exploring the superior mobility of sediment mixtures demonstrate that the size ratio (D_c/D_f), in addition to the fine feed content, has an important influence upon sediment transport rates following a fine grain input to a coarse mobile bed.

The first set of experiments explored the role of grain size ratio. The transition from the one-size equilibrium bed slope, to the two-size equilibrium bed slope depends upon the fine grain diameter, a previously undocumented finding. For a given fine sediment feed rate, the largest amount of degradation occurs at the greatest grain size ratio. Progressively less degradation occurs as the grain size ratio decreases, until a transition from degradation to aggradation occurs. Despite the influence of the size ratio upon the channel response, collapse of the bed slope evolution curves is feasible. The slope collapse demonstrates that an exponential decay is a good description of the behavior, and also reveals similarity in the characteristics determining the channel response, irrespective of the grain size ratio. Further, the evolution of

the slope over time is controlled by the initial and final equilibrium slopes. Consequently, if these values are known, it would be possible to predict slope evolution over time for any size of fine grain input.

The second set of experiments explored the role of fine content in the total feed. The transition from one-size equilibrium bed slope to two-size equilibrium bed slope depends upon the fine feed content. The greatest amount of degradation occurred at the smallest fine feed content. As the fine feed content increases, the amount of degradation is reduced, until there is a transition from degradation to aggradation. An increase in the sediment transport rates for the coarse component, which results in bed degradation, is feasible only when the bedload layer is able to interact with the underlying coarse bed. The fine content at which the bed response transitions from degredation to aggradation depends upon the infiltration characteristics, the grain size ratio and the vertical bed structure. This is the first explanation, to the authors' knowledge, why the equilibrium bed slope changes at a given fine feed content.

Chapter 4: Testing reproducibility in a fluvial context

The purpose of this chapter is to present the experiments undertaken at Simon Fraser University (SFU), Vancouver, Canada with two-size mixtures of spherical glass beads. By following the same experimental procedure as the experiments presented in Chapters 2 and 3, the reproducibility of the Irstea results is tested. Comparison of the experimental results is both qualitative and quantitative.

4.1 Experimental Arrangement

The experiments were undertaken in a flume (see Figure 4.1) located at Simon Fraser University (SFU), Vancouver, Canada. The flume was designed to mimic the channel at Irstea, but included variations in the materials and construction. The flume at SFU has a wood structure coated with epoxy, with the exception of the front-wall, which is Plexiglas®, and a gap in the back-wall, which is also Plexiglas® and behind which is a backlight. The base was formed of a random arrangement of spherical glass beads of 3 mm to 6 mm in diameter, glued to a stainless steel flatbar and covered in epoxy; this prevents a regular arrangement of grains developing within the sediment bed. The total length of the flume was 4.88 m, although the experimental length was 2.51 m. The slope was fixed at $10.1 \pm 0.1\%$ (same as Irstea). The experimental section of the flume had a width of 10.3 mm (same as Irstea). The Plexiglas® front-wall is 0.455 m high and 25 mm wide. To cause bed formation, a 64 mm high obstacle was inserted into the end of the flume (same as Irstea).

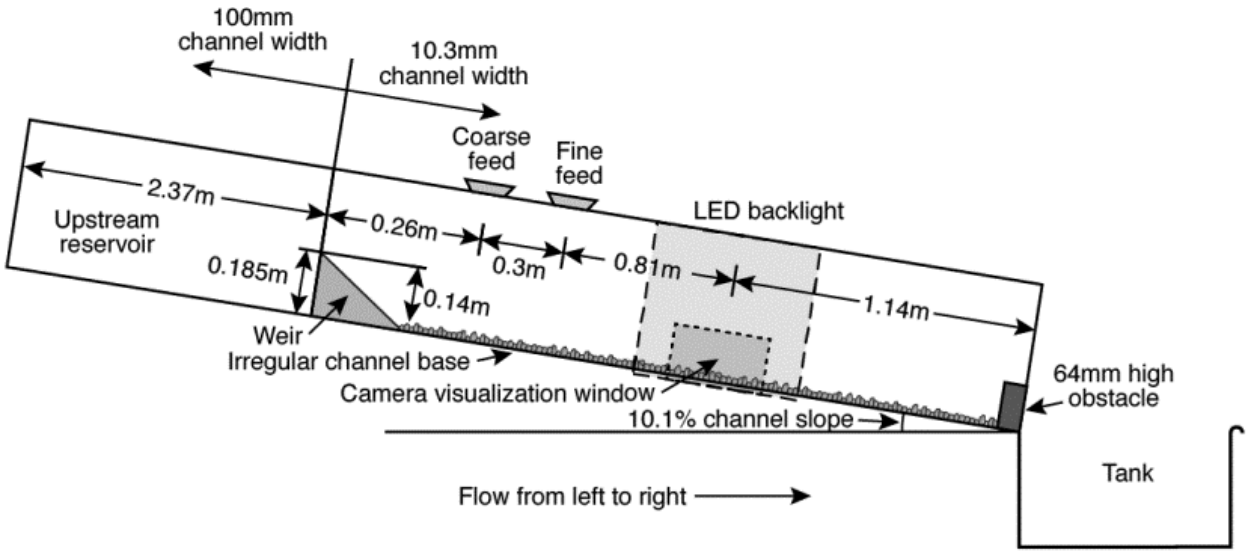

Figure 4.1 Schematic diagram of the experimental arrangement at SFU, containing no beads.

The water system was a closed circuit, containing two reservoirs and a pump. The pump was a 1/12 horsepower Portable Utility Pump. One reservoir was located at the channel outlet (labeled 'tank'), and the other at the upstream end of the flume. The flow rate was measured using an electromagnetic flow meter, and controlled with a Y-valve. The water system at SFU was less consistent than at Irstea, and consequently the flow rates used in the SFU experiments varied between experiments (details provided in Section 4.2). The reservoir at the upstream end of the flume was 2.37 m long and 0.1 m wide, and was separated from the experimental section of the flume by a triangular weir. The height of the triangular weir was 0.185 m from the base of the reservoir, and 0.14 m from the irregularly arranged beads on the steel flatbar within the experimental section.

Spherical glass beads were utilized in the experiments, and were from the same manufacturer as those used in the Irstea experiments (Chapters 2 and 3). The diameter of the

beads forming the coarse component was fixed at 5.0 ± 0.3 mm, therefore ensuring consistent void spacing within the bed for all the experiments. The diameter of the fine component varied; diameters of 1.5 ± 0.2 mm, 2.0 ± 0.2 mm and 3.0 ± 0.3 mm were used. Additionally, one set of material below 1 mm in diameter was used; D_{50} of 0.9 mm (0.75 – 1 mm). All of the beads used in the experiments have a density of 2500 kg/m^3, and all are transparent except the 0.9 mm beads, which are translucent pink.

Two 'Tinker' distributors were used to introduce sediment into the flume; one to feed the coarse component and another to feed the fine component. The coarse and fine feeders were located 2.25 m and 1.95 m upstream of the flume outlet respectively. The 'Tinker' distributor is less consistent when feeding material compared with the K-Tron© device used at Irstea. Consequently, it was not possible to fix the coarse feed rate with no variability between the experiments, as done in the Irstea experiments (details given in Section 4.2).

All of the experiments were recorded using a Manta© black-and-white high-speed camera, provided by Allied Vision Technologies©, which was positioned perpendicular to, and inclined to the same angle as, the channel. The camera recorded at 130 frames per second, and the images from the camera visualization window are 1024 by 500 pixels. A LED backlight was placed within the back-wall and spanned between 0.895 and 1.45 m upstream of the channel outlet. The center of the camera visualization window was approximately 1.14 m upstream of the channel outlet.

4.2 Experimental Procedure

As with the Irstea experiments, a consistent procedure, with two stages, was followed for each experiment: (1) one-size equilibrium was achieved with the coarse grains (see Figure 4.2 and

Table 4.1 for details). One-size equilibrium is theoretically achieved when the sediment input rate equals the sediment output rate, and the bed and water slope match the flume slope. Due to the variability in the flow rate and feed rate, the initial sediment bed slope (S_o) was not always equal to 10.1 % in the SFU experiments (see Table 4.2). However, to ensure the input rate was approximately equal to the output rate, two two-minute samples of the sediment output were taken. The output rate was always within 8 % of the input rate, with the exception of one sample, from one experiment, which had a 17 % difference between the input and output rate. The nominal coarse feed rate and the flow rate were not changed throughout the experiment. (2) Fines of a fixed diameter and a fixed feed rate were introduced into the channel (see Table 4.2). The bed response to the fine grain input was filmed using the high-speed camera.

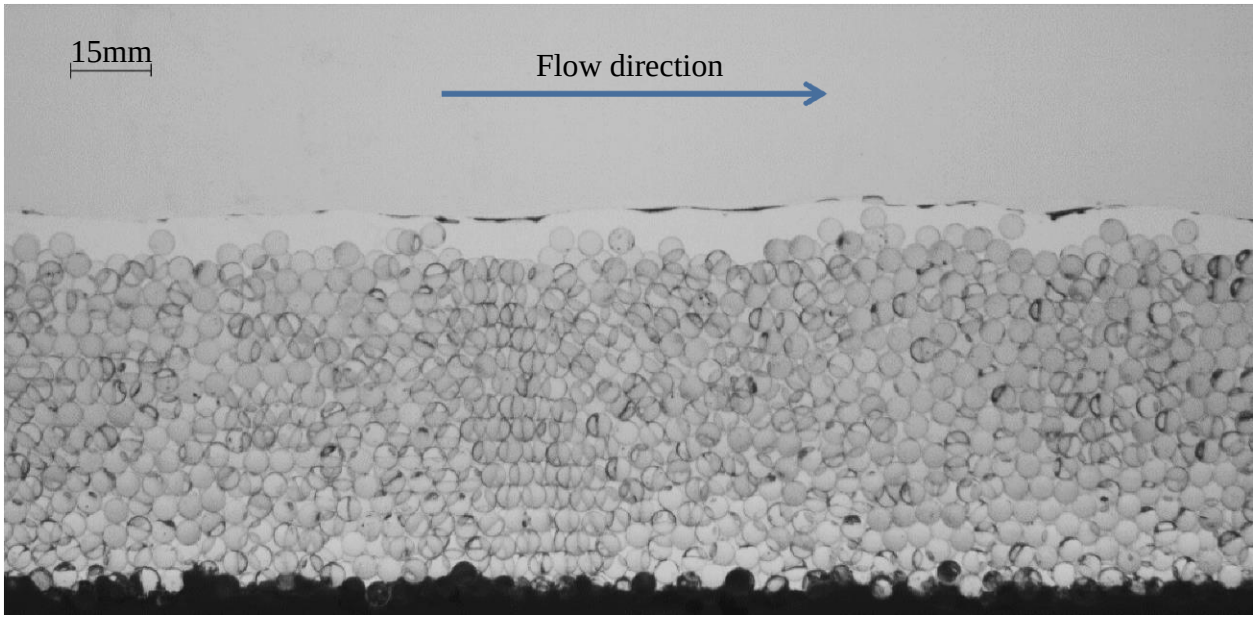

Figure 4.2 5 mm bed in one-size equilibrium at SFU.

Table 4.1 Experimental conditions for one-size equilibrium[*].

Lab	Mean flow rate (mL/s)	Mean coarse feed rate (g/s)	Mean flow depth, h (mm)	Submergence ratio (h/D_c)	Side-wall corrected dimensionless shear stress	Mean Velocity, U (m/s)	Froude Number ($\frac{U}{\sqrt{gh}}$)	Water temperature (Celsius)	Kinematic viscosity, ν (mm^2/s)	Reynolds Number ($\frac{4UR_h}{\nu}$)
Irstea	49.5	2.22	8.02 ± 0.38	1.6 ± 0.18	0.076 ± 0.011	0.60 ± 0.03	2.14 ± 0.15	25	0.8926	8420 ± 237
SFU	40.3 ± 1.16	2.24 ± 0.12	6.75 ± 1.23	1.35 ± 0.31	0.064 ± 0.023	0.59 ± 0.14	2.31 ± 0.84	15	1.1386	6001 ± 859

[*]Details of how the hydraulic parameters were calculated are given in Appendix B. Details of the Irstea experiments have been included for comparison.

Table 4.2 Experimental conditions for the fine grain inputs.

Experiment number	Fine grain diameter (D_f) (mm)	Grain size ratio (D_c/D_f)	Coarse grain feed rate (g/s)	Fine grain feed rate (g/s)	Fine feed rate/ Total feed rate (%)	Average initial one-size equilibrium bed slope, S_o (%)
S.1	0.9	5.56	2.23	0.67	23.1	10.13
S.2	0.9	5.56	2.23	1.52	40.5	10.28
S.3	0.9	5.56	2.22	4.72	68.0	9.70
S.4	1.5	3.33	2.35	1.58	40.2	9.70
S.5	2	2.5	2.21	0.72	24.6	9.84
S.6	2	2.5	2.30	1.53	39.9	10.59
S.7	3	1.67	2.31	1.65	41.7	10.04

Despite the same channel width and slope, coarse bead diameter, and very similar coarse bead feed rates, the flow rate required for one-size equilibrium differed between the Irstea (49.5 ml/s) and SFU (40.3 ± 0.52 ml/s) experiments[1]. The exact reasoning for this dissimilarity, causing the lower flow rate in the SFU experiments, is unknown. However, several possible reasons have been identified:

[1] The values measured by the electromagnetic flow meter at SFU were confirmed manually.

(1) Both of the flume walls at Irstea were glass, whereas one of the flume walls at SFU was epoxy covered wood and the other was Plexiglas®. The different wall materials may have resulted in different surface frictions.

(2) The base of the Irstea flume was an irregularly corrugated bottom, whereas the flume base at SFU consisted of a random arrangement of spherical glass beads glued to a stainless steel flatbar and covered in epoxy. The difference in the flume bases may have resulted in differences in the packing arrangements, and consequently differences in the infiltration flow.

(3) The experiments were undertaken at Irstea over summer, between June and August, and it is estimated that the water temperature was approximately 25°C, whereas the SFU experiments were undertaken over the autumn/winter, between October and December, and it is estimated that the water temperature was approximately 15°C. Differences in the water temperature between the two locations, will have changed the kinematic viscosity of the water (see Table 4.1 for details).This results in a 28 % higher kinematic viscosity in the SFU experiments, and consequently a higher bulk and roughness Reynolds number.

(4) The inlet flow and sediment feed arrangements were different between the two sets of experiments.

Following the fine sediment input, the channel passed through a transient phase to ultimately reach a new, two-size equilibrium bed slope, whereby the sediment input rate was again approximately equal to the sediment output rate for each size component. Two two-minute samples of the sediment output from the channel were taken at the end of each experiment to

confirm that the bed had reached two-size equilibrium. The samples were oven dried and then sieved to separate the fine and coarse components to enable comparison between the input and output rates. The results of the two two-minute samples are presented in Table 4.3. The percentage difference between the input rate and the output rate is consistently less than 13 %, with the exception of two of the samples in Experiment S.1, which may be a consequence of the low total feed rate and the 0.9 mm grain size in this case.

Table 4.3 Percentage difference between the input rate and the output rate during two two-minute samples.

Experiment number	**Fine size (mm)**	**Fine feed / total feed (%)**	**Fine sediment**		**Coarse sediment**	
			Percentage difference in sample 1 (%)	**Percentage difference in sample 2 (%)**	**Percentage difference in sample 1 (%)**	**Percentage difference in sample 2 (%)**
S.1	0.9	23.1	-0.33	-24.97	11.64	15.13
S.2	0.9	40.5	0.08	3.70	5.09	12.55
S.3	0.9	68.0	-3.69	-2.77	0.40	-0.14
S.4	1.5	40.2	-12.06	-5.38	0.19	0.61
S.5	2	24.6	9.66	5.01	-2.37	-3.14
S.6	2	39.9	6.46	6.73	-0.22	0.52
S.7	3	41.7	-3.35	4.34	2.40	-1.60

In many cases the channel had aggraded or degraded to reach the new equilibrium slope, consequently the bed and water slopes were no longer parallel to flume slope. The bed slope was measured manually and using image analysis with the same method as outlined for the Irstea

experiments (see Section 2.2 for details). Figure 4.3 presents the slopes measured manually and using image analysis for the experiments undertaken with a 41 % fine feed content. Good agreement can be seen between the two types of measurement.

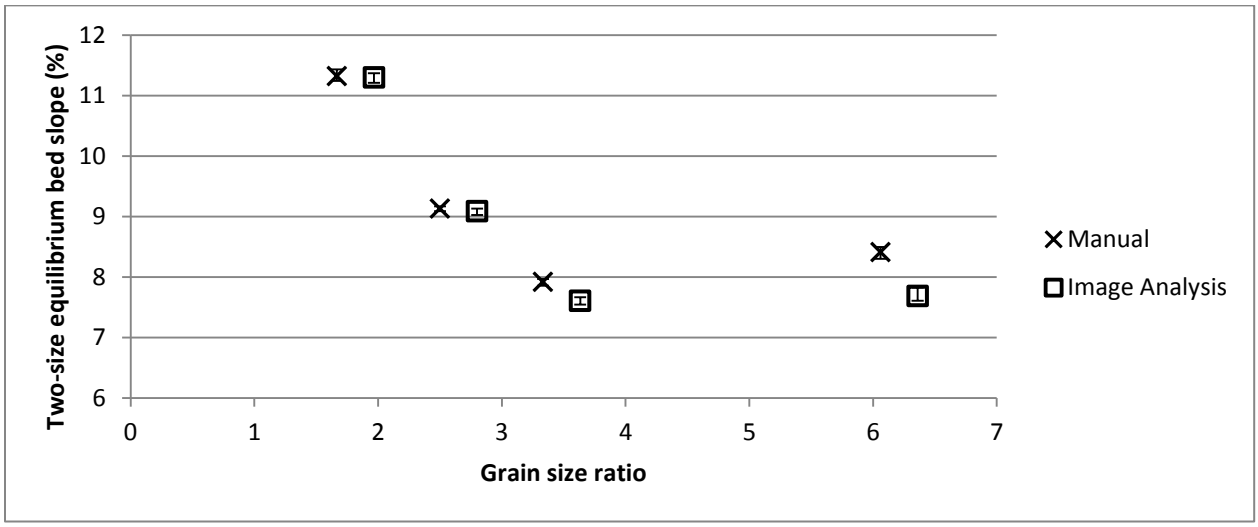

Figure 4.3 Comparison of the two-size equilibrium bed slope values measured manually and determined from image analysis for the experiments with a 41 % fine feed content*.

***The image analysis data have been offset by 0.3 (increased) on the x-axis to permit comparison of the data. For the manual measurements, the slope was calculated five times for each experiment. For both the manual and image analysis values, the range in the results falls within the symbols.**

4.3 Results

These experiments were designed to undertake a formal test of the reproducibility of the Irstea results. The majority of the experimental conditions at SFU were the same as at Irstea, however there were a few key differences. The flume at SFU was longer and made of different materials, the coarse grain feeder and water supply were less consistent, and the one-size equilibrium flow rate required for the 5 mm beads at a feed rate of approximately 2.2 g/s was lower. Overall, the

results from the Irstea experiments are qualitatively reproducible; suggesting that the same processes control the behavior in the two sets of experiments. The quantitative results were slightly different. It is expected that these slight differences are a result of the minor variations in the experimental conditions.

Following the fine grain introduction, the new sediment propagated downstream as a wave, infiltrating into the underlying bed where possible. The experiments with the 0.9 mm fines produced partially impeded static percolation profiles. The experiments with the 1.5 mm and 2 mm fines produced bridging profiles, and the introduced 3 mm fines were not able to infiltrate into the coarse bed by spontaneous percolation, as at Irstea. Once this initial wave of fine sediment had just moved through the camera visualization window, it was possible to measure the projected area of the bed which had been infiltrated due to spontaneous percolation. The results of this analysis for the experiments which were undertaken with a 41 % fine feed content are presented in Figure 4.4, alongside the results for the corresponding Irstea experiments to enable comparison. There is close agreement between the SFU and the Irstea results in Figure 4.4, although the SFU data consistently plot below the Irstea data.

The two-size equilibrium bed slopes (S_{eq}), measured manually, divided by the initial one-size equilibrium bed slope (S_o) for the Irstea and the SFU experiments are presented in Figure 4.5. The black dashed line indicates the $S_{eq}/S_o = 1$ condition; therefore experiments with data points above this line ($S_{eq}/S_o>1$) aggraded in response to the fine grain input, and experiments with data points below this line ($S_{eq}/S_o<1$) degraded. The SFU experiments appear to follow the same trends as the Irstea experiments, although full comparison is not possible as fewer experiments were undertaken in the SFU set. The SFU experiments consistently have a higher S_{eq}/S_o value, when compared to the Irstea experiments.

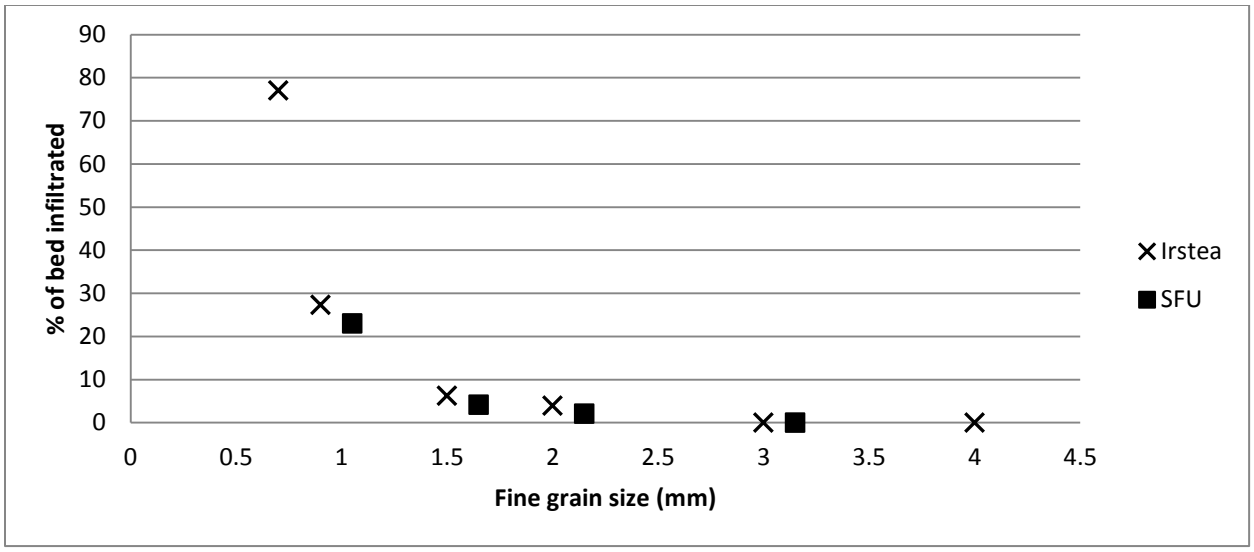

Figure 4.4 The projected area within the camera visualization window infiltrated purely due to spontaneous percolation immediately after the fine sediment infiltration wave had passed through the window. The figure permits comparison between the amount of infiltration in the Irstea and the SFU experiments*.

***The SFU experiments have been offset by 0.15 (increased) on the x-axis to permit clear visualization.**

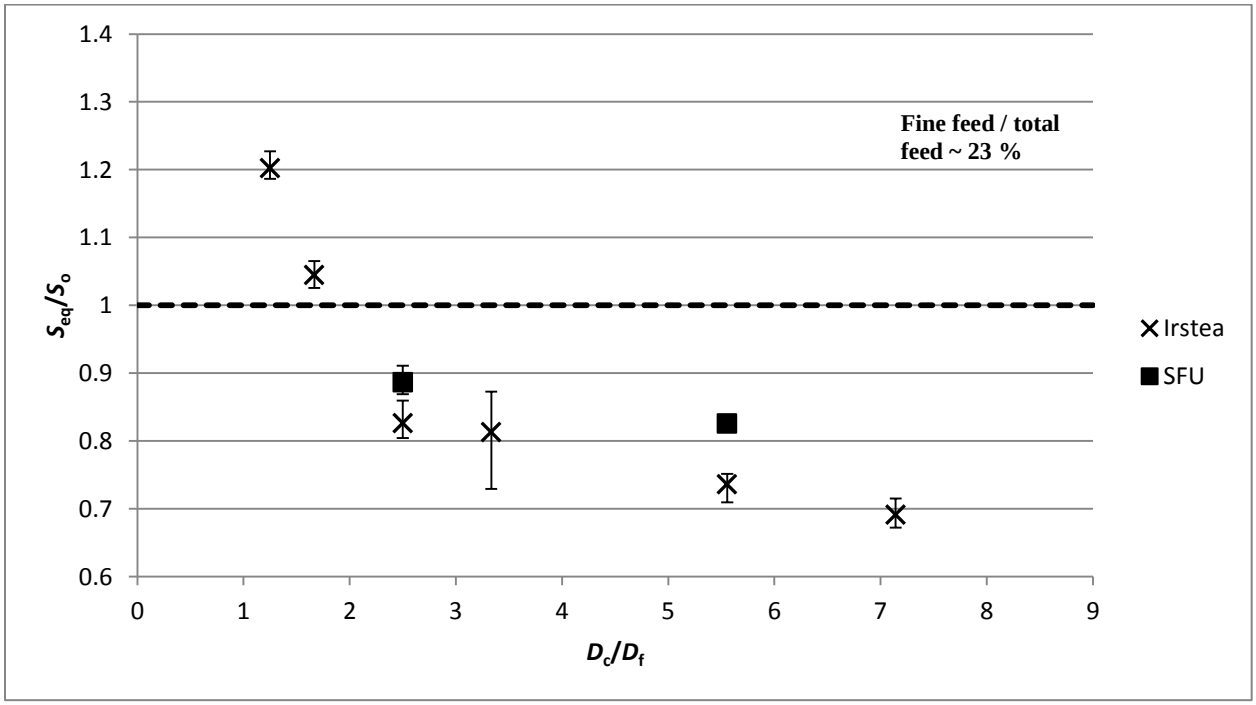

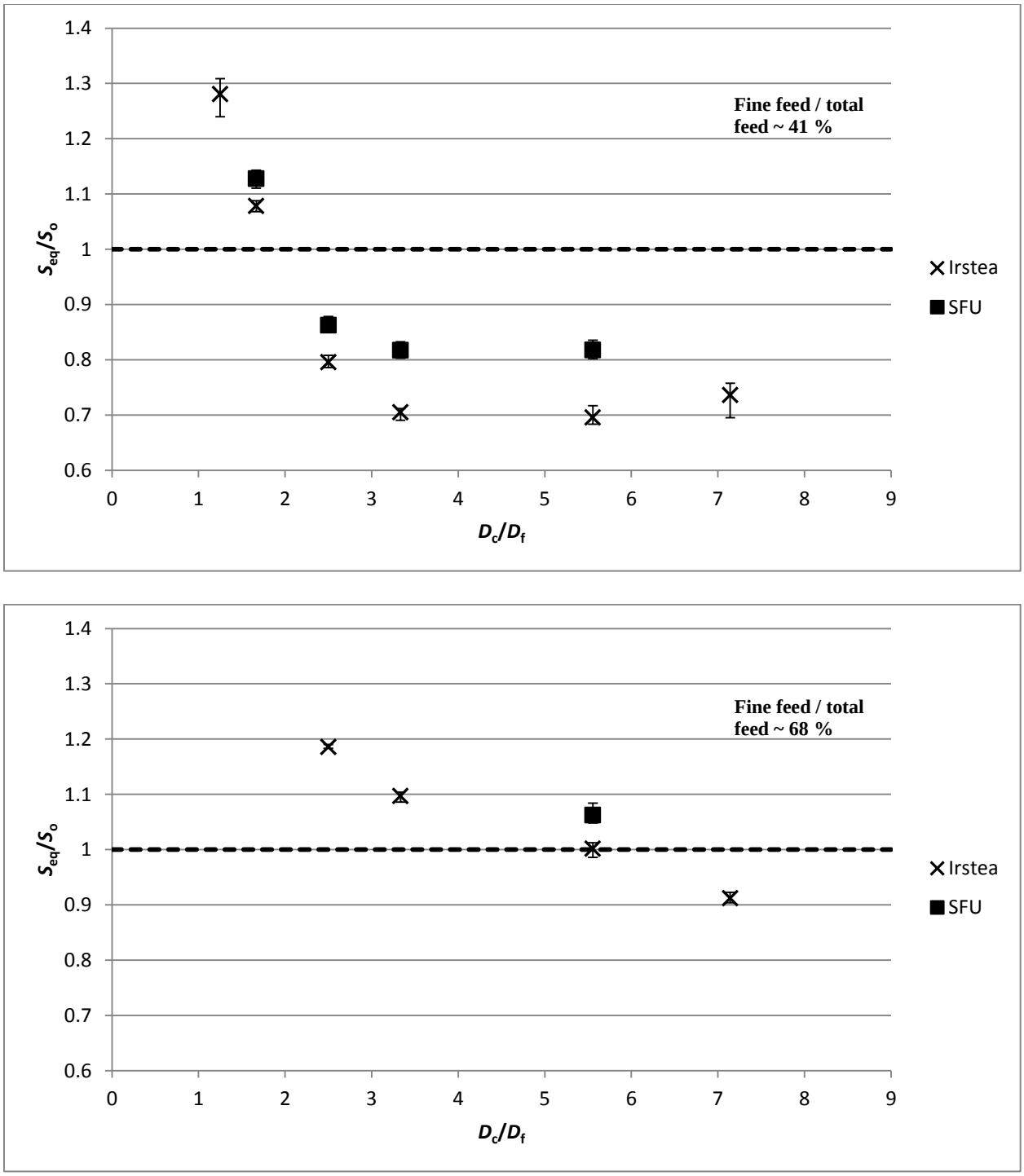

Figure 4.5 Two-size equilibrium bed slopes (S_{eq}), measured manually, divided by the initial one-size equilibrium bed slope (S_o) for the Irstea and the SFU experiments*.

*** For each experiment the slope was measured five times. Error bars show absolute range of measurements.**

Figure 4.6 presents the slope evolution curves over time, permitting further examination of the channel response to the fine grain input in the SFU experiments. Figure 4.6a presents the experiments undertaken with a variety of fine grain diameters, at a fine feed content of 41 %. The experiments with fine grain diameters of 0.9 mm and 1.5 mm show clear degradation in response to the fine grain input. The 2 mm experiment also exhibited degradation, but less than in the 0.9 mm and 1.5 mm experiments. In contrast the 3 mm fine grain input caused the channel to aggrade. Figure 4.6b shows the slope evolution curves for the experiments undertaken with a 0.9 mm fine feed component at a variety of fine feed concentrations. Clear degradation can be seen in the 23 % and 41 % fine feed content experiments. The two-size equilibrium slope in the 68 % case is very similar to the initial one-size equilibrium bed slope.

Further analysis of the experiments with a 0.9 mm diameter input was undertaken, examining the bed behaviour at 'time 1' and 'time 2' (labelled in Figure 4.6b). 'Time 1' is when the bed slope is still responding to the fine grain input, and 'time 2' is when the bed appears to be in two-size equilibrium in all of the experiments. As observed in the Irstea experiments, a positive relation between the fine feed content and the quasi-static fine layer thickness was exhibited in the SFU 0.9 mm experiments (see Figure 4.7), and with a thicker layer occurring at 'time 2', when the channel was in two-size equilibrium, than at 'time 1' when the bed was still responding to the fine grain input. The SFU 0.9 mm experiments also displayed a negative relation between the fine feed content and the number density of 5 mm bedload grains (see Figure 4.8); when the fine feed content was low the 5 mm bedload motion was 'congested', whereas when the fine feed content was high the motion was 'smooth'.

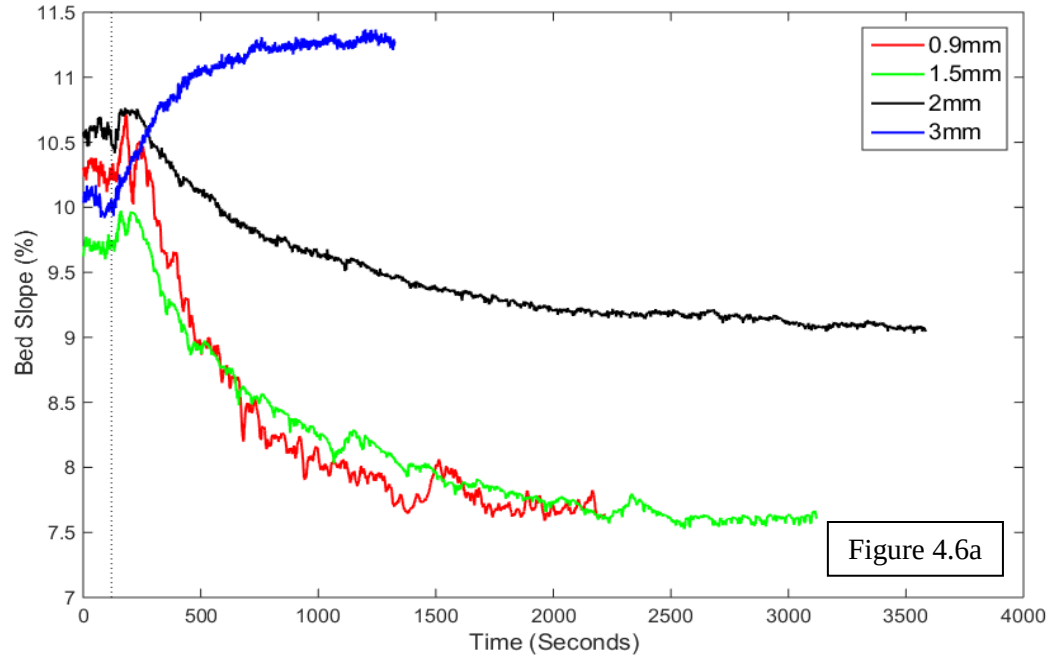

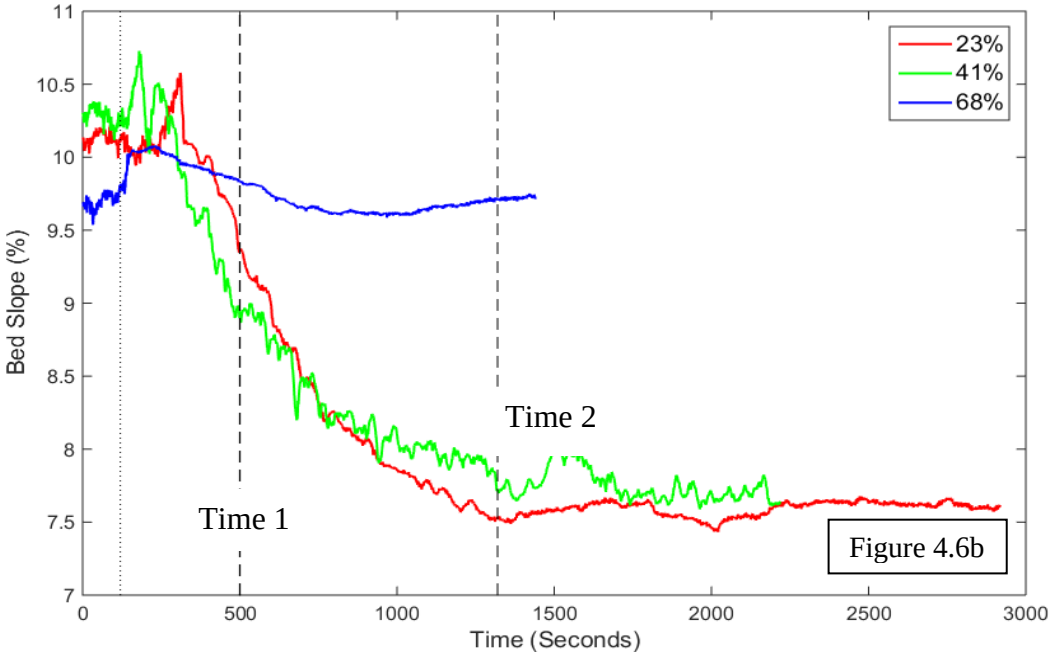

Figure 4.6 Bed slope evolution over time for the experiments with a 41 % fine feed content at a range of fine feed diameters (Figure 4.6a), and with a 0.9 mm fine grain size at a range of fine feed concentrations (Figure 4.6b)*.

*** 'Time 1' and 'time 2' are defined in the text. The fines were introduced to the channel after 120 seconds (indicated with vertical dotted line).**

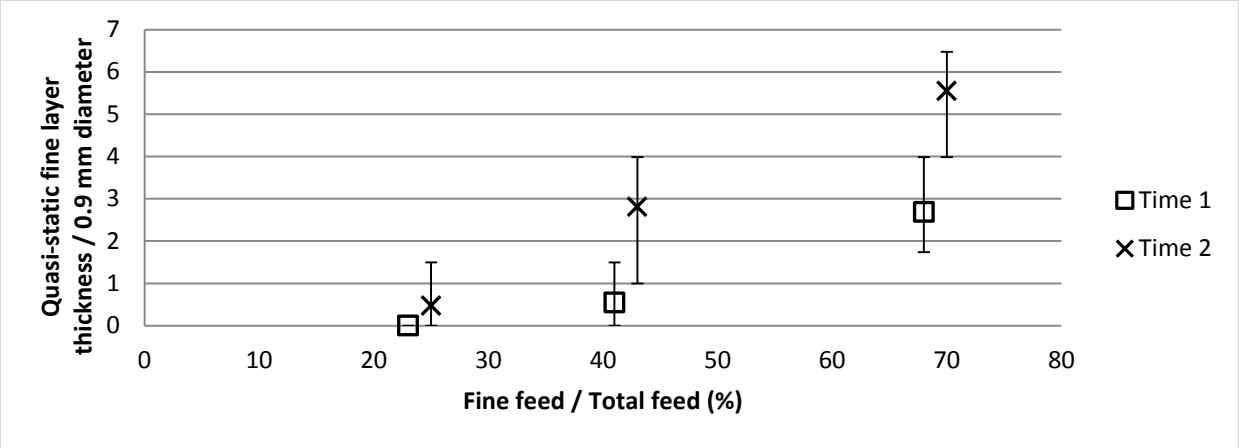

Figure 4.7 Quasi-static fine layer thickness for the 0.9 mm experiments at 'time 1' and 'time 2', divided by the fine grain diameter*.

***Measurements were taken at one second intervals, over 10 seconds, starting at 'time 1' and 'time 2'. The error bars show the range in the quasi-static fine layer thickness over these ten measurements. The 'time 2' data have been offset by 2 % (increased) on the x-axis to enable comparison.**

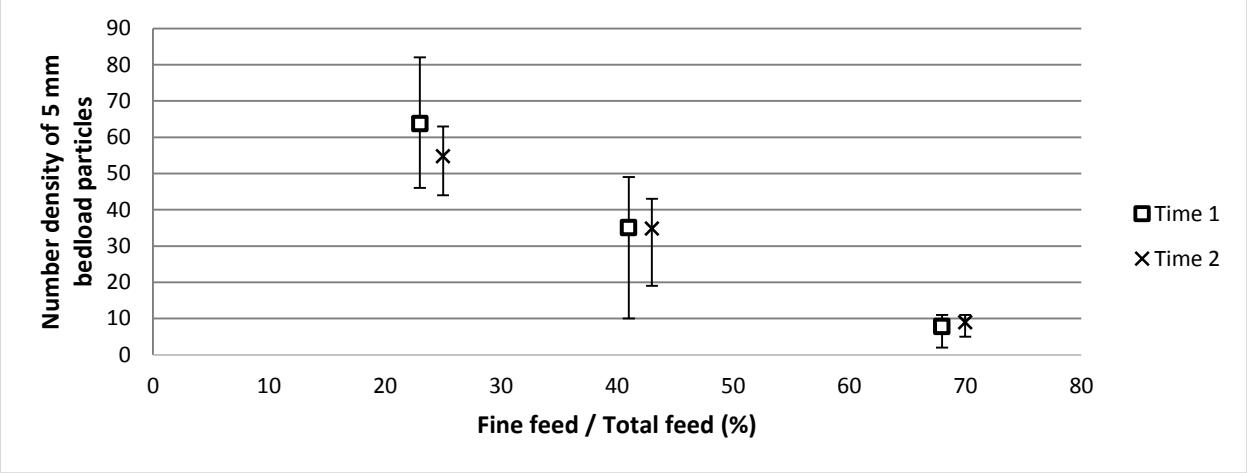

Figure 4.8 Number density of 5 mm bedload particles within the camera visualisation window for the 0.9 mm experiments at 'time 1' and 'time 2'*.

***The number density counted every 5 seconds, over two minutes, starting at 'time 1' and 'time 2'. The error bars show the range in number density over the twenty four measurements. The 'time 2' data have been offset by 2 % (increased) on the x-axis to enable comparison.**

4.4 Discussion

Whilst the experimental procedure at SFU mimicked that at Irstea as closely as possible, one key difference was the flow rate required for one-size equilibrium of the 5 mm beads at a feed rate of approximately 2.2 g/s. Whilst at Irstea a flow rate of 49.5 ml/s was required, at SFU approximately 40.3 ml/s was necessary. The reason for this dissimilarly is not known, but possible causes were put forward in Section 4.2.

Table 4.1 presents the hydraulic data for both sets of experiments. In the Irstea experiments, the flow rate was 23 % higher, the flow depth 19 % higher, and the side-wall corrected dimensionless shear stress 19 % higher. In both sets of experiments, electromagnetic flow meters were used to measure the flow rate, and consequently there is substantial confidence in these figures. However, defining and measuring the flow depth is very difficult in cases of such low submergence, resulting in uncertainty in the values. Where does one define the stationary bed line? Does one include the rolling beads or not? Over what time scale does one consider if the beads are moving? When the flow depth is much larger than the diameter of the grains, these decisions result in small potential errors in the flow depth measurements, but in these experiments these decisions result in large possible changes to the flow depth values. The flow depth values presented herein were measured with image analysis techniques. Using one frame per second for two minutes, the bed surface profile and the water line were detected using the methods described in Lafaye de Micheaux et al. (2015). The mean bed elevation was then subtracted from the mean water line to give an average flow depth. A different definition of the flow depth would potentially result in a difference in the flow depth, and therefore the values presented herein should be considered as rough estimates. The other hydraulic parameters presented in Table 4.1 are calculated using the flow rate and flow depth. Given the uncertainty in

the flow depth, there will also be considerable uncertainty in other parameters, including the side-wall corrected dimensionless shear stress.

Whilst the differences in the hydraulic parameters could be seen as an inconvenience, the consistency in the dominant processes between the two sets of experiments, despite the hydraulic differences, provides confidence in our observations. Following the introduction of fines to the channel, the infiltration characteristics were qualitatively the same for the two sets of experiments. The same infiltration profiles were formed at certain grain size ratios, and the projected area of the bed infiltrated due to spontaneous percolation increased with D_c/D_f. However, in the SFU experiments, for the same grain size ratios, the percentage of the projected area infiltrated due to spontaneous percolation was consistently lower than in the Irstea experiments. Huston and Fox (2015) found that a combination of the coarse bed porosity and roughness Reynolds number, indicating an influence by the pore water velocity distribution of the initially un-infiltrated coarse bed, was a good predictor of maximum bridging depth. Whilst the coarse bed porosity should be similar for the SFU and Irstea experiments, the roughness Reynolds number will have been higher in the Irstea experiments, providing an explanation for the larger amount of infiltration in that case.

The bed slope response was also qualitatively similar in the Irstea and SFU experiments, with the same trends emerging for the two-size equilibrium bed slope (S_{eq}) divided by the initial one-size equilibrium bed slope (S_o). However, the S_{eq}/S_o values are consistently higher in the SFU experiments when compared to the Irstea results. It is thought that this systematic difference is a result of the lower flow rate utilized in the SFU experiments.

In both the Irstea and the SFU experiments, the quasi-static fine layer thickness was shown to have a positive relation with the proportion of fines in the total feed. Additionally, as

seen in the Irstea experiments, the SFU experiments exhibited a thicker quasi-static fine layer when the bed was in two-size equilibrium compared to when the bed was still responding to the fine grain input. For the bed to degrade there must be interaction between the bedload layer and the underlying quasi-static coarse bed, which means the quasi-static fine layer must be relatively thin.

4.5 Conclusion

Experiments were undertaken to test the reproducibility of a preceding set of experiments, examining the response of a coarse grained mobile bed to a finer grain input, using spherical glass beads. Differences were apparent in the quantitative results between the two sets of experiments. The differences were consistent, and in this case, likely stem from the different flow rates required for the initial one-size equilibrium bed, which establishes flow (or shear stress) as an additional variate conditioning the quantitative expression of two-size mixture transport. Despite these differences, the overall processes controlling the channel response were the same; that is the experiments were qualitatively reproducible, as illustrated in the infiltration profiles formed and the channel behaviour.

Chapter 5: The influence of grain shape

The purpose of this chapter is to elucidate the influence of grain shape upon channel response to a finer grain input. This will be achieved through a series of experiments undertaken with natural materials. Both quantitative and qualitative comparison is undertaken between the experiments using spherical glass beads (presented in Chapters 2-4) and those using natural materials (this chapter).

5.1 Experimental Arrangements

The same experimental setup at SFU was used for these experiments as those presented in Chapter 4[1].

Two sets of experiments were undertaken:

(1) An intermediate set of experiments utilizing spherical glass beads for the coarse component (5±0.3 mm diameter), and natural materials for the fine component. This set of experiments will be referred to as SFU_{mix}.

(2) A set of experiments utilizing natural materials for both the coarse and fine components. This set of experiments will be referred to as SFU_{nat}.

The natural materials were sourced from the Fraser River and west Jericho beach, both near Vancouver, British Columbia, Canada. The material from west Jericho beach consists of fine gravel and sand sourced from the Fraser River. During the SFU_{nat} experiments, the diameter of the coarse component was fixed at 4 mm (3.55 – 4 mm). The diameter of the fine component

[1] The experiments presented in Chapter 4 using spherical glass beads, will be referred to as SFU_{beads}.

varied: diameters of D_{50} = 0.6 mm (0.5 – 0.63), 0.8 mm (0.8 – 0.9 mm), 2 mm (1.8 – 2 mm) and 3 mm (2.8 – 3.15 mm) were used. Figure 5.1 is a photograph of the 4 mm natural sediment illustrating the variability in particle shape.

Figure 5.1 Photograph of the natural 4 mm diameter sediment.

In the SFU_{mix} experiments with the spherical, transparent, glass beads, it was possible to observe the behaviour of the sediment in the bed at a high level of detail using the Manta© camera. However, in the experiments with the natural materials, the Manta© camera was limited in its ability to capture detailed images of the bed as it is black-and-white. In order to capture more information about the experiments with natural materials, a digital Sony Alpha 58 SLR colour camera was also used to record the experiments.

5.2 Experimental Procedure

The same two-stage experimental procedure was undertaken as in Chapter 4: (1) one-size equilibrium was achieved using the coarse grains (see Table 5.1 for details). To ensure the input

rate was approximately equal to the output rate, two two-minute samples of the sediment output were taken. In the experiments with the spherical glass beads, the output rate was always within 9 % of the input rate, with the exception of one sample, from one experiment, which had a 18 % difference between the input and output rate. In the experiments with natural materials, the output rate was always within 11 % of the input rate. The nominal coarse feed rate and the flow rate were not changed throughout the experiment. (2) Fines of a fixed diameter and a fixed feed rate were introduced into the channel (see Table 5.2 for details on SFU_{mix} and Table 5.3 for details on SFU_{nat}). The bed response to the fine grain input was filmed using the cameras.

Once the bed had reached a new, two-size equilibrium state, the bed slope was measured both manually and using image analysis. The manual measurements were undertaken using the same method as outlined for the Irstea experiments (see Section 2.2 for details). The two-size equilibrium slope values from the image analysis in the preceding chapters were determined by calculating the mean, maximum and minimum values after the slope had stabilised. For the SFU_{nat} experiments, this was difficult as, in several of the experiments, the slope did not become stable (see results and discussion). Therefore, the two-size equilibrium slope value for the image analysis in these experiments was determined by finding the mean, maximum and minimum values over the final four minutes of the recording. As manual measurements were taken over approximately four minutes, both sets of measurements should be compared over the same time period. Figure 5.2 presents the slopes measured manually and using image analysis for the experiments undertaken with a 41 % fine feed content for the SFU_{nat} experiments. Good agreement can be seen between the two types of measurement.

Table 5.1 Experimental conditions for one-size equilibrium*.

Experimental Description	Mean flow rate (mL/s)	Mean coarse feed rate (g/s)	Mean flow depth, h (mm)	Submergence ratio (h/D_c)	Side-wall corrected dimensionless shear stress	Mean Velocity, U (m/s)	Froude Number ($\frac{U}{\sqrt{gh}}$)	Kinematic viscosity, ν (mm^2/s)	Reynolds Number ($\frac{4UR_h}{\nu}$)
Irstea	49.5	2.22	8.02 ± 0.38	1.6 ± 0.18	0.076 ± 0.011	0.60 ± 0.03	2.14 ± 0.15	0.8926	8420 ± 237
SFU_{beads} and SFU_{mix}	40.3 ± 1.16	2.24 ± 0.12	6.75 ± 1.23	1.35 ± 0.31	0.064 ± 0.023	0.59 ± 0.14	2.31 ± 0.84	1.1386	6001 ± 859
SFU_{nat}	68.05 ± 0.55	2.24 ± 0.07	12.07 ± 0.63	3.21 ± 0.35	0.157 ± 0.021	0.55 ± 0.02	1.59 ± 0.12	1.1386	6945 ± 202

***D_c is the diameter of the coarse grains (5±0.3 mm for the spherical glass beads, and 4 mm (3.55-4 mm) for the natural materials). Details of how the hydraulic parameters were calculated are given in Appendix B. Details of the Irstea experiments have been included for comparison.**

Table 5.2 Experimental conditions for SFU_{mix}

Experiment number	Fine grain diameter (D_f) (mm)	Grain size ratio (D_c/D_f)	Coarse grain feed rate (g/s)	Fine grain feed rate (g/s)	Fine feed rate/ Total feed rate (%)	Average initial one-size equilibrium bed slope, S_o (%)
S.8	0.6	8.33	2.27	0.67	22.8	9.57
S.9	0.6	8.33	2.21	1.6	42.0	9.48
S.10	0.6	8.33	2.22	4.67	67.8	9.72
S.11	0.8	6.25	2.26	0.68	23.1	10.05
S.12	0.8	6.25	2.26	1.58	41.1	10.12
S.13	2	2.5	2.25	0.7	23.7	10.28
S.14	2	2.5	2.24	1.55	40.9	9.86
S.15	3	1.67	2.25	1.54	40.6	9.95

Table 5.3 Experimental conditions for SFU_{nat}

Experiment number	Fine grain diameter (D_f) (mm)	Grain size ratio (D_c/D_f)	Coarse grain feed rate (g/s)	Fine grain feed rate (g/s)	Fine feed rate/ Total feed rate (%)	Average initial one-size equilibrium bed slope, S_o (%)
S.16	0.6	6.67	2.25	0.67	22.9	10.67
S.17	0.6	6.67	2.24	1.62	42.0	10.49
S.18	0.6	6.67	2.24	4.66	67.5	10.09
S.19	0.8	5	2.17	0.62	22.2	10.42
S.20	0.8	5	2.24	1.57	41.2	10.46
S.21	0.8	5	2.27	4.62	67.1	10.26
S.22	2	2	2.24	0.69	23.5	10.17
S.23	2	2	2.29	1.61	41.3	10.25

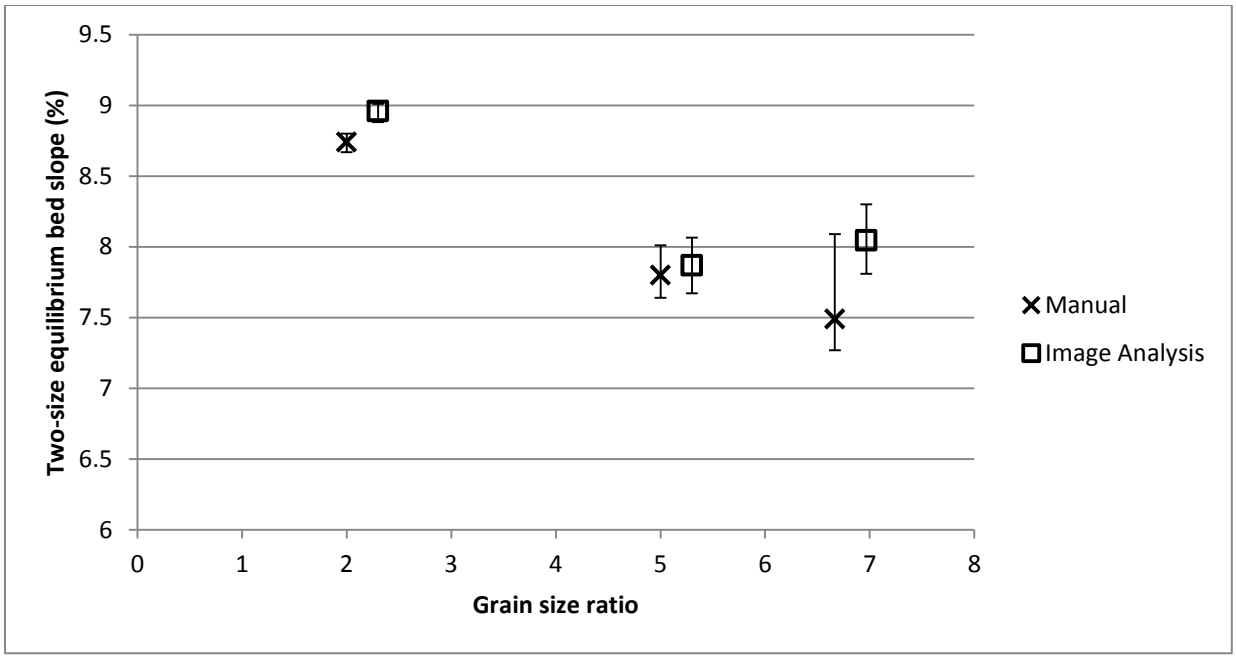

Figure 5.2 Comparison of the two-size equilibrium bed slope values measured manually and determined from image analysis for the experiments with a 41 % fine feed content for the SFU_{nat} experiments*.

*** The image analysis data have been offset by 0.3 (increased) on the x-axis to permit comparison of the data. For the manual measurements, the slope was calculated five times for each experiments and the range in the results is shown in the error bars.**

5.2.1 Supporting Information

The phenomena described in this chapter were identified from the experimental videos taken with the Sony Alpha 58 SLR colour camera. Clips taken from these video recordings can be accessed at: http://hdl.handle.net/2429/59561

The details of these clips are reported in Appendix D.

5.3 Results

5.3.1 Mixed Experiments

The SFU_{mix} experiments utilized spherical glass beads with 5 mm diameter for the coarse component, and natural materials for the fine component. The aim of these experiments was to provide an intermediate step between the SFU_{beads} experiments which utilized spherical glass beads for both the fine and coarse component, and the SFU_{nat} experiments which utilized natural materials for both components. The differences and similarities between the SFU_{mix}, and the SFU_{beads} and Irstea experiments will be discussed in this section.

The results of the two two-minute samples taken to confirm that the bed was in two-size equilibrium for the SFU_{mix} experiments are presented in Table 5.4. The percentage difference between the input rate and the output rate is consistently less than 9 %, with the exception of one sample in Experiment S.15.

The use of natural material for the fine component in the SFU_{mix} experiments introduce a shape factor. Comparison of the infiltration profiles formed, and the projected area of infiltration due to spontaneous percolation, during the SFU_{mix}, Irstea and SFU_{beads} experiments is shown in Table 5.5 and Figure 5.3 respectively. Table 5.5 illustrates that all the experiments exhibited a transition from bridging when D_f = 2 mm to no spontaneous percolation when D_f = 3 mm. The diameter of the finest grains introduced differed slightly between the three sets of experiments. However, in all the experiments, partially impeded static percolation occurred when $D_f \leq 0.9$ mm. Additionally, it can be seen in Figure 5.3 that the projected area of the bed infiltrated purely due to spontaneous percolation in the SFU_{mix} experiments is consistent with the values from the Irstea and SFU_{beads} experiments.

Table 5.4 Percentage difference between the input rate and the output rate during two two-minute samples (SFU_{mix}).

Experiment number	Fine size (mm)	Fine feed / total feed (%)	Fine sediment		Coarse sediment	
			Percentage difference in sample 1 (%)	Percentage difference in sample 2 (%)	Percentage difference in sample 1 (%)	Percentage difference in sample 2 (%)
S.8	0.6	22.8	0.48	3.97	2.61	2.28
S.9	0.6	42.0	1.70	0.05	-2.12	1.25
S.10	0.6	67.8	-2.58	-2.6	-2.09	-2.10
S.11	0.8	23.1	-4.63	-2.14	1.04	1.40
S.12	0.8	41.1	-3.32	-4.69	-3.99	-2.99
S.13	2	23.7	-2.90	0.35	3.87	3.70
S.14	2	40.9	-1.39	-8.94	0.58	0.00
S.15	3	40.6	-8.22	-24.93	-1.84	-1.58

Table 5.5 Infiltration profiles formed by the fine sediment during the Irstea, SFU_{beads} and SFU_{mix} experiments with a variety of fine grain diameters[*].

Fine grain diameter (mm)	Irstea	SFU_{beads}	SFU_{mix}
0.6			Partially impeded static percolation
0.7	Partially impeded static percolation		
0.8			Partially impeded static percolation
0.9	Partially impeded static percolation	Partially impeded static percolation	
1.5	Bridging	Bridging	
2	Bridging	Bridging	Bridging
3	No spontaneous percolation	No spontaneous percolation	No spontaneous percolation

[*]For all of the experiments, the coarse component was formed of spherical glass beads of 5 mm diameter. Boxes are blank where no experiment was undertaken.

Despite the similarities in the infiltration characteristics, the two-size equilibrium bed slopes which resulted from fine grain inputs in the SFU_{mix} experiments differed when compared to the values exhibited in the Irstea and SFU_{beads} experiments; see Figure 5.4. For the cases in which a partially impeded static percolation profile occurred, the two-size equilibrium bed slope was lower than expected in the 23 % fine feed concentration experiments, in line with previous results in the 41 % experiments, and higher than expected in the 68 % experiments (only 0.6 mm

data, D_c/D_f =8.33, is presented for the 68 % case). For the 2 mm bridging case, the slope was in line with previous results for the 23 % fine feed experiments, but higher than expected for the 41 % experiments. The 3 mm experiment resulted in a higher than expected two-size equilibrium bed slope.

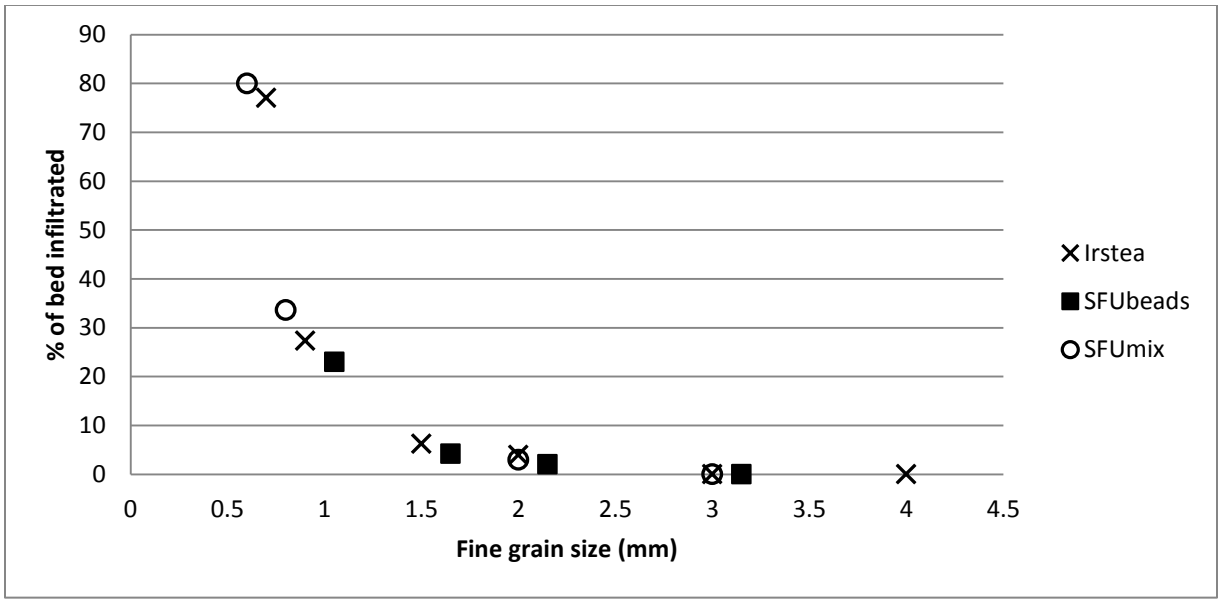

Figure 5.3 The projected area within the camera visualization window infiltrated purely due to spontaneous percolation immediately after the fine sediment infiltration wave had passed through the window. The figure permits comparison between the amount of infiltration in the Irstea and the SFU_{beads} and SFU_{mix} experiments*.

***The SFU_{beads} experiments have been offset by 0.15 (increased) on the x-axis to permit clear visualization.**

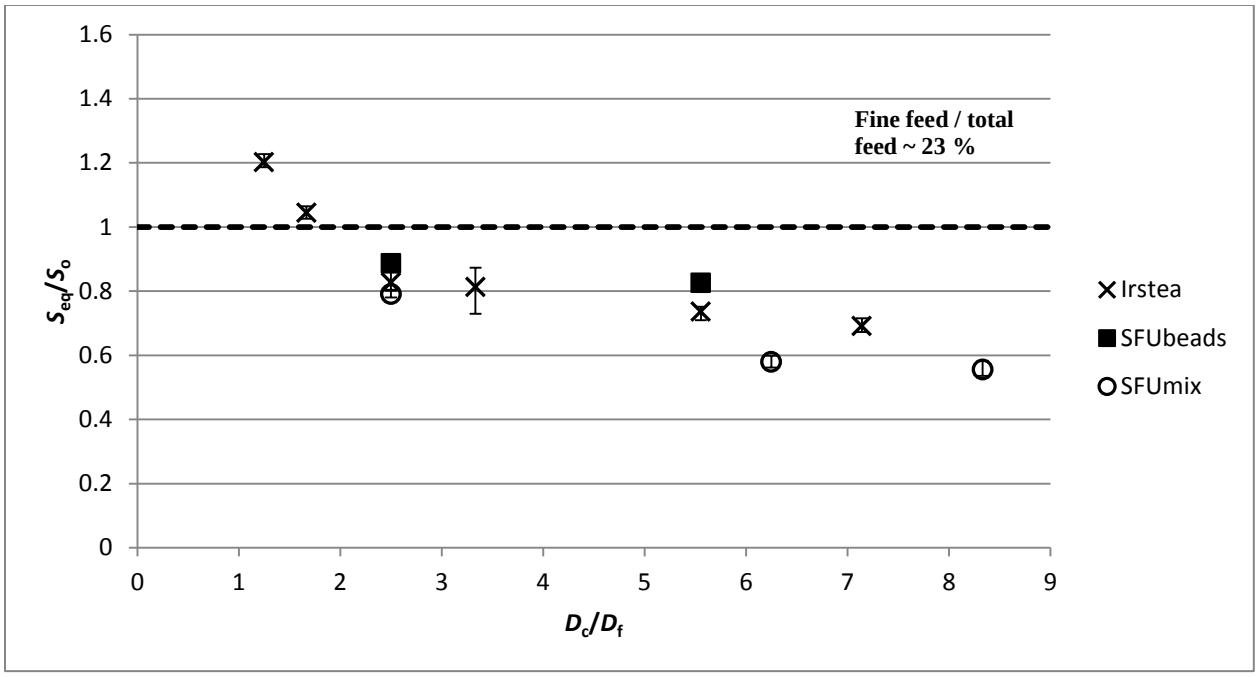
Fine feed / total feed ~ 23 %
S_{eq}/S_o
D_c/D_f
Irstea
SFUbeads
SFUmix

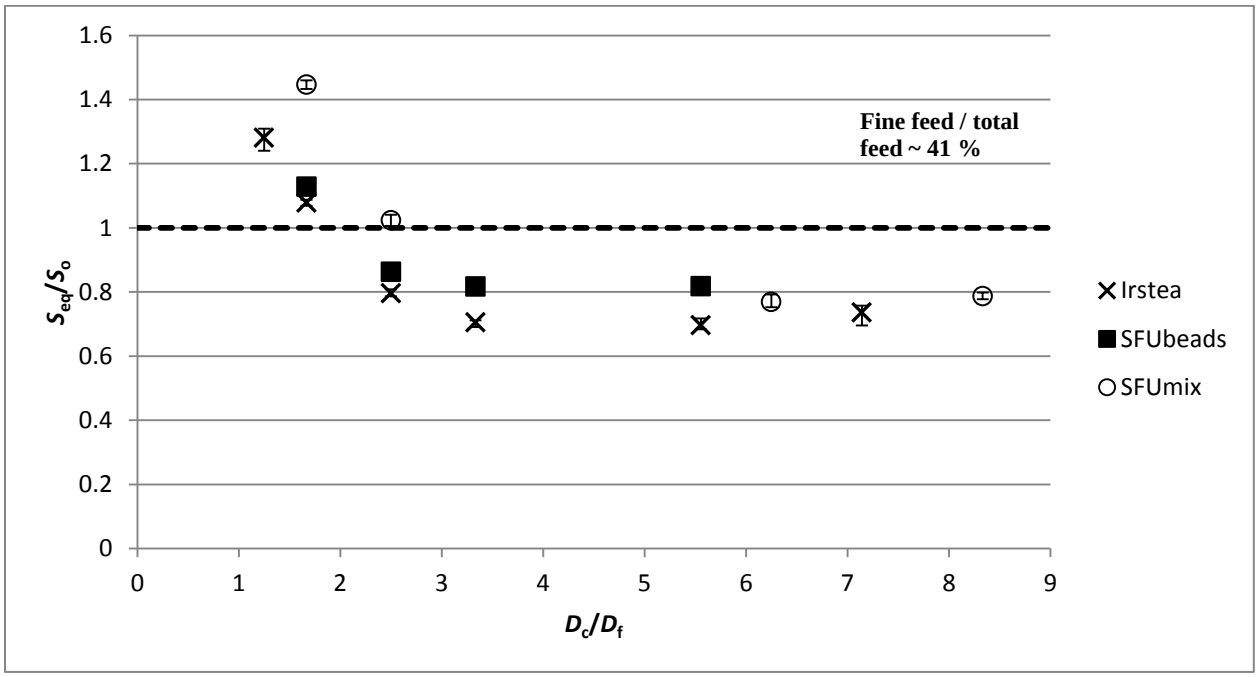
Fine feed / total feed ~ 41 %
S_{eq}/S_o
D_c/D_f
Irstea
SFUbeads
SFUmix

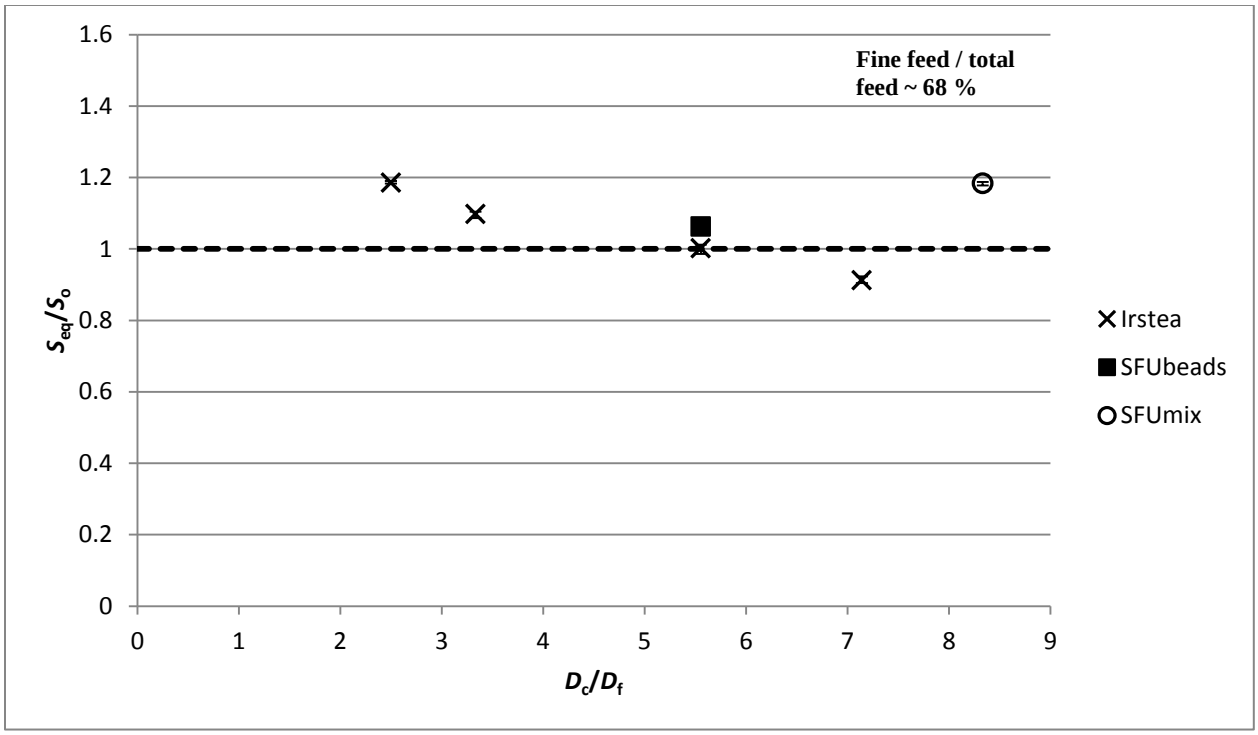

Figure 5.4 Two-size equilibrium bed slopes (S_{eq}), measured manually, divided by the initial one-size equilibrium bed slope (S_o) for the Irstea, SFU_{beads} and SFU_{mix} experiments*.

***For each experiment the slope was measured five times. Error bars show the absolute range of measurements.**

5.3.2 Natural Materials

The SFU_{nat} experiments were undertaken using natural sediments for both the fine and coarse component, introducing an additional shape factor compared to the SFU_{mix} experiments. In each experiment, before the fine feed was introduced, a two-minute recording of the 4 mm grains in one-size equilibrium was taken (video clip: Video_S14). Figure 5.5 illustrates the characteristic, undulating bed structure of the one-size equilibrium bed. When the bed was in one-size equilibrium, the average local intergrain roughness was approximately $0.4D_c$, and the longer wavelength bed undulations were on average approximately $1.65D_c$ in amplitude, and reached a

maximum of approximately $3D_c$. The water surface was in phase with the bed surface, fitting the general description of antidunes, which are common on steep slopes (Knighton, 1998).

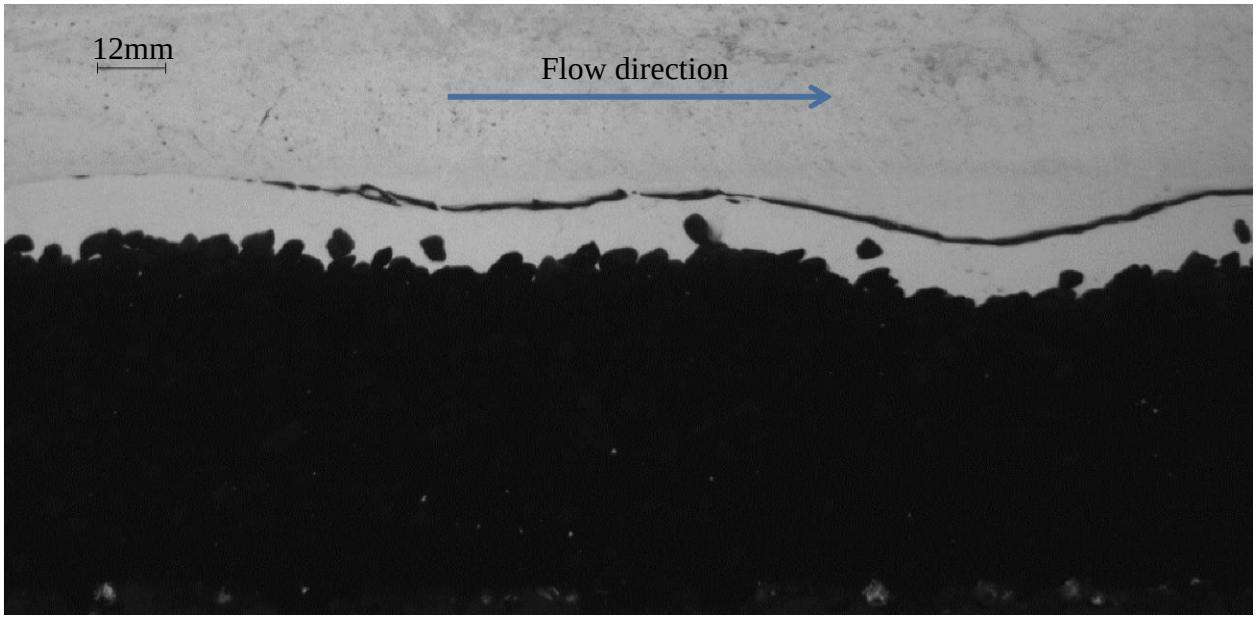

Figure 5.5 Image from the high-speed Manta© camera of the bed in one-size equilibrium during the SFU_{nat} experiments.

After the fines were introduced to the channel, they migrated downstream, during which time they infiltrated into the underlying quasi-static coarse bed where feasible (supporting videos: Video_S15, Video_S16 and Video_S17). Table 5.6 presents the infiltration profiles formed by the fine grains within the coarse bed for the SFU_{nat} experiments, along with the profiles formed during the Irstea, SFU_{beads} and SFU_{mix} experiments. For the SFU_{nat} experiments, a bridging profile was exhibited in the experiment with a grain size ratio (D_c/D_f) of 6.67. For the other sets of experiments (Irstea, SFU_{beads} and SFU_{mix}), partially impeded static percolation was exhibited for grain size ratios smaller than 6.67.

Table 5.6 Infiltration profiles formed by the fine sediment during the Irstea, SFU_{beads}, SFU_{mix} and SFU_{nat} experiments*.

Grain size ratio (D_c/D_f)	**Irstea**	**SFU_{beads}**	**SFU_{mix}**	**SFU_{nat}**
8.33			Partially impeded static percolation	
7.14	Partially impeded static percolation			
6.67				Bridging
6.25			Partially impeded static percolation	
5.56	Partially impeded static percolation	Partially impeded static percolation		
5.0				Bridging
3.33	Bridging	Bridging		
2.5	Bridging	Bridging	Bridging	
2.0				No spontaneous percolation
1.67	No spontaneous percolation	No spontaneous percolation	No spontaneous percolation	

***For the Irstea, SFU_{beads} and SFU_{mix} experiments, the coarse component was formed of spherical glass beads of 5 mm diameter. For the SFU_{nat} experiments, the coarse component was formed of natural sediment of 4 mm diameter. Boxes have been left blank when no experiment was undertaken.**

The two-size mixture bedload motion was intriguing in the 0.6 mm and 0.8 mm experiments with a fine feed proportion of 23 % and 42 %, and in the 2 mm experiment with a fine feed proportion of 23 % (supporting videos: Video_S18, Video_S19, Video_S20). In these experiments, the bed surface profile was often undulating as a result of collections of the two-size sediment load coming to rest, and then moving downstream together. The collection of bedload upon the bed surface produced peaks, between which were troughs. Within the collections of bedload material, the coarse particles rested upon a base of fine sediment. An example of these structures is shown in Figure 5.6. These collections of bedload migrated downstream, in a stop-start fashion. An undulating bed surface during these experiments is also present during the initial condition of the 4 mm material in one-size equilibrium. In both cases, the water surface profile matched the bed surface profile.

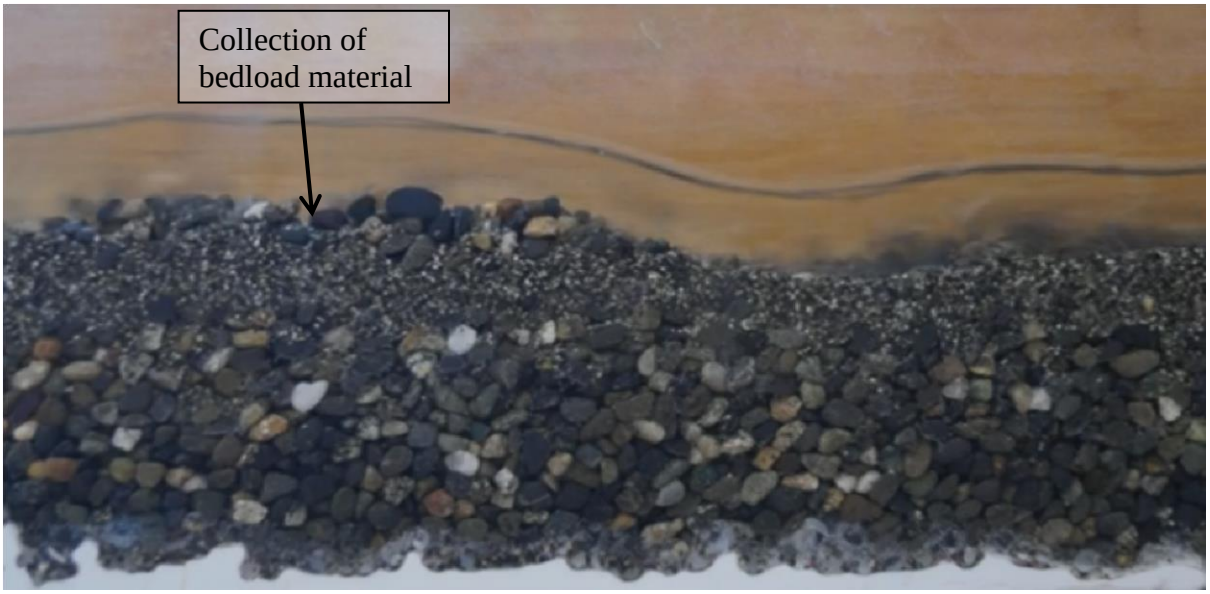

Figure 5.6 Image from the SLR camera of the undulations in the bed surface during the SFU_{nat} Experiment S.17 (D_f =0.6 mm, fine feed/total feed = 42 %). Flow from left to right.

Examination of the experimental videos revealed the dynamics of the collections of bedload (see Video_S21). For the collection of bedload to form, the first coarse particle came to rest, often on the upward slope of a trough. Further particles built up behind this grain, with the fine grains at the base, due to kinetic sieving, and the coarse grains on top. This collection of grains grew, both in height and length. As the flow moved over these grains, it plunged onto the bed just downstream of the coarse grain which initiated the collection, evacuating the sediment from the bed surface and creating a trough. The creation of this trough often removed the fine grains from the bed surface and revealed the underlying quasi-static coarse bed (see Figure 5.7). During the formation of the collection of bedload, not all of the coarse bedload arriving in the area joined the collection and became static; part of the coarse bedload continued to move downstream, saltating overtop. Entrainment from the underlying quasi-static coarse bed often occurred within the trough (depending upon the thickness of the fine layer remaining upon the bed surface), particularly due to collisions with the saltating grains moving downstream. The creation of the trough and the accumulating sediment resulted in the collection of bedload tending towards a convex shape. The initial grain was therefore on the downward slope of the downstream trough, with a relatively small pivoting angle. Eventually, the initiating grain was knocked, usually by a saltating coarse grain, causing the structure to collapse and the sediment to move downstream, where the process repeated. As the collection of grains moved downstream through the trough, it often caused entrainment from the quasi-static bed.

Figure 5.7 Image from the SLR camera of a trough forming during the SFU_{nat} Experiment S.17 (D_f =0.6 mm, fine feed/total feed = 42 %). Flow from left to right.

The undulations in the bed surface profile during these experiments due to the sediment moving as collections are apparent when examining the slope evolution profiles (see Figure 5.8). Due to these undulations, determining when the bed reached equilibrium was challenging. Two two-minute samples were taken to confirm that the sediment input rate was approximately equal to the sediment output rate; the results are presented in Table 5.7. Despite the overall slope appearing stable, there were large, short term, differences between the sediment input and output rates as the transport rate varied dramatically over time in experiments S.16, S.17, S.19, S.20 and S.22.

In the experiments when the undulations were not present (example: Video_S22), the style of bedload motion was similar to the bead experiments. The difference between the sediment input rate and the sediment output rate for experiments S.18, S.21 and S.23 was always less than 3 %.

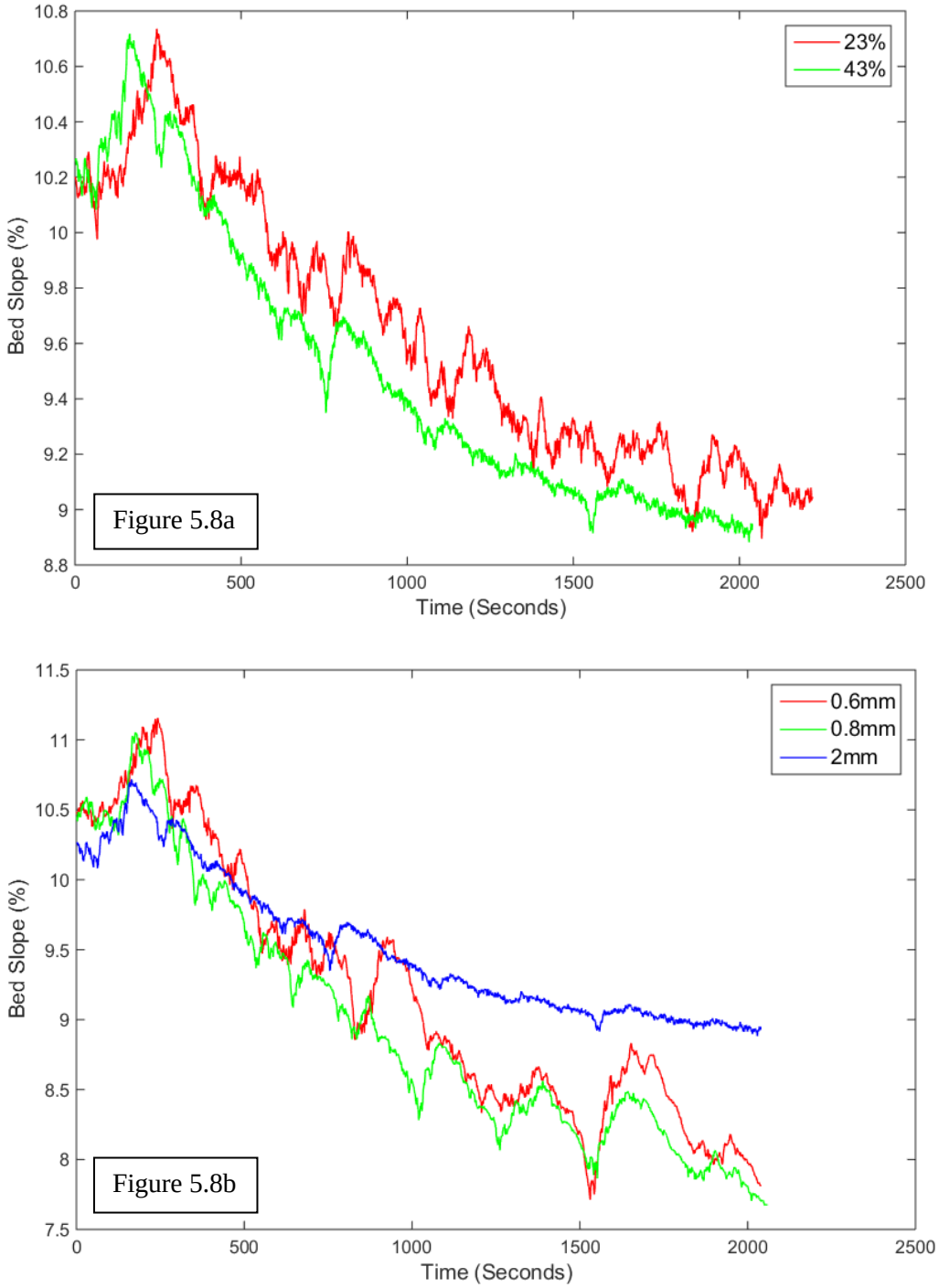

Figure 5.8 Bed slope evolution over time for the experiments with a 2 mm grain input at a range of fine feed concentrations (Figure 5.8a), and with a 42 % fine feed content at a range of fine grain diameters (Figure 5.8b)*.

***The fines were introduced to the channel after 120 seconds.**

Table 5.7 Percentage difference between the input rate and the output rate during two, two-minute samples (SFU_{nat})*.

Experiment Number	Fine size (mm)	Fine feed rate / total feed rate (%)	Fine sediment		Coarse sediment	
			Percentage difference in sample 1 (%)	Percentage difference in sample 2 (%)	Percentage difference in sample 1 (%)	Percentage difference in sample 2 (%)
S16	0.6	22.9	-26.62	5.43	-21.47	3.27
S17	0.6	42.0	-90.97	23.59	15.98	19.84
S18	0.6	67.5	-2.81	-2.60	-1.85	-1.16
S19	0.8	22.2	3.82	141.24	23.73	30.24
S20	0.8	41.2	-58.94	58.16	-44.64	35.86
S21	0.8	67.1	-1.67	-0.97	2.49	0.24
S22	2	23.5	-33.03	5.31	-3.68	2.12
S23	2	41.3	-1.06	-0.67	1.86	2.07

***The experiments in which the undulations were not present are highlighted in yellow.**

In order to examine the repeatability of the two-size equilibrium bed slopes measured for experiments S.16, S.17, S.19 and S.20, an additional set of experiments was undertaken, as detailed in Table 5.8. The difference between the input and output rate during the two two-minute samples taken at the end of the repeat experiments were in a similar range to the original experiments. However, the S_{eq}/S_o values were comparable, providing confidence (see Table 5.9).

Table 5.8 Experimental conditions for the repeat experiments.

Fine grain diameter (D_f) (mm)	Grain size ratio (D_c/D_f)	Coarse grain feed rate (g/s)	Fine grain feed rate (g/s)	Fine feed rate/ Total feed rate (%)	Initial one-size equilibrium bed slope, S_o (%)
0.6	6.67	2.24	0.68	23.3	10.14
0.6	6.67	2.25	1.6	41. 6	10.34
0.8	5	2.24	0.63	22.0	10.18
0.8	5	2.28	1.6	41.2	10.29

Table 5.9 S_{eq}/S_o values for the original and repeat experiments.

Original experiment number	S_{eq}/S_o values	
	Original experiment	Repeat experiment
S.16	0.92±0.03	0.93±0.03
S.17	0.71±0.06	0.70±0.04
S.19	0.82±0.02	0.86±0.04
S.20	0.75±0.02	0.74±0.02

The manually measured bed slopes for the SFU_{nat} experiments are presented in Figure 5.9. The relation between S_{eq}/S_o and fine feed/total feed contains differences compared to those exhibited in the previous experiments (Irstea, SFU_{beads} and SFU_{mix}). In the previous experiments, a generally positive relation existed between S_{eq}/S_o and fine feed/total feed, although the values at 23 % and 41 % fine feed content were often very similar. However, in the SFU_{nat} experiments, the S_{eq}/S_o value is lower at 41% fine feed content than at 23% fine feed content, for all of the grain size ratios examined. However, S_{eq}/S_o is then higher at 68 % fine feed content than at 41 %

content, agreeing with the previously observed positive relation. The SFU_{nat} S_{eq}/S_o results are plotted alongside the other experimental sets in Figure 5.10. Overall, the SFU_{nat} data fits well with the S_{eq}/S_o values from the other experiments. Although the 0.6 mm experiment (D_c/D_f = 6.67) in the 23 % case degraded less than expected.

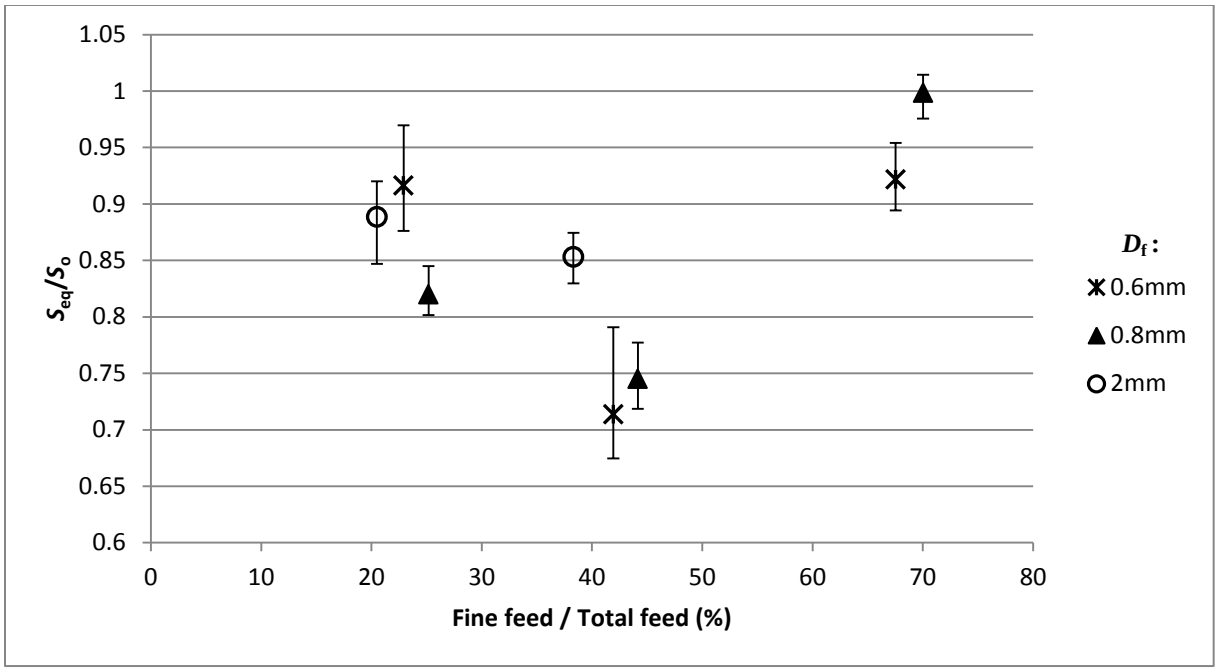

Figure 5.9 Two-size equilibrium bed slopes (S_{eq}), measured manually, divided by the initial one-size equilibrium bed slope (S_o) for the SFU_{nat} experiments*.

*** The 0.8 mm data have been offset by 3 % (increased), and the 2 mm data by 3 % (decreased) on the x-axis to permit comparison. For each experiment the slope was measured five times. Error bars show absolute range of measurements.**

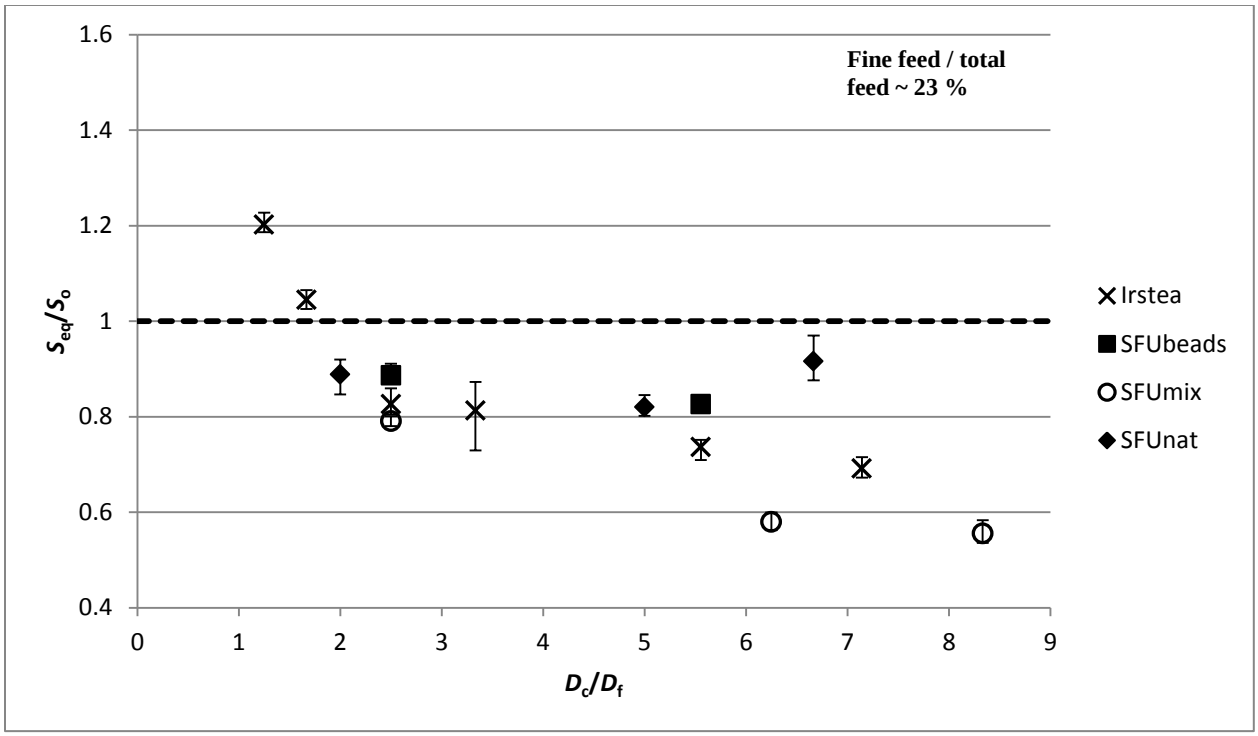
Fine feed / total feed ~ 23 %
1.6
1.4
1.2
1
0.8
0.6
0.4
0
1
2
3
4
5
6
7
8
9
S_{eq}/S_o
D_c/D_f
Irstea
SFUbeads
SFUmix
SFUnat

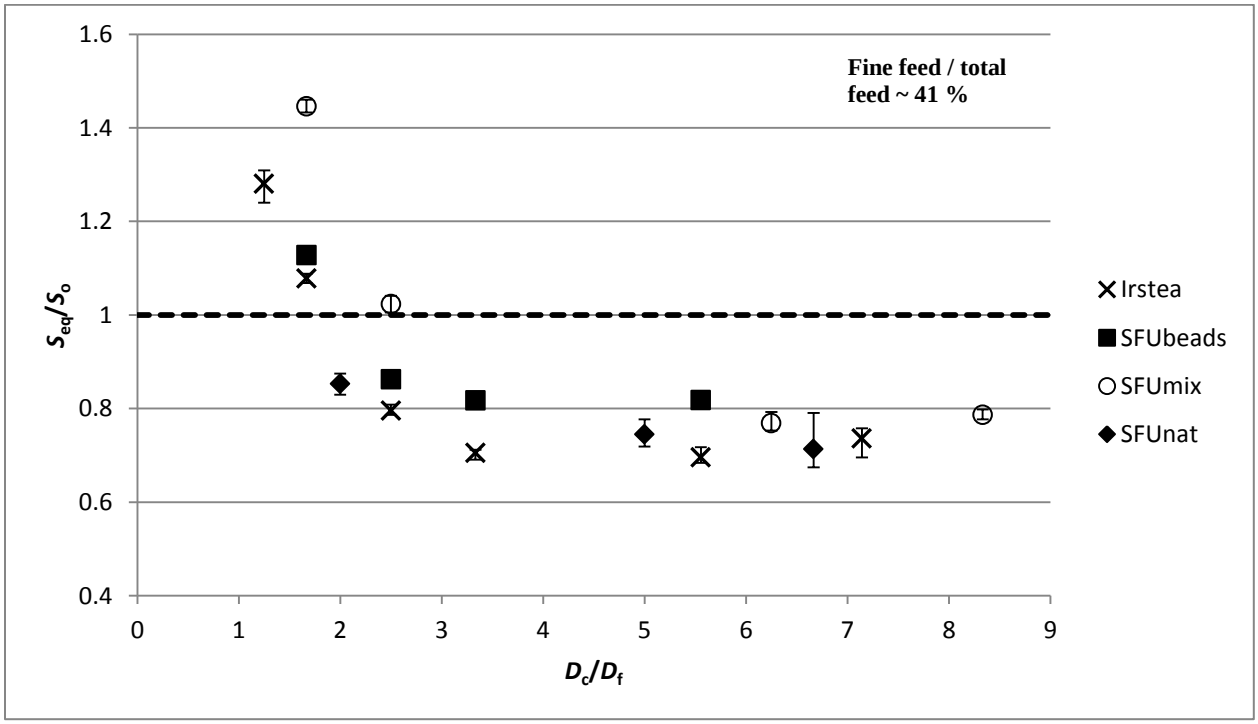
Fine feed / total feed ~ 41 %
1.6
1.4
1.2
1
0.8
0.6
0.4
0
1
2
3
4
5
6
7
8
9
S_{eq}/S_o
D_c/D_f
Irstea
SFUbeads
SFUmix
SFUnat

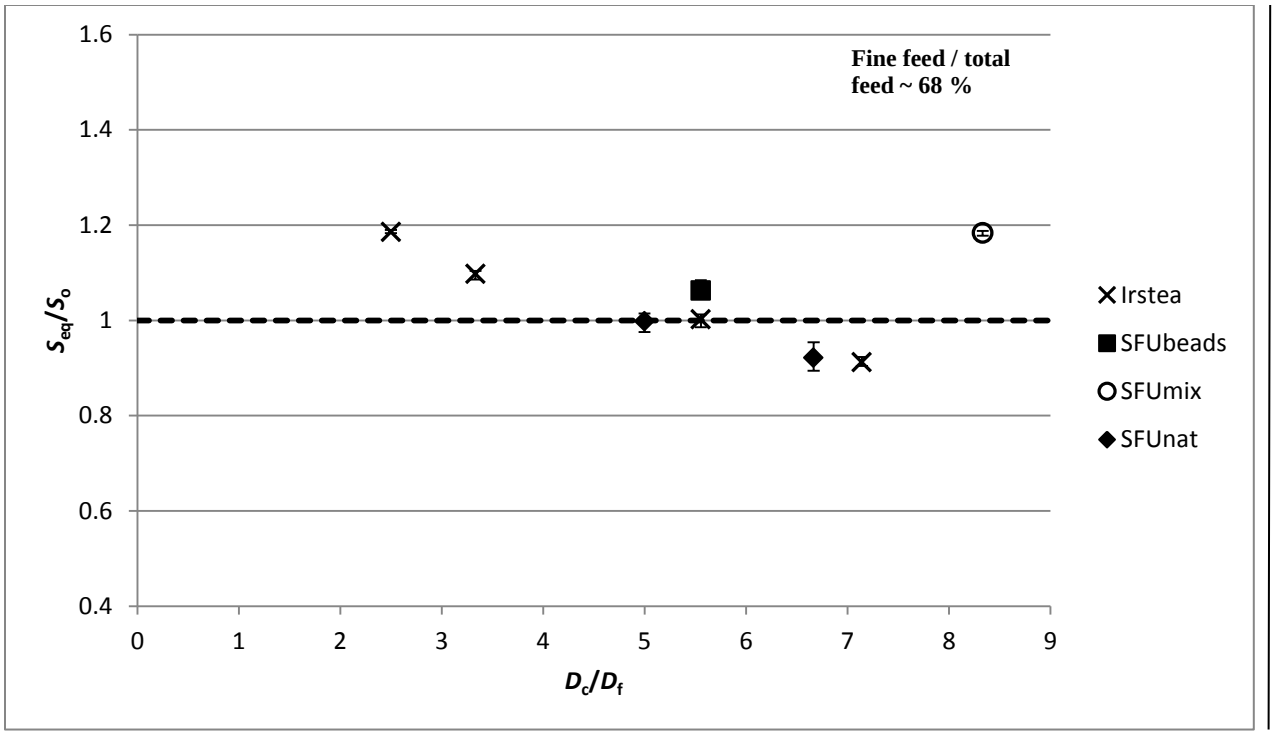

Figure 5.10 Two-size equilibrium bed slopes (S_{eq}), measured manually, divided by the initial one-size equilibrium bed slope (S_o) for the Irstea, SFU_{beads}, SFU_{mix} and SFU_{nat} experiments*.

***For each experiment the slope was measured five times. Error bars show absolute range of measurements.**

5.4 Discussion

The SFU_{mix} experiments were undertaken as an intermediate step, exploring the influence of using natural fines instead of the fine spherical glass beads with the same one-size equilibrium conditions as the SFU_{beads} experiments; the same flow rate and therefore side-wall corrected non-dimensionalised shear stress for the initial condition. Consequently, it can be assumed that any differences between the results in the SFU_{beads} and SFU_{mix} experiments are due to the change in fine particle shape.

In some cases, the natural fine grain size differed slightly from the size of the fine spherical glass particles, but in both sets of experiments 2 mm and 3 mm fines were utilized. The

boundary between bridging and no spontaneous percolation was the same in the SFU_{beads} and SFU_{mix} experiments; the 2 mm fine introduction resulted in the development of a bridging profile, and the 3 mm fine introduction was unable to spontaneously percolate into the bed. For the SFU_{beads} experiments, the largest fine grain size for which a partially impeded static percolation profile was formed was 0.9 mm, and the same profile was formed using the 0.8 mm fines in the SFU_{mix} experiments. Additionally, the percentage of the projected area of the bed infiltrated due to spontaneous percolation in the SFU_{mix} experiments is consistent with what is expected from the SFU_{beads} and Irstea experiments. Overall, the transitions between the different infiltration profiles occur at comparable grain size ratios, within the resolution of the ratios employed. However, as a continuous range of ratios has not been tested, it is possible that fine-scale differences may be exhibited between the examined ratios.

Differences in the S_{eq}/S_o values could be seen for the SFU_{mix} experiments when compared to the SFU_{beads} experiments, suggesting that the channel response is influenced by the fine particle shape. The relation between S_{eq}/S_o and the proportion of fines in the total feed appeared to be exaggerated in the SFU_{mix} experiments (see Figure 5.4). At 41 % fine feed proportion for the partially impeded static percolation profiles, and at 23 % proportion for the bridging experiment, the S_{eq}/S_o values were in line with the values expected. Yet around these values, the positive relation between the fine feed proportion and S_{eq}/S_o is exaggerated compared to the SFU_{beads} experiments. In attempting to understand why this exaggeration occurs, it is necessary to consider how the factors which cause an enhancement in sediment mobility following a fine grain input may be influenced by the fine particle shape.

In the 0.6 mm and 0.8 mm experiments, with a 23 % fine feed content, the bed degraded to a greater extent than expected. It is possible that this is due to an influence of the underlying

particle shape upon the pivoting angle of a grain. Although it has been suggested that the shape of the underlying material influences the pivoting angle (e.g. Kirchner et al., 1990), it appears that no tests elucidating the impact of this factor alone have been undertaken. Miller and Byrne (1966) compared the results from their experiments with those of Eagleson and Dean (1959), suggesting that a difference in the pivoting angle of a sphere between the experiments was due to a difference in the underlying bed material, however, these two sets of experiments were not undertaken in consistent conditions and were for uniform materials (diameter of the grain was the same as the diameter of the material forming the bed). It is hypothesized that, for a spherical bead, the pivoting angle required for entrainment may be lower when the finer underlying grains are natural material compared to when they are spherical glass particles. The natural grains were classified by their intermediate axis[1], however, they may lie flat on the bed surface with their smallest axis exposed, consequently reducing the pivoting angle.

The higher than expected S_{eq}/S_o values in many of the SFU_{mix} experiments may be a result of the flow structure. One of the reasons for the enhancement in sediment mobility following a fine grain input to a coarse bed is the smoother surface leading to flow acceleration close to the bed, therefore increasing drag force (Venditti et al., 2010b). The natural fine surface is likely to be rougher compared to the spherical glass particles, which may reduce the effective drag force. This reduced drag force, particularly in the high fine feed content experiments, may cause the larger than expected S_{eq}/S_o values. Further experiments which examine the flow properties would enable this hypothesis to be confirmed or disputed.

[1] The intermediate axis is also an imperfect measure (Church, 2003).

The SFU_{nat} experiments were undertaken using natural materials for both the coarse and fine components. Use of natural material for the coarse component added an additional shape factor when compared to the SFU_{mix} experiments. The initial conditions for the SFU_{nat} experiments were different to those in the SFU_{beads} and SFU_{mix} experiments. To achieve one-size equilibrium with the 4 mm natural grains at approximately 2.2 g/s, the flow rate required was much higher than for the 5 mm spherical glass beads. The requirement of a higher flow rate is likely attributable to the particle shape; Komar and Li (1986) found that the pivoting angle depends upon the grain shape; specifically, the grains 'rollability' which they assessed as the ratio of the intermediate axis diameter (D_b) to the short axis diameter (D_c), and the angularity of the grain which may result in interlocking. A higher D_b/D_c results in a larger pivoting angle, therefore spherical particles are easier to entrain than ellipsoids (Li and Komar, 1986).

The transitions between the different infiltration profiles in the SFU_{nat} experiments did not occur at comparable grain size ratios to the bead experiments. A contributory reason could be that the coarse component of the natural materials was classified by the intermediate axis, which is an imperfect measure (Church, 2003). A bridging profile was exhibited when $D_c/D_f = 6.67$ in the SFU_{nat} experiments. Whilst a partially impeded static percolation profile occurred at a smaller grain size ratio in the SFU_{mix} (D_c/D_f=6.25) and SFU_{beads} experiments (D_c/D_f=5.56). The use of natural materials for the coarse component will have modified the pore sizes and shapes within the bed, with the results demonstrating that the bed became harder to infiltrate. This result is in agreement with Frostick et al. (1984), which found that pore shape exerts an influence over the spontaneous percolation behaviour.

The use of natural materials for the coarse component modified the behavior of the bedload in the 0.6 mm and 0.8 mm experiments with a fine feed proportion of 23 % and 41 %,

and in the 2 mm experiment with a fine feed proportion of 23 %. The movement of the bedload as a collection, migrating downstream, has been observed previously by other researchers. The motion we observe is very similar to that which can be seen in the videotapes of the experiments from Curran and Wilcock (2005a). In their videos the formation of the collection of bedload, the bed surface profile, and the eventual collapse and downstream movement of the grains, exhibit dynamics analogous to those described in Section 5.3.2. The size of the collections of bedload in the videotapes from the Curran and Wilcock (2005a) experiments are greater than those observed during our experiments, which may be attributable to their larger channel and widely sorted sediment.

These collections of moving bedload share some similarities with the characteristic behavior of 'bedload sheets' (Whiting et al., 1988) (not to be confused with the term 'sheet flow'). Once entrained, the transport of sediment in gravel bed rivers has been observed to occur in the form of migrating patches (Nelson et al., 2009). These migrating patches were first documented by Whiting et al. (1988), and termed 'bedload sheets'. 'Bedload sheets' have been observed to be 1-2 grains in height, have a length to height ratio of between 25 and 300, with coarse fronts and fining material towards the tail. Recking et al. (2009) proposed that bedload sheets are produced due to vertical and longitudinal sorting within the bed, which results in periodic aggradation and scour of the bed locally. The coarse particles come to rest as they become caught in the wake of other coarse particles; this accumulating collection of coarse grains forms the front of the bedload sheet (Whiting et al., 1988). The sheet then migrates due to a "catch and mobilise process" according to Whiting et al. (1988). The "catch and mobilise process" occurs when the fine sediment moves across the coarse grains which form the front of the bedload sheet, and infiltrate into the interstices. The arrival of the fines then remobilises the

coarse grains and cause the sheet to migrate downstream. Nelson et al. (2009) proposed that the size ratio (D_c/D_f) between the fine and coarse sediment plays an important role in the behaviour of the bedload sheets, as it will control how the fines infiltrate into the coarse framework. Nelson et al. (2009) also observed that sediment supply had an important influence upon the bedload sheets, with a reduction in supply leading to a reduced migration rate and larger spacing between the sheets.

Bedload sheets have been linked to the spatial and temporal variations in transport rate (Whiting et al., 1988; Nelson et al., 2009; Recking et al., 2009). Nelson et al. (2009) proposed that the passage of the head of the bedload sheet containing the coarse material would result in high sediment transport rates, whilst the space between bedload sheets and the tail material would cause low sediment transport rates.

Similarities between our observations and those of characteristic bedload sheets are: (1) The length of the structures is much greater than the height, in agreement with the observations of Whiting et al. (1988). (2) The periodic aggradation and scour occurring locally, which was documented by Recking et al. (2009), was present. (3) An influence of both grain size ratio and sediment supply, noted by Nelson et al. (2009), was observed in these experiments. (4) Large variations in the transport rate occurred, leading to sizeable disparity between the sediment input rate and the sediment output during the two two-minute samples at the end of the experiments.

Differences between the bedload structures we observed and the characteristic behavior of bedload sheets were also present. Within typical bedload sheets downstream fining occurs within each sheet. This characteristic was not present within the bedload sheets we observed in the SFU_{nat} experiments as the sediment was finely graded bimodal material.

As the bedload did not move as a collection in the bead experiments, this behaviour may be attributable to the natural coarse-grain particle shape. Interestingly, the conditions under which this behaviour arose coincides with the conditions under which the bed was congested in the bead experiments. The coarse particle shape in the natural material experiments may have caused an exaggeration of this congested behaviour, resulting in the migrating collections of bedload.

The question of confirming equilibrium remains an issue in cases when the bedload moves as collections, causing surging behaviour. This behaviour makes it difficult to confirm a stable output (see Table 5.7) or a stable slope (see Figure 5.8). In our experiments, empirical evidence for the two-size equilibrium slope is given by the repeat experiments. However, in previous experiments (e.g. Iseya and Ikeda, 1987; Ikeda and Iseya, 1988; Curran and Wilcock, 2005b), two-size equilibrium slope values have been reported, with no evidence that the bed slope was stable at this time, or even fell within a range of possible values. In the reporting of those experiments, feed and transport rates have been provided, but there is often a large disparity between the values, the potential implications of which have not been discussed.

The SFU_{nat} experiments with $D_c/D_f = 2$ were of particular importance. During these experiments, the fine sediment did not infiltrate into the coarse bed. However, both of the experiments undertaken with this grain size ratio, at 23 % and 41 % fine feed content, degraded in response to the fine grain input. In contrast to experiments using spherical glass beads when the fines were unable to spontaneously percolate into the underlying bed, the input of the fines in the SFU_{nat} $D_c/D_f = 2$ experiment did not result in the formation of a quasi-static fine layer upon the bed surface which isolated the underlying bed. Instead the bedload layer continued to interact

with the underlying bed, with the fine grains moving into any available space due to kinetic sieving, resulting in the channel degradation (see Video_S23).

The relation between S_{eq}/S_o and the fine feed content was different in the SFU_{nat} experiments when compared the SFU_{beads} and SFU_{mix} results. In the SFU_{nat} experiments, the S_{eq}/S_o values demonstrated that the channel degraded further in the experiments with a 41 % fine feed content than in those with a 23 % content. However, the experiments with a 68 % fine feed content degraded less than those with the 41 % content. This behavior suggests an inflection point occurs between a fine feed content of 23 % and 68 %. Similar behavior was observed by Ikeda and Iseya (1988); in an experiment with a grain size ratio of 5, an inflection point was observed at approximately 43 % fine feed content, and in another experiment with a grain size ratio of 7.03, an inflection point was observed at approximately 54 % content.

5.5 Conclusion

Experiments exploring the consequences of using natural sediment rather than spherical glass beads demonstrated that particle shape has an important quantitative impact upon the channel response to a fine grain input.

The first set of experiments utilized spherical glass beads as the coarse component and natural sediment for the fine component. The infiltration profiles formed, and the percentage of the bed infiltrated are comparable to the experiments undertaken using spherical glass beads for both components. However, the use of natural materials for the fine component resulted in different two-size equilibrium bed slopes compared to the experiments where both the fine and coarse component were formed of spherical glass beads.

In the second set of experiments, natural materials were utilized for both the fine and coarse component. In these experiments, important differences arose compared to the experiments using spherical glass beads. The change in pore shape and size, as a result of the bed being formed of natural material, resulted in reduced amounts of infiltration. Additionally, the behaviour of the bedload in some of the experiments with natural materials was more complex, with migrating collections of bedload occurring. However, overall, the S_{eq}/S_o values from the SFU_{nat} experiments are comparable with the results from the other experimental sets.

Chapter 6: Perspectives and Conclusion

The simplified experiments undertaken for this research have enabled us to focus upon the control exerted by grain-grain interactions when a channel is responding to a fine grain input. A reductionist approach to the problem was chosen in order to amplify our understanding of what happens in the field by focusing upon a key element of the phenomena in order to gain understanding at a fundamental level. Although there are limitations associated with simplified physical models, a great deal of useful information can be derived from their use.

6.1 Perspectives

In Chapter 2 the difference between previously observed grain size ratios at which certain vertical infiltration profiles arise and the boundaries occurring during this research with spherical glass beads was highlighted. The transition we observe between spontaneous percolation with the 2 mm fines, and no spontaneous percolation with the 3 mm fines, can be understood in consideration of the packing arrangements of uniform spheres. The 5 mm packing arrangement in the bed was haphazard (Gray, 1968), and we can assume similar to Scott and Kilgour's (1969) 'random close packing'. However, it is known that boundaries cause particles to pack less densely, which is likely to be a factor in the present experiments due to the narrow flume. Allen (1982) showed that, with a void fraction of 0.3954, the largest possible sphere ($D_{f,max}$) which can fit into the largest void in a packing arrangement of spheres (D_c), is $D_c/D_{f,max} = 1.895$ – close to our value of 1.67 (which may not be the critical limit) for non-infiltration. When $D_c = 5$ mm, then the largest possible sphere in the void space is 2.64 mm. Hence the 2 mm particles (D_c/D_f of 2.5) are able to infiltrate into a 5 mm bed, but the 3 mm particles cannot. This is the first time, to

the author's knowledge, that agreement between the theoretical packing behavior of spheres and processes in fluvial sedimentation has been demonstrated.

The experiments in this research involved feeding fines of different diameters, at a variety of feed rates, and examining the influence upon the bed slope. In some cases, the fine grain input resulted in an enhancement of coarse grain mobility so great that the output rate initially surpassed the input rate, and the channel degraded. In other cases, the bed aggraded in response to the fine grain input. By varying the grain size ratio and the fine sediment feed concentration, the roughness of the bed and the total supply to the channel varied between the experiments. These factors will have had an influence upon how the channel responds to the fine grain input. However, this research also identified a distinct physical control upon the channel response. Demonstration that the transition between a fine grain input causing degradation and aggradation is a function of the infiltration and grain sorting characteristics has not previously been documented.

The findings from these experiments have important implications for the field of fluvial geomorphology. The findings have demonstrated the importance of examining the infiltration processes as they may provide essential information regarding sediment transport. The significance of the infiltration behaviour upon channel response suggests substantial complications in the computation of sediment transport rates.

6.2 Conclusions

Simplified flume experiments were undertaken to address a series of research questions. Questions 1 to 5 form the main research goals. Questions 6 and 7 are auxiliary questions, designed to address wider concerns.

Question 1: The main body of research on kinetic sieving has been undertaken in an industrial context. What are the defining characteristics of this sorting process in a fluvial context?

Kinetic sieving – a previously under-studied process in fluvial geomorphology – occurs in the moving bed surface; the fine sediment is displaced to the bottom of the bedload layer, and the coarse sediment moves to the top. The process is similar to that described by Savage and Lun (1988) for dry granular materials in an inclined free surface flow. Consequently, the body of knowledge formulated for industrial purposes is apt to be applicable to fluvial contexts.

Question 2: A bed with a mobile surface will be subject to both spontaneous percolation and kinetic sieving. How do the two sorting processes interact and influence each other? Is the previously observed spontaneous percolation behaviour modified by the presence of a mobile bed surface?

Question 3: How does grain size ratio (D_c/D_f) impact upon spontaneous percolation and kinetic sieving processes in a bed with a mobile surface?

Below the moving bedload layer is a quasi-static bed. When the grain size ratio permits, the fine sediment infiltrates into the quasi-static deposit through spontaneous percolation. For all of the grain size ratios explored during these experiments (D_c/D_f from 7.14 to 1.25), kinetic sieving takes place in the bedload layer. However, the amount of infiltration and the fine sediment profile formed within the static coarse framework bed due to spontaneous percolation will depend upon the deposit geometry, grain size distribution and the amount of remaining void space. A summary of the behavior and the controlling grain size ratios for the experiments undertaken using spherical glass particles is given in Figure 2.9.

Following the input of fines to the mobile bed, under certain circumstances the bed degrades. For the bed to degrade, quasi-static grains have to be entrained. Grain-grain collisions between the coarse bedload and the quasi-static coarse grains were observed to be essential for entrainment to occur. When a quasi-static coarse grain is nudged by a grain in motion, fines move into the previously occupied space. When the movement of the coarser grain results in an opening of a previously blocked, uninfiltrated void space, additional spontaneous percolation by the fine sediment may occur into the bed. Consequently, the mobile bed surface increases the amount of spontaneous percolation into the bed and mobilizes additional coarse grains.

Question 4: How does grain size ratio influence sediment mobility within the bed?

Question 5: Can changes in mobility at different grain size ratios be explained by the sorting processes? (The purpose of the research is not to simply observe the effect of changing the grain size ratio upon the mobility, but to understand the cause).

Changes in sediment mobility were determined in the experiments by monitoring the bed slope adjustment following the fine grain input. The bed slope adjustment varied depending upon the grain size ratio between the bed and the fine grain input. The larger the grain size ratio, the greater the increase in sediment mobility, and therefore the lower the two-size equilibrium bed slope. Despite the variation in bed response depending upon the grain size ratio, it was possible to collapse the majority of the slope evolution curves using an exponential decay function, demonstrating similarity in the behaviour.

The experiments were undertaken with a fixed coarse grain diameter, and a variety of fine grain diameters. Each grain size ratio will result in a different bed roughness, and also a different load to transport, depending upon the volume of fines able to infiltrate into the bed. In

addition to these factors, a physical control determining whether a fine grain input resulted in degradation or aggradation of the bed slope was observed.

The bed slope adjustment is related to the grain sorting behaviour. Examination of the experimental videos revealed that, if the fines are able to infiltrate into the underlying quasi-static bed through spontaneous percolation, the bedload layer is able to interact with the quasi-static coarse bed and grain-grain collisions occur, resulting in entrainment and, consequently, degradation. When spontaneous percolation is not geometrically feasible, a quasi-static layer of fine grains is formed upon the bed surface, which prevents interaction between the bedload layer and the underlying coarse bed, inhibiting degradation.

In an attempt to understand a wider range of controls, experiments were also undertaken varying the proportion of fines in the total feed for each grain size ratio. These experiments revealed that, for a given grain size ratio, the content of fines in the total feed has an important influence upon the channel response. Distinct boundaries emerged between a fine grain input of a given diameter which resulted in degradation and one which resulted in aggradation, depending upon the fine feed content. If the fine sediment input rate exceeds the current ability of the flow to transport the material, it forms a quasi-static layer underneath the transport layer that inhibits entrainment from the underlying bed, resulting in channel aggradation and an increase in bed slope.

Despite the limitations of reductionist experiments, the present work has provided important insight into the grain-grain behaviour, which would have otherwise been very difficult to isolate for clear observation. This approach would be useful to tackle other questions for which a greater understanding of a complex process is required.

Question 6: Are the results of an experiment in the domain of fluvial geomorphology reproducible?

Testing of reproducibility is an important aspect of the scientific method. It both tests the reliability of results, and also encourages clear reporting of experimental arrangements and procedures. Experiments testing the reproducibility of the current results were undertaken in a different laboratory, using a similar experimental arrangement and procedure. The same behavior was observed to control the channel response to a fine grain input in both cases. However, a difference in the quantitative values was observed. These differences were consistent; the S_{eq}/S_o (two-size equilibrium bed slope/one-size equilibrium bed slope) values for the replicate experiments were consistently higher and the percentage of the bed infiltrated was consistently lower. It is proposed that these variances are a result of differences in the flume construction and arrangement, causing a lower flow rate to be required for one-size equilibrium conditions in the replicate experiments.

Question 7: What is the impact of using spherical beads instead of natural materials?

The experiments using spherical glass beads enabled investigation of the phenomena at the grain scale, permitting important observations of the dominant processes. In order to develop our understanding towards natural systems, further experiments were undertaken using the same experimental procedure, but with natural materials. These experiments introduce the element of particle shape. The successive outcomes move us one step closer to the ultimate question of what controls channel response in more widely graded natural sediments.

Comparison between the experiments with spherical glass beads and natural materials reveals that particle shape has an important influence upon channel response to a fine grain input.

Kinetic sieving takes place within the mobile bedload layer, but the effect of the coarse particle shape upon the void spacing means that less infiltration by spontaneous percolation occurs within the bed. Additionally, in several of the experiments the behaviour of the bedload is different than that in the bead experiments, with collections of bedload migrating downstream together. However, overall, when comparing the S_{eq}/S_o values for the experiments with the natural materials with the values from the other experimental sets, the behaviour is similar.

6.3 Future Work

In order to develop our understanding towards conditions in a natural fluvial system, the desirable next step of research would involve a wider range of grain sizes. An initial step, using three grain sizes is suggested. By using three grain sizes (D_c, D_i and D_f), it would be possible to test which grain size ratio (D_c: D_i, D_c: D_f or D_i: D_f) controls the channel response, or whether new behaviours emerge. Beyond these experiments, successively wider grain size distributions should be tested.

Deeper analysis of the granular behaviour is advisable. Tracking of the particles to gain information on solid fraction and particle velocity over time and over depth in the bed will provide even more information regarding the channel response. Additional analysis also needs to be undertaken to explore the role of flume width and slope upon the results.

Finally, further work examining why differences in grain behaviour are exhibited when using natural materials instead of spherical glass particles should also be undertaken. This work will provide important insight into the limitations of physical models of fluvial systems using idealised materials, while at the same time enhancing our understanding of the natural phenomena.

Bibliography

Allan AF, Frostick L. 1999. Framework dilation, winnowing, and matrix particle size: the behavior of some sand-gravel mixtures in a laboratory flume. *Journal of Sedimentary Research* **69** : 21–26.

Allen JRL. 1982. *Sedimentary structures: their characters and physical basis Volume 1*. Elsevier Scientific Publishing Company: Amsterdam.

Allen, JRL. 1983. Gravel overpassing on humpback bars supplied with mixed sediment: examples from the Lower Old Red Sandstone, southern Britain. *Sedimentology* **30** : 285-294.

Allen JRL. 1985. *Principles of physical sedimentology*. George Allen & Unwin: London.

Andreotti B, Forterre Y, Pouliquen O. 2013. *Granular media: between fluid and solid*. Cambridge University Press: Cambridge.

Bacchi V, Recking A, Eckert N, Frey P, Piton G, Naaim M. 2014. The effects of kinetic sorting on sediment mobility on steep slopes. *Earth Surface Processes and Landforms* **39**(8) : 1075-1086.

Baker M. 2016. Is there a reproducibility crisis? *Nature* **533** : 452 – 454.

Begley CG, Ellis LM. 2012. Raise standards for preclinical cancer research. *Nature* **483** : 531-533.

Beschta RL, Jackson WL. 1979. The intrusion of fine sediments into a stable gravel bed. *Journal of the Fisheries Research Board of Canada* **36** : 204–210.

Böhm T, Frey P, Ducottet C, Ancey C, Jodeau M, Reboud J-L. 2006. Two-dimensional motion of a set of particles in a free surface flow with image processing. *Experiments in Fluids* **41** : 1–11.

Bridgwater J, Sharpe NW, Stocker DC. 1969. Particle mixing by percolation. *Transactions of the Institute of Chemical Engineers* **47** : T114-T119.

Calantoni J, Thaxton CS. 2008. Simple power law for transport ratio with bimodal distributions of coarse sediments under waves. *Journal of Geophysical Research* **113** : C03003.

Camerer CF, Dreber A, Forsell E, Ho T-H, Huber J, Johannesson M, Kirchler M, Almenberg J, Altmejd A, Chan T, Heikensten E, Holzmeister F, Imai T, Isaksson S, Nave G, Pfeiffer T, Razen M, Wu H. 2016. Evaluating replicability of laboratory experiments in economics. *Science* **351**(6280) : 1433-1436.

Carling PA. 1984. Deposition of fine and coarse sand in an open-work gravel bed. *Canadian Journal of Fisheries and Aquatic Sciences* **41** : 263–270.

Carling PA, Breakspear RMD. 2006. Placer formation in gravel-bedded rivers: A review. *Ore Geology Reviews* **28** : 377–401.

Carling PA, Kalsey A, Glaister MG. 1992. Effect of bed roughness, particle shape and orientation on imition motion criteria.In *Dynamics of gravel bed rivers*, Billi P, Hey RD, Thorne CR, Tacconi P (eds). John Wiley & Sons Ltd.: Chichester; 23-39.

Carling PA, McCahon CP. 1987. Natural siltation of brown trout (Salmo trutta L.) spawning gravels during low-flow conditions. In *Regulated streams: advances in ecology*, Craig JF, Kemper JB (eds). Plenum Press: New York; 229-244.

Carling PA, Orr H, Kelsey A. 2006. The dispersion of magnetite bedload tracer across a gravel point-bar and the development of heavy-mineral placers. *Ore Geology Reviews* **28** : 402-416.

Church M. 2003. Grain size and shape. In *Encyclopedia of Sediments and Sedimentary Rocks*, Middleton GV (ed). Kluwer : Dordrecht; 338-345.

Church M. 2006. Bed Material Transport and the Morphology of Alluvial River Channels. *Annual Review of Earth and Planetary Sciences* **34** : 325–354.

Cui Y, Parker G, Lisle TE, Gott J, Hansler-Ball ME, Pizzuto JE, Reed JM. 2003. Sediment pulses in mountain rivers: 1. Experiments. *Water Resources Research* **39**(9) : 1239.

Cui Y, Wooster JK, Baker PF, Dusterhoff SR, Sklar LS, Dietrich WE. 2008. Theory of fine sediment infiltration into immobile gravel Bed. *Journal of Hydraulic Engineering* **134** : 1421–1429.

Curran JC, Wilcock PR. 2005a. Characteristics dimensiones of the step-pool bed configuration: An experimental study. *Water Resources Research* **41** : W02030.

Curran JC, Wilcock PR. 2005b. Effect of sand supply on transport rates in a gravel-bed channel. *Journal of Hydraulic Engineering* **131** : 961–967.

Dermisis D, Papanicolaou TAN. 2014. The effects of protruding rock boulders in regulating sediment intrusion within the hyporheic zone of mountain streams. *Journal of Mountain Science* **11** : 1466–1477.

Diplas P, Parker G. 1992. Deposition and removal of fines in gravel-bed streams. In *Dynamics of Gravel-Bed Rivers,* Billi P, Hey RD, Thorne CR, Tacconi P (eds). John Wiley & Sons Ltd: New York; 313–329.

Duran J. 1999. *Sands, powders and grains : an introduction to the physics of granular materials (Partially ordered systems).* Springer: New York.

Eagleson PS, Dean RG. 1959. Wave-induced motion of sediment particles. *Transactions of the American Society of Civil Engineers.* **3225** : 1162-1186.

Einstein HA. 1968. Deposition of suspended particles in a gravel bed. *J. Hydraul. Div. Am. Soc. Civ. Engrs* **94** : 1197-1205.

Fenton JD, Abbott JE. 1977. Initial movement of grains on a stream bed: The effect of relative protrusion. *Proceedings of the Royal Society Series A.* **352** : 523-537.

Ferguson RI, Church M. 2004. A simple universal equation for grain settling velocity. *Journal of Sedimentary Research* **74** : 933-937.

Ferguson RI, Prestegaard KL, Ashworth PJ. 1989. Influence of sand on hydraulics and gravel transport in a braided gravel bed river. *Water Resources Research* **25** : 635–643.

Flueck JA. 1978. The role of statistics in weather modification experiments. *Atmosphere-Ocean* **16**(4) : 377–395.

Fraser HJ. 1935. Experimental study of the porosity and permeability of clastic sediments. *The Journal of Geology* **43**(8) : 910-1010.

Frey P, Dufresne M, Böhm T, Jodeau M, Ancey C. 2006. Experimental study of bed-load on steep slopes. In *River Flow 2006*, Ferreira RML, Alves ECTL, Leal JGAB, Cardoso AH (eds). Taylor & Francis Group: London; 887-893.

Frey P, Church M. 2011. Bedload: A granular phenomenon. *Earth Surface Processes and Landforms* **36**(1) : 58-69.

Frey P. 2014. Particle velocity and concentration profiles in bedload experiments on a steep slope. *Earth Surface Processes and Landforms* **39**(5) : 646-655.

Frostick LE, Lucas PM, Reid I. 1984. The infiltration of fine matrices into coarse-grained alluvial sediments and its implications for stratigraphical interpretation. *Journal of the Geological Society London* **141** : 955–965.

Gibson S, Abraham D, Heath R, Schoellhamer D. 2009. Vertical gradational variability of fines depositied in a gravel framework. *Sedimentology* **56** : 661–676.

Gibson S, Abraham D, Heath R, Schoellhamer D. 2010. Bridging process threshold for sediment infiltrating into a coarse substrate. *Journal of Geotechnical and Geoenvironmental Engineering* **136** : 402–406.

Gilbert GK. 1914. The transportation of debris by running water, Professional paper 86. US Geologial Survey: Washington DC, 261pp.

Gray WA. 1968. *The packing of solids*. Chapman and Hall Ltd: London.

Hales TC. 2005. A proof of the Kepler conjecture. *Annals of Mathematics* **162** : 1065-1185.

Hergault V, Frey P, Métivier F, Barat C, Ducottet C, Böhm T, Ancey C. 2010. Image processing for the study of bedload transport of two-size spherical particles in a supercritical flow. *Experiments in Fluids* **49**(5) : 1095-1107.

Hill KM, Gioia G, Tota VV. 2003. Structure and kinematics in dense free-surface granular flows. *Physical Review Letters* **91**(6) : 064302.

Hill KM, Zhang J. 2008. Kinematics of densely flowing granular mixtures. *Physical Review E - Statistical, Nonlinear and Soft Matter Physics* **77** : 061303.

Horsfield HT. 1934. The strength of asphalt mixtures. *Journal of the Society of Chemical Indsutry* **53** : T107-T115.

Houssais M, Lajeunesse E. 2012. Bedload transport of a bimodal sediment bed. *Journal of Geophysical Research* **117** : F04015.

Houssais M, Ortiz CP, Durian DJ, Jerolmack DJ. 2015. Onset of sediment transport is a continuous transition driven by fluid shear and granular creep. *Nature Communications* **6** : 6527.

Huston DL, Fox JF. 2015. Clogging of fine sediment within gravel substrates : Dimensional analysis and macroanalysis of experiments in hydraulic flumes. *Journal of Hydraulic Engineering* **141** : 04015015.

Ikeda H, Iseya F. 1988. Experimental study of heterogeneous sediment transport. *Environmental Research Center Paper No. 12, Univ. of Tsukuba, Tsukuba, Japan.*

Iseya F, Ikeda H. 1987. Pulsations in bedload transport rates induced by longitudinal sediment sorting: a flume study using sand and gravel mixtures. *Geografiska Annaler, Series A* **69** : 15–27.

IUPAC. 1997. *Compendium of Chemical Terminology, 2nd ed. (the "Gold Book")*. Compiled by McNaught AD, Wilkinson A. Blackwell Scientific Publications : Oxford.

Jackson WL, Beschta RL. 1984. Influences of increased sand delivery on the morphology of sand and gravel channels. *Water Resources Bulletin American Water Resources Association* **20** : 527-533.

Kaiser, J. 2016. If you fail to reproduce another scientist's results, this journal wants to know. Retrived April 2016 from http://www.sciencemag.org/news/2016/02/if-you-fail-reproduce-another-scientist-s-results-journal-wants-know

Kemp P, Sear D, Collins A, Naden P, Jones I. 2011. The impacts of fine sediment on riverine fish. *Hydrological Processes* **25** : 1800–1821.

Kirchner JW, Dietrich WE, Iseya F, Ikeda H. 1990. The variability of critical shear stress, friction angle, and grain protrusion in water-worked sediments. *Sedimentology.* **37** : 647-672.

Knighton D. 1998. *Fluvial forms and processes: a new perspective*. Arnold : London.

Komar PD, Li Z. 1986. Pivoting analyses of the selective entrainment of sediments by shape and size with application to gravel threshold. *Sedimentology* **33** : 425-436.

Lafaye de Micheaux H, Dudill A, Frey P, Ducottet C. 2015. Image processing to study the evolution of channel slope and water depth in bimodal sediment mixtures. In *10th Pacific Symposium on Flow Visualisation and Image Processing,* G. Cardone (ed).

Lane EW. 1955. The importance of fluvial morphology in hydraulic engineering. *Am. Soc. Civil Eng Proc.* **81**(745) : 17.

Li Z, Komar PD. 1986. Laboratory measurments of pivoting angles for applications to selective entrainment of gravel in a current. *Sedimenology*. **33** : 413-423.

Lisle TE. 1989. Sediment transport and resulting deposition in spawning gravels, North Coastal California. *Water Resources Research* **25** : 1303–1319.

Major JJ, Pierson TC, Dinehard RL, Costa JE. 2000. Sediment yield following severe volcanic disturbance – A two-decade perspective from Mount St. Helens. *Geology* **28**(9) : 819-822.

Manegold E, Hofman R, Solf K. 1931. Ueber Kapillarsysteme XII. I. Die mathematische Behandlung idealer Kgelpackungen und das Hohlraumvolumen realer Geruststrukturen. *Kolloidzeitschrift* **56** : 142-159.

Mao L, Cooper JR, Frostick LE. 2011. Grain size and topographical differences between static and mobile armour layers. *Earth Surface Processes and Landforms* **36** : 1321–1334.

Martin RL, Purohit PK, Jerolmack DJ. 2014. Sedimentary bed evolution as a mean-reverting random walk: Implications for tracer statistics. *Geophysical Research Letters* **41** : 6152-6159.

Meiron DI, Baker GR, Orszag, SA. 1982. Analytic structure of vortex sheet dynamics. Part 1. Kelvin-Helmholtz instability. Journal of Fluid Mechanics **114** : 283-298.

Meyer-Peter E, Müller R. 1948. *Formulas for bed-load transport*. Proceedings of the 2nd meeting of the International Association for Hydraulic Structures Research; 39-64.

Middleton GV. 1970. Experimental studies related to problems of flysch sedimentation. In *Flysch Sedimentology in North America*, Lajoie J. (ed). Geological Association of Canada: St John's Canada; 253-272.

Miller RL, Byrne RJ. 1966. The angle of repose for a single grain on a fixed rough bed. *Sedimentology*. **6** : 303-314.

Montgomery DR, Panfil MS, Hayes SK. 1999. Channel-bed mobility response to extreme sediment loading at Mount Pinatubo. *Geology* **27** : 271-274.

Nelson PA, Venditti JG, Dietrich WE, Kirchner JW, Ikeda H, Iseya F, Sklar LS. 2009. Response of bed surface patchiness to reductions in sediment supply. *Journal of Geophysical Research* **114** : F02005.

Onoda GY, Liniger EG. 1990. Random loose packings of uniform spheres and the dilatancy onset. *Physical Review Letters* **64** : 2727-2730.

Open Science Collaboration. 2015. Estimating the reproducibility of psychological science. *Science* **349**(6251) : aac4716.

Parker G, Klingeman PC. 1982. On why gravel bed streams are paved. *Water Resources Research* **18** : 1409–1423.

Pugnaloni LA, Barker GC. 2004. Structure and distribution of arches in shaken hard sphere deposits. *Physica A: Statistical Mechanics and Its Applications* **337** : 428–442.

Recking A, Frey P, Paquier A, Belleudy P. 2009. An expeirmental investigation of mechanisms involved in bed load sheet production and migration. *Journal of Geophysical Research* **114** : F03010.

Sakthivadivel R, Einstein HA. 1970. Clogging of porous column of spheres by sediment. *Journal of the Hydraulics Division, American Society of Civil Engineers* **96** : 461–472.

Savage SB, Lun CKK. 1988. Particle-size segregation in inclined chute flow of dry cohesionless granular solids. *Journal of Fluid Mechanics* **189** : 311–335.

Schumm SA, Stevens MA. 1973. Abrasion in place : A mechanism for rounding and size reduction of coarse sediments in rivers. *Geology* **1** : 37–40.

Scott GD, Kilgour DM. 1969. The density of random close packing of spheres. *Journal of Applied Physics D: Applied Physics* **2** : 863-866.

To K, Lai PY, Pak HK. 2002. Flow and jam of granular particles in a two-dimensional hopper. *Physica A: Statistical Mechanics and Its Applications* **315** : 174–180.

Venditti JG, Dietrich WE, Nelson PA, Wydzga MA, Fadde J, Sklar L. 2010a. Effect of sediment pulse grain size on sediment transport rates and bed mobility in gravel bed rivers. *Journal of Geophysical Research: Earth Surface* **115** : F03039.

Venditti JG, Dietrich WE, Nelson PA, Wydzga MA, Fadde J, Sklar L. 2010b. Mobilization of coarse surface layers in gravel-bedded rivers by finer gravel bed load. *Water Resources Research* **46** : W07506.

White HE, Walton SF. 1937. Particle packing and particle shape. *Journal of the American Ceramic Society* **20** : 155-166.

Whiting PJ, Dietrich WE, Leopold LB, Drake TG, Shreve RL. 1988. Bedload sheets in heterogeneous sediment. *Geology* **16** : 105-108.

Wilcock PR, Kenworthy ST, Crowe JC. 2001. Experimental study of the transport of mixed sand and gravel. *Water Resources Research* **37** : 3349–3358.Wooster JK, Dusterhoff SR, Cui Y, Sklar LS, Dietrich WE, Malko M. 2008. Sediment supply and relative size distribution effects on fine sediment infiltration into immobile gravels. *Water Resources Research* **44** : W03424.

Wooster JK, Dusterhoff SR, Cui Y, Sklar LS, Dietrich WE, Malko M. 2008. Sediment supply and relative size distribution effects on fine sediment infiltration into immobile gravels. *Water Resources Research* **44**(3) : W03424.

Appendices

Appendix A

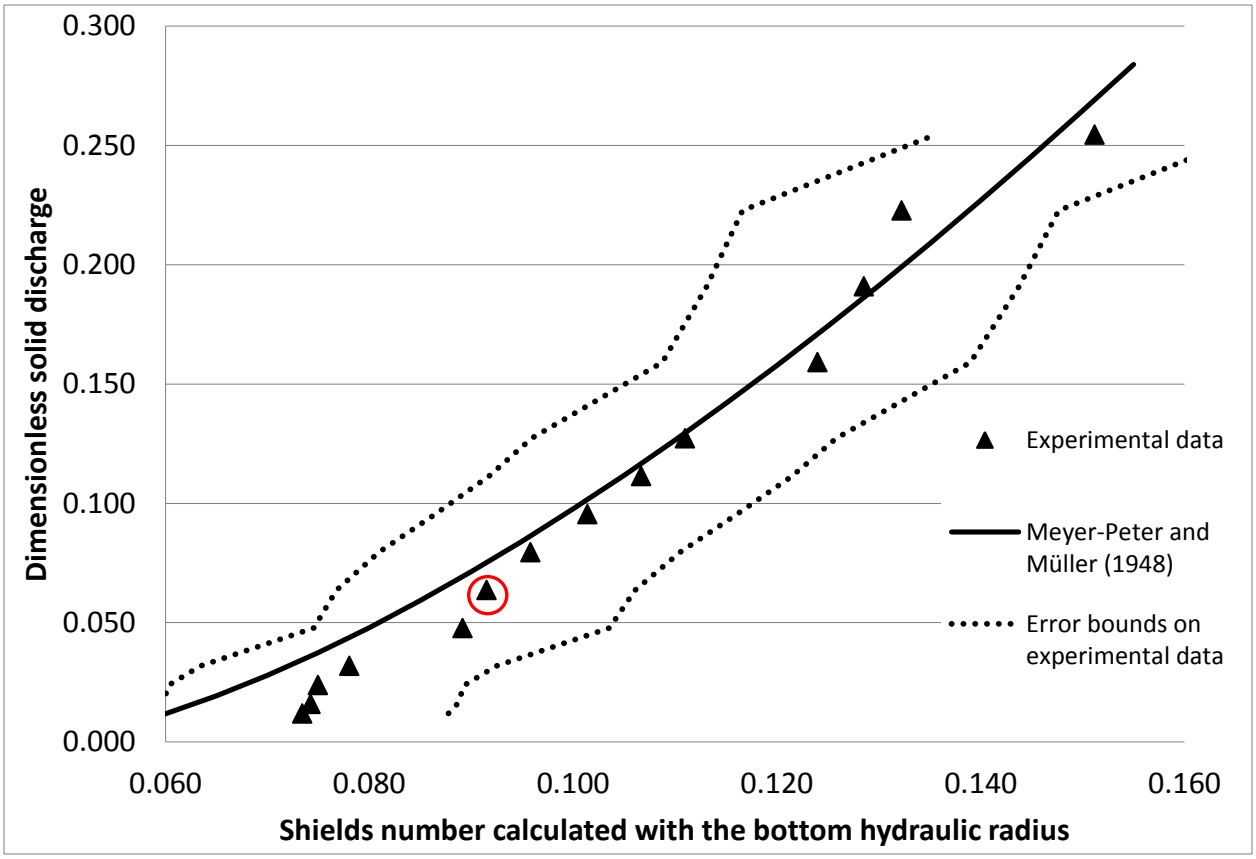

Figure A.1 The relation between dimensionless solid discharge and Shields number calculated with the bottom hydraulic radius for experimental data and the classic semi-empirical Meyer-Peter and Müller (1948) bedload formula. The data is presented on linear-linear axes.

A series of additional experiments was undertaken at Irstea to demonstrate the agreement, during supercritical flow, between sediment transport rates in this flume and classical semi-empirical bedload formulae; the results are presented in Figure 6.1. The experiments were undertaken using the same channel width (10.3 mm) and channel slope (10.1 %). Fifteen experiments were

performed, using the 5 mm diameter grains, each with a different bead feed rate. The lowest feed rate tested was 0.04 kg/s/m, and the highest was 0.97 kg/s/m (the data point circled in red shows the conditions during the experiments presented in this paper: 0.216 kg/s/m). For each feed rate, the flow rate required for equilibrium conditions was determined (sediment input rate equal to sediment output rate, and flume slope parallel to bed slope).

The Einstein dimensionless solid discharge was used:

$$\Phi = \frac{q_s}{\sqrt{(s-1).g.D^3}}$$

With q_s as the bedload transport rate per unit width (m3/s/m); $s=\rho_s/\rho$ = sediment density / water density (=1.5).

The Shields number was calculated using the bottom hydraulic radius (R_{hb}), as in the following definition

$$\theta = \frac{R_{hb}.S}{(s-1).D}$$

The bottom hydraulic radius R_{hb} was calculated by the classical Einstein or Vanoni Brooks method, taking into account sidewall dissipation. The methodology applied to our specific channel is fully described in Frey et al. (2006).

Good agreement is achieved between the experimental data and the classical semi-empirical bedload formulae of Meyer-Peter and Müller (1948).

Appendix B

The following parameters are constants (Irstea experiments):

$\boldsymbol{D_c}$	Coarse grain diameter	5±0.3 mm
$\boldsymbol{g}$	Gravitational constant	9.81 m/s^2
$\boldsymbol{k}$	von Karman constant	0.4
$\boldsymbol{Q}$	Flow rate	49.5 ml/s
$\boldsymbol{R}$	Submerged specific density (glass beads)	1.5
$\boldsymbol{S}$	Slope	10.1 %
$\boldsymbol{W}$	Channel width	10.3 mm
$\boldsymbol{\alpha}$	Channel angle	0.101 radians
$\boldsymbol{\nu}$	Kinematic viscosity (at 25°C)	0.8926 mm^2/s
$\boldsymbol{\rho}$	Water density (at 25°C)	0.997 g/cm^3

The following parameters were calculated as detailed:

Mean flow depth, *h*:

The flow depth values presented in this thesis were measured using image analysis techniques. Using one frame per second for two minutes, the bed surface profile and the water line were detected using the methods described in Lafaye de Micheaux et al. (2015) (see Figure 6.2 for an example). The mean bed elevation was then subtracted from the mean water line to give an average flow depth. This analysis was performed for every experiment with Chapter 3: Set 1.

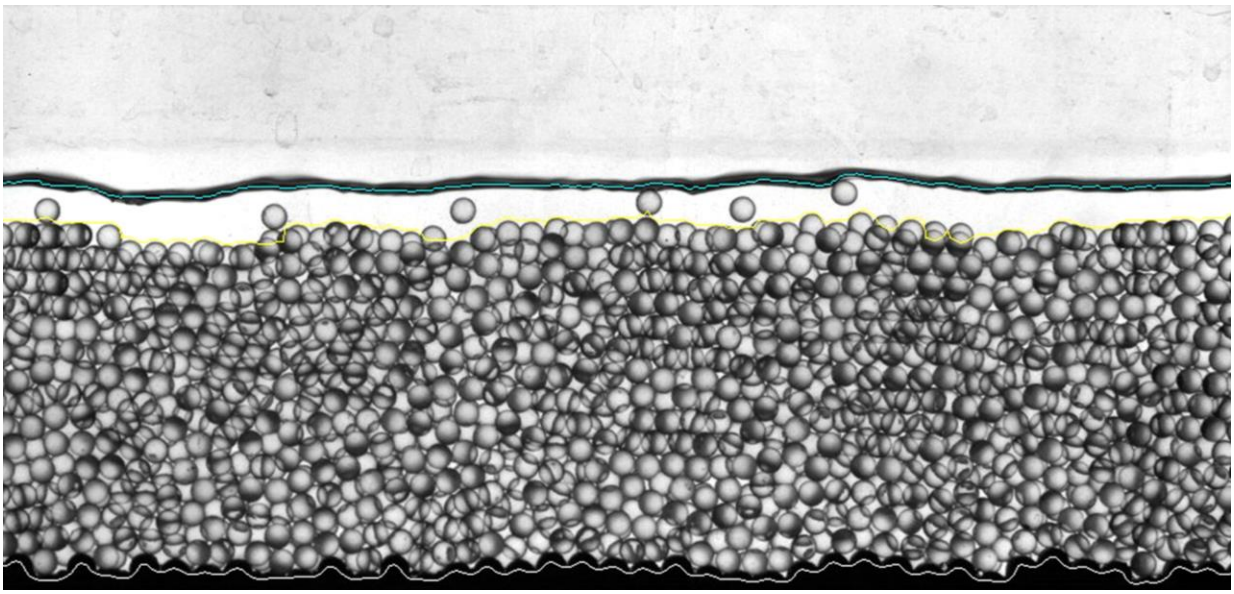

Figure B.1 Example camera visualization frame demonstrating the bed and water line detection.

Submergence ratio $= \frac{h}{D_c}$

Side-wall corrected dimensionless shear stress $= \frac{R_{hb} sin\alpha}{RD_c}$

R_{hb} is the bottom hydraulic radius calculated using the classical Einstein and Vanoni Brooks method, taking into account sidewall dissipation. The methodology to compute R_{hb} is fully described in Frey et al. (2006): Section 3.2.

Mean velocity, $U = \frac{Q}{Wh}$

Froude Number $= \frac{U}{\sqrt{gh}}$

Reynolds Number $= \frac{4UR_{\mathrm{h}}}{\nu}$

R_{h} is the hydraulic radius $\left(R_{\mathrm{h}} = \frac{Wh}{2h+W}\right)$

Roughness Reynolds Number $= \frac{u_* D_{\mathrm{c}}}{\nu}$

u_* is the shear velocity $\left(u* = \sqrt{\frac{\tau_o}{\rho}}\right)$, τ_{o} is the shear stress ($\tau_{\mathrm{o}} = \rho g R_{\mathrm{hb}} S$)

Rouse Number $= \frac{w_{\mathrm{s}}}{k u_*}$

w_{s} is the fall velocity calculated using the Ferguson and Church (2004) equation $\left(W_S = \frac{RgD_{\mathrm{c}}^2}{C_1 \upsilon + (0.75 C_2 RgD_{\mathrm{c}}^3)^{0.5}}\right)$, $C_1 = 18$ and $C_2 = 0.4$ which are appropriate for smooth spheres.

The uncertainty in the reported hydraulic parameters is a result of the uncertainty in the mean flow depth and diameter of the coarse grains.

Appendix C

Supporting videos for Irstea experiments: Video_S1, Video_S2, Video_S3, Video_S4, Video_S5, Video_S6, Video_S7, Video_S8, Video_S9, Video_S10, Video_S11, Video_S12, Video_S13

For all videos, the AVI (how many frames form one second of the video) is 30.

In all videos, flow is from right to left.

Video Name	**Description**	**Start of the video**	**End of the video**	**Frame rate (frames/second)**
Video_S1	The 5 mm bed in one-size equilibrium	Frame 6000 (46.2 seconds into the recording)	Frame 7625 (58.7 seconds into the recording)	130
Video_S2	Experiment I.1 - 0.7 mm beads infiltrating into the 5 mm bed	Frame 20506 (37.7 seconds after the fine feed was introduced)	Frame 23744 (62.6 seconds after the fine feed was introduced)	130
Video_S3	Experiment I.2 - 0.9 mm beads infiltrating into the 5 mm bed	Frame 18243 (20.3 seconds after the fine feed was introduced)	Frame 21670 (46.7 seconds after the fine feed was introduced)	130
Video_S4	Experiment I.1 (0.7 mm fines) - bed degrading	Frame 35000 (149.2 seconds after the fine feed was introduced)	Frame 37000 (164.6 seconds after the fine feed was introduced)	130
Video_S5	Experiment I.2 (0.9 mm fines) - bed in	Frame 155787 (1078.4 seconds after	Frame 156287 (1082.2 seconds after	130

	two-size equilibrium	the fine feed was introduced)	the fine feed was introduced)	
Video_S6	Experiment I.3 – 1.5 mm beads infiltrating into the 5mm bed	Frame 16500 (6.9 seconds after the fine feed was introduced)	Frame 19900 (33.1 seconds after the fine feed was introduced)	130
Video_S7	Experiment I.4 – 2 mm beads infiltrating into the 5 mm bed	Frame 16000 (3.1 seconds after the fine feed was introduced)	Frame 19106 (27.0 seconds after the fine feed was introduced)	130
Video_S8	Experiment I.4 (2 mm fines) - bed degrading	Frame 31000 (118.5 seconds after the fine feed was introduced)	Frame 131000 (887.7 seconds after the fine feed was introduced)	1.3
Video_S9	Experiment I.5 – 3 mm fines introduced to the 5 mm bed	Frame 15830 (1.8 seconds after the fine feed was introduced)	Frame 19830 (32.5 seconds after the fine feed was introduced)	65
Video_S10	Experiment I.5 (3 mm fines) – bed in two-size equilibrium	Frame 158999 (1103.1 seconds after the fine feed was introduced)	Frame 159999 (1110.8 seconds after the fine feed was introduced)	130
Video_S11	Experiment I.7 (0.7 mm fines) - bed in two-size equilibrium	Frame 198999 (1410.8 seconds after the fine feed was introduced)	Frame 199999 (1418.5 seconds after the fine feed was introduced)	130
Video_S12	Experiment I.8 (0.7 mm fines) – bed in	Frame 134999 (918.5 seconds after the fine	Frame 135999 (926.1 seconds after the fine	130

	two-size equilibrium	feed was introduced)	feed was introduced)	
Video_S13	Experiment I.10 – 2 mm fines introduced to the 5 mm bed	Frame 17000 (10.8 seconds after the fine feed was introduced)	Frame 20500 (37.7 seconds after the fine feed was introduced)	65

Appendix D

Supporting videos for SFU_{nat} experiments: Video_S14, Video_S15, Video_S16, Video_S17, Video_S18, Video_S19, Video_S20, Video_S21, Video_S22, Video_S23.

In all videos, flow is from right to left.

Video Name	**Description**	**Length (seconds)**
Video_S14	The 4 mm bed in one-size equilibrium.	30
Video_S15	Experiment S.17– 0.6 mm fines infiltrating into the 4 mm bed.	48
Video_S16	Experiment S.20 – 0.8 mm fines infiltrating into the 4 mm bed.	17
Video_S17	Experiment S.23 – 2 mm fines infiltrating into the 4 mm bed.	21
Video_S18	Experiment S.17 (0.6 mm fines) – undulating bedload movement.	60
Video_S19	Experiment S.19 (0.8 mm fines) – undulating bedload movement	45

Video_S20	Experiment S.22 – (2 mm fines) – undulating bedload movement.	59
Video_S21	Experiment S.16 (0.6 mm fines) – highlighting features of the two-size bedload movement.	29
Video_S22	Experiment S.21 (0.8 mm fines) – smooth bedload movement.	50
Video_S23	Experiment S.23 (2 mm fines) – Example of 4 mm entrainment.	68